universität wien

MASTERARBEIT

Titel der Masterarbeit

"Construction of different mutants of *Natrialba magadii* and the influence of different ϕCh1 ORFs on *N. magadii*"

verfasst von

Léa Schöner, Bsc

angestrebter akademischer Grad

Master of Science (MSc)

Wien, 2013

Studienkennzahl lt. Studienblatt:	A 066 830
Studienrichtung lt. Studienblatt:	Masterstudium Molekulare Mikrobiologie und Immunbiologie
Betreut von:	Ao. Univ.-Prof. Dipl.-Biol. Dr. Angela Witte

Table of Contents

1. Introduction

1.1. *Archaea*

1.1.1. Classification of the living world and the third domain of life

The classification of living organisms has a long history. Until the 20th century the living world was grouped into two kingdoms, Plants and Animals, and assigning organisms being plants or animals was quite easy as they do not resemble each other. This dichotomy was first questioned with the discovery of single-cell organisms. They resembled both, plants and animals, and generally they were considered to be plants. In 1866 Haeckel realized that these unicellular organisms are neither plants nor animals, so he proposed that the tree of life has 3 branches with the third kingdom, the Protists. In 1938 Copeland distinguished between single-cell organisms having a distinct nucleus and cells without one. Therefore he proposed a fourth kingdom the Monera, comprising unicellular organisms without a distinct nucleus, today termed Bacteria [1]. At the same time Chatton realized the importance to differentiate between nucleated and non-nucleated cells. Therefore he introduced an additional concept for classification, he proposed to divide the living world additionally into Prokaryotes and Eukaryotes [2]. Finally, in 1969 Whittaker proposed his five-kingdom system, which is the most accepted view on organization of life today. He divided the living world into Animalia, Plantae, Fungi, Protista (protozoa, algae and slime moulds), and Monera (bacteria). The five-kingdom system existed in parallel with Chattons eukaryote-prokaryote concept until 1977, when Carl Woese discovered the archaebacteria and introduced a new taxon of the highest level - the domain [1].

Woese intended to determine phylogenetic relationships with the aim to construct a phylogenetic tree of life that incorporates all cellular life. He was searching for a molecule that can be used as a universal chronometer. He used small-subunit ribosomal-RNA (16S/18S rRNA) for comparative sequence analysis because of its properties: it is a component of all self-replicating organisms, it shows significant sequence conservation but also some moderate variability and it is easy to isolate. In 1977 Woese and Fox presented that prokaryotes are not only made up of the group bacteria, which was an astonishing revelation. Beside the bacteria and eukaryotic cells, there exists "a third kingdom", the archaebacteria. He defined the three groups as urkingdoms comprising eubacteria (all typical bacteria), archaebacteria (methanogenic bacteria) and urkaryotes (eukaryotes). Each urkingdom had specific signatures in the conserved 16S/18S rRNA molecule [3]. In 1990 Woese

proposed to establish a new taxon called domain as the highest level above kingdom and introduced the three-domain system. The universal tree of life is based on 16S/18S rRNA sequencing, with the three domains *Bacteria*, *Archaea* and *Eukarya,* and each domain contains 2 or more kingdoms [4].

This classification system divides the prokaryotic world into *Bacteria* and *Archaea*, and the tree of life shows that *Archaea* are distantly related to *Eukarya*, and moreover, *Archaea* appear to be closer related to eukaryotes than to *Bacteria*. Woese subdivided *Archaea* into the kingdom *Euryarchaeota,* initially comprising methanogens and relatives, and the kingdom *Crenarchaeota*, comprising extremely thermophilic *Archaea* [4].

Since the establishment of the phylogenetic tree of life, new groups beside the *Euryarchaeota* and *Crenarchaeota* have been described (Fig. 1). *Nanoarchaeota* are represented by the only member *Nanoarchaeum equitans* [5], and members of *Korarchaeota* are indicated only by DNA sequences of environmental samples of unculterable *Archaea* deriving from volcanic hot springs [6].

Figure 1: The phylogenetic tree of life based on 16S/18S rRNA sequences.

The tree of life represents the three domain system. The domain *Bacteria* is separated from the domains *Archaea* and *Eukarya*, and *Archaea* and *Eukarya* are distantly related - they have a common ancestor. *Archaea* are subdivided into 4 kingdoms. Members of the *Euryarchaeota* include mainly methanogen and halophile species, and represents the most diverse kingdom. Members of the *Crenarchaeota* include mainly hyperthermophile species. The kingdom *Nanoarchaeota* is represented only by *Nanoarchaeum equitans,* and the kingdom *Korarchaeaota* is indicated by DNA sequences of uncultered microbes.
(Adapted from Allers and Mevarech, 2005; Nature Reviews|Microbiology [12])

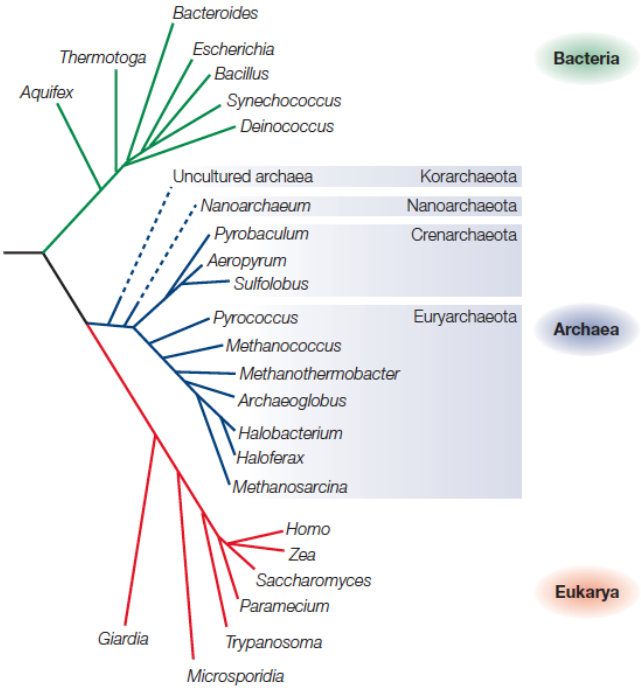

1.1.2. Diversity of *Archaea* and the two major phyla - An overview

Before 16S/18S rRNA sequences revealed *Archaea* as the third domain of life, they have been wrongly classified as *Bacteria* for decades, since they resemble each other in appearance. The first member of *Archaea* was probably described in 1880 by Farlow, under the name *Sarcina morrhuae* (today termed *Halococcus morrhuae*), which is a halophilic member of the *Euryarchaeota* [7].

Originally, *Archaea* were considered to be thoroughly extremophiles, because they were mainly isolated from environments most bacteria and eukaryotes would not survive. *Archaea* are predominant in hyperthermal regions (thermophiles), but in all other environments with extreme conditions like hypersalinity (halophiles), high or low pH (acidophiles and alkalophiles), low temperature (psychrophiles), high pressure (barophiles) or radiation, *Archaea* are found together with *Bacteria* and *Eukarya*. Extremophiles need adaption to overcome these hostile conditions in order to protect their cytoplasm membrane, proteins, DNA and other cellular components [8]. Except for methanogenesis, which is only known for *Archaea*, all other metabolic pathways found in *Archaea* also exist among *Bacteria*. However, not all *Archaea* are extremophiles just because they are found at the limits of extreme environments. Culture independent surveys revealed a different picture [9,10]. *Archaea* have been detected in non-extreme regions that are also habitats for *Bacteria*, such as oceans and lakes, or soil.

The *Euryarchaeota* and the *Crenarchaeota* present the two major phyla of the *Archaea*. Members of the ***Euryarchaeota*** form the best-characterized and most diverse group including mainly halophiles, methanogens but also some thermoacidophiles (*Thermoplasma*) and some hyperthermophiles (*Archaeoglobus*) [9]. Methanogens colonize strictly anoxic habitats, including for example marine environments or gastrointestinal tracts of animals. An example is *Methanocaldococcus jannaschii*, which was isolated from a submarine hydrothermal vent. Methanogens are able to reduce carbon dioxide, acetic acid or various one-carbon compounds like methanol, to produce methane [11]. Extreme halophilic *Archaea*, also called haloarchaea, tolerate oxygen, and grow as heterotrophs in hypersaline environments like salt lakes with salt concentration close to saturation or saturation. They are able to withstand the osmotic pressure by accumulation of inorganic salts in the cytoplasm. Halophilic *Archaea* are also found in alkaline environments (haloalkaliphilic *Archaea*) where they grow at pH values above 10 [12]. (Halophilic and haloalkaliphilic *Archaea* will be discussed in more detail later in this chapter)

Members of the ***Crenarchaeota*** form a less diverse group compared to the *Euryarchaeota*. Members are thermophiles, growing optimal between 60-85°C, or hyperthermophiles growing between 80-100°C. *Pyrolobus fumarii* is found in hydrothermal vents growing at temperatures up to 113°C. Acidophile organisms have a pH optimum for growth at 3-4 or below. Acidophile *Archaea* are often thermophile, called thermoacidophile, like members of the order *Sulfolobales. Sulfolobus solfataricus* colonizes hot springs in Yellowstone National Park with an optimal growth temperature of 75-80°C and a pH of 2-3 [12]. The metabolism of *Crenarchaeota* ranges from chemoorganotrophy to

chemolithoautotrophy. Cultivation independent studies revealed that there exists a widespread diversity of mesophilic *Archaea* under the *Crenarchaeota* that colonize non-extreme terrestrial and marine habitats. It was shown that *Archaea* are abundant components of marine plankton. They colonize marine environments and moreover, 20% of all microbial cells in the oceans constitute of *Archaea* [9,10,13].

About 75% of the earth biosphere is cold (≥5°C). Cold habitats such as cold marine water, deep sea and sea ice, and also non-marine environments like alpine and polar habitats are home for psychrophilic *Archaea*. Psychrophilic organisms have an optimal growth temperature of 10°C or lower. *Archaea* isolated from such environments are for example methanogens, like *Methanogenium frigidum* isolated from Ace Lake in Antarctica, and also non-thermophilic members of the *Crenarchaeota* like *Crenarchaeum symbiosum*, isolated from coast water. *Halorubrum lacusprofundi*, a member of haloarchaea, was isolated in Deep Lake in Antarctica [14]. Organisms living in deep sea are exposed to high pressure. The barophilic archaeon *Thermococcus barophilus* was isolated from a hydrothermal vent at 3550m depth and enrichments were done under a pressure of 40MPa, whereas the atmospheric pressure on the earth surface is 101,325kPa [15].

Environments that are associated with high levels of ionizing radiation are populated by radioresistant organisms. A well-known representative of a bacterial radioresistant species is *Deinococcus radiodurans*. The radioresistant archaeon *Thermococcus gammatolerans* was isolated from a submarine hydrothermal vent where natural radioactivity is a hundred times higher then on the earth surface. *Thermococcus gammatolerans* is able to withstand extreme high levels of γ-irradiation up to 30kGy, a dose that is lethal to all other organisms [16,17].

1.1.3. Unique features of *Archaea*

Archaea have similarities with both, *Bacteria* and *Eukarya*. Many components of archaeal information process systems, like DNA replication, transcription and translation, have similarities to the eukaryal ones [11]. On the other hand, they also have many traits in common with *Bacteria*. Beside the morphological resemblance, they have similarities, such as the organization of the chromosomal DNA, the use of 70S ribosomes, the organization of genes into operons or metabolic pathways. However, *Archaea* do have unique characteristics that distinguish them from the other 2 domains. To mention is the cytoplasmic membrane which is composed of unique lipids, and in contrast to *Bacteria*, archaeal cell walls do not contain peptidoglycan [18].

1.1.3.1. Ether-linked lipids - an archaeal signature

Archaeal lipids of the cytoplasmic membrane are different to that of *Bacteria* and *Eukarya*. The membrane of *Archaea* is composed of ether-linked lipids, whereas in the other 2 domains, lipids are ester-linked [19]. The phospholipids of bacteria and eukaryotes consist of linear hydrophobic fatty acids that are ester-linked to a glycerol backbone (Fig. 2A). Instead of fatty acid chains, the hydrophobic part (lipid core) of archaeal lipids consist of branched isoprenoid acyl chains which are covalently bound to the glycerol backbone through ether bonds [19]. Ether bonds are much more resistant to hydrolysis than ester linkages which is an important advantage for *Archaea* living in extreme environments [20]. The bilayers of archaeal cytoplasmic membranes are commonly made up of lipids with a C20 isoprenoid acyl chain (Fig. 2B).

Also found in archaeal membranes are the unique tetraether lipids. These lipids have C40 isoprenoid acyl chains and both ends of the chains are bound to the hydrophilic groups. They span the membrane, which allows the formation of a very stable monolayer instead of a bilayer (Fig. 2C). Such monolayer membranes are important for adaption to extreme environments. In the matter of thermophily, these membranes are very resistant to heat denaturation and the branched lipid core increases membrane fluidity, which is required for growth at high temperatures. For example, such membranes are found in the thermoacidophile species *Sulfolobus solfataricus* or *Thermoplasma acidophilum* [19–21]. Moreover, archaeal and bacterial/eukaryal lipids differ in stereochemistry - the glycerol-phosphate backbones have enantiomeric configuration (Fig. 2) [21].

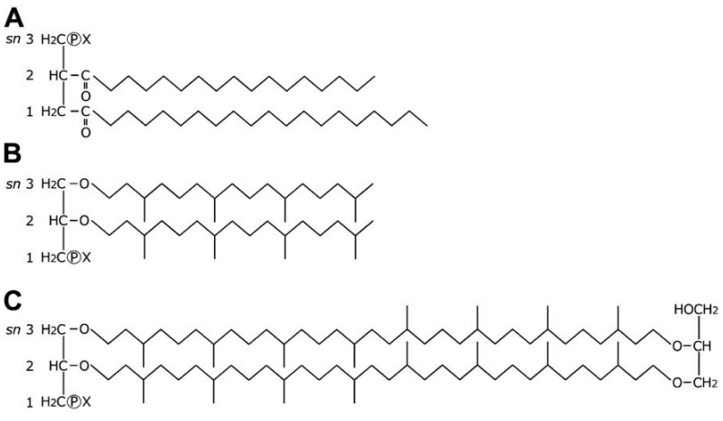

Figure 2: Cytoplasmic membrane lipids of *Archaea* and *Bacteria/Eukarya*.
(A) Phospholipids of *Bacteria* and *Eukarya*: The fatty acid chains (hydrophobic region) are linked via ester bonds to a glycerol-3-phosphate backbone (hydrophilic region). **(B/C)** The hydrophobic region of archaeal lipids is made up of branched isoprenoid acyl chains that are linked vie ether bonds to a glycerol-1-phosphate backbone.
(C) Tetraether lipids are composed of 2 hydrophilic groups connected by 40 carbon isoprene chains, which allows the formation of a monolayer membrane.
(Matsumi R. *et al*, 2010 [21])

1.1.3.2. Diversity of archaeal cell walls

The diverse structures of prokaryotic cell walls reflects the adaption to specific ecological and environmental conditions [22]. Beside the ether-linked lipids, another unique archaeal characteristic is the composition of the cell wall. As already mentioned, compared to bacteria, archaeal cell walls do not contain peptidoglycan, and they are chemically and structurally diverse. Almost found in all *Archaea* is the protective S-layer (surface layer), which is mostly anchored to the cytoplasmic membrane and composed of protein or glycoprotein species (Fig. 3) [23]. The S-layer proteins build a two dimensional array that surrounds the cytoplasmic membrane. In some *Archaea*, the S-layer is the only component of the cell wall, whereas other cell walls contain multiple polymers (like pseudomurein and methanochondroitin) and additional S-layer proteins. The cell wall component **pseudomurein** is somehow similar to bacterial peptidoglycan. In peptidoglycan, N-acetylmuramic acid is α-1,4 linked to D- N-acetylglucosamine. Pseudomurein is composed of N-acetylglucosamine that is β-1,3 linked to L-N-acetylalosaminuronic acid. Another cell wall polymer is **methanochondroitin**, produced by members of *Methanosarcina* (Fig. 3). It differs from pseudomurein in chemical structure, and interestingly, it is only produced when cells aggregate, single cells only have the S-layer [23,24].

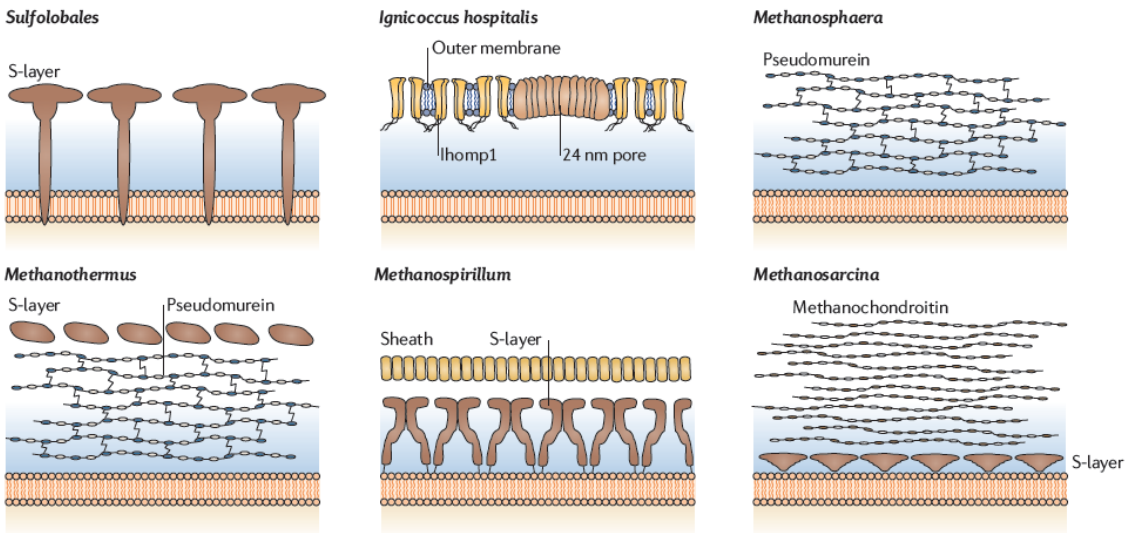

Figure 3: Schematic presentations of some cell wall profiles of different *Archaea*. The S-layer of *Sulfolobus* is composed of two proteins, with the smaller protein the S-layer is anchored into the membrane. *Ignococcus hospitalis* is the only archaeon having an outer membrane. *Methanosphaera* and *Methanothermus* have pseudomurein in their cell walls. *Methanopirillum* possesses a proteinaceous sheath. *Methanochondroitin* is produced by cell aggregates of *Metahnosarcina* species.
(Adapted from Albers and Meyers, 2011; Nature Reviews|Microbiology [23])

The most complex cell envelope is that of *Methanospirillum hungatei* and *Methanosaeta concilii* (Fig. 3). Cells are covered by an extraordinary stable **proteinaceous sheath**, which is different to S-layer proteins. Another cell envelope example is that of the extreme halophile *Halococcus morrhuae*, which is a layer of **heteropolysaccharides**. Also to mention is *Ignicoccus hospitalis*, which is the only known archaeon that possesses an outer membrane (Fig. 3). Members of the *Thermoplasmatales* represent another interesting exception. Members live in environments with very low pH values (1-2) and temperatures around 60°C, and despite these conditions, they don't even have a cell wall. Instead they have a cell-surface coat made of glycoproteins and glycolipids, called glycocalyx, which is thought have protective functions [23,24]. Another rigid cell wall polymer was found in the haloalkaliphilic archaeon *Natronococcus occultus*; the polymer consists of **glutaminylglycan** [24].

1.1.4. *Archaea* compared to the other 2 domains

As already mentioned, *Archaea* share characteristics with both, *Bacteria* and *Eukarya*. At first sight, *Archaea* resemble *Bacteria* more then *Eukarya* because of the prokaryotic character. They have similar cell sizes and lack a membrane-enclosed nucleus and organelles, and both have large circular chromosomes and plasmids. As found in *Bacteria*, archaeal genes are organized into polycistronic transcription units. Most archaeal transcriptional regulators are homologues to bacterial ones, which indicates that *Archaea* use the bacterial way to regulate transcription. Archaeal mRNAs often contain a Shine-Dalgarno binding site and *Archaea* and *Bacteria* share the same 70S ribosome structure. Another bacterial attribute found in several archaeal species is the cell division protein FtsZ. However, the core components of the transcription, translation and replication machinery show much more similarities to the eukaryal ones. In some aspects, *Archaea* seem to be a mosaic of eukaryal and bacterial features that were believed to be unique and exclusive to either *Bacteria*, and *Eukarya*, and the functions of up to 50% of genes that are exclusive for *Archaea* are unknown [12,25].

1.1.4.1. Transcription and Translation

The similarities of transcription and translation systems in *Archaea* and *Eukarya* were first recognized in the 1980s by Wolfram Zillig who studied archaeal DNA-dependent RNA polymerases (RNAP)[26]. The basal transcription machinery of *Archaea* resembles that of eukaryotes, but is much simpler. *Archaea* have one RNAP, and the subunit composition resembles that of the RNAPII of eukaryotes [27]. Transcription initiation in eukaryotes is much more complex then that of *Archaea*, but still there are some similarities: archaeal promoters contain a TATA-like element for promoter recognition - an A-T rich sequence. The TATA-box is located about 30bp upstream of the

transcriptional initiation site and like the RNAPII, the archaeal RNAP needs transcription factors for promoter recognition - the highly conserved TATA-box binding protein (TBP) and TFB, which is homolog to eukaryal TFBII [28]. For transcriptional initiation in eukaryotes, much more transcription factors are needed. The bacterial RNA polymerase contains only 5 subunits and the enzyme binds to the promoter, which has 2 conserved sequences (-10 and -35 region), with the help of sigma factors [27]. Many archaeal promoters contain the additional element BRE, which is located upstream and adjacent to the TATA-like element. It was shown that it determines promoter strength and transcription orientation in hyperthermophilic *Archaea*. It was suggested that *Halobacterium salinarum* also contains a BRE element, and moreover, *Hbt. salinarum* and *Hfx. volcanii* have multiple TFB and TBP proteins which might have a regulatory effect on gene expression [29]. Although the archaeal transcription apparatus is more of a eukaryal type, the majority of putative transcriptional regulators are homolog to activators and repressors of *Bacteria* [30], which goes well together with the fact that in *Archaea* functionally related genes are mostly organized into operons, which is typical for *Bacteria*. An example is the organization of the ribosomal operon, which arranged in the order 16S-23S-5S rDNA in *Bacteria*. *Archaea* have the same organization with a $tRNA^{Ala}$ gene inserted between the 16S and 23S genes in halophiles and methanogens [25].

Like transcription, the translation system of *Archaea* has similarities to eukaryal and to bacterial components. Initiation factors (IFs) of translation are more of the eukaryotic character. *Archaea* and *Eukarya* have more then 10 IFs whereas *Bacteria* have 3 [12]. The way archaeal ribosomes recognize the mRNA seems to be similar to *Bacteria*. Both use polycistronic mRNAs that contain the Shine-Dalgarno sequence upstream of the start codon, which is bound by the 16S rRNA of small ribosomal subunit (30S). Together with the large subunit (50S) both build the 70S ribosome of the initiation complex. Like *Bacteria*, *Archaea* usually use the start codon AUG, but also GUG and UUG exist. On the other hand, like eukaryotes, the initiator tRNA used by *Archaea* is Methionine, whereas *Bacteria* use N-formylmethionine. Also to mention is the translation of leaderless mRNAs that lack a SD sequence, and start directly with the start codon. Such leaderless mRNAs are found in *Bacteria* and *Eukarya*, and seem to be abundant in many archaeal species [12,27,28].

1.1.4.2. Replication

Like *Bacteria*, *Archaea* have a single circular chromosome. Therefore one would expect that replication of *Archaea* resembles that of *Bacteria*. Nevertheless, the proteins of the archaeal replication machinery are of a eukaryal type. *Bacteria* have a single origin of replication (*ori*C): an AT-rich DNA region containing multiple copies of the DnaA box. DnaA proteins bind to the origin and

unwind the DNA so that bidirectional replication can start [31]. Unlike bacteria, eukaryotes have multiple origins of replication (also AT rich), which are bound by the origin recognition complex (ORC) composed of 6 polypeptides: Orc1-6. The ORC recruits additional proteins to the origin, one of which is Cdc6 [31]. Like eukaryotes, *Archaea* can have multiple origins of replication. This was discovered in *Sulfolobus solfataricus* and *Sulfolobus acidocaldarius*, both have three origins of replication [32]. The origin is composed of short repetitive DNA sequences, called origin recognition boxes (ORBs). These ORBs are bound by an Orc1-Cdc6 family replication initiator protein, which has homology to both, the ORC family of eukaryotic initiator proteins, and to Cdc6. Multiple bound Orc1-Cdc6 proteins serve as a platform for the assembly of all components of the replication machinery [33].

Proteins that are involved in the elongation during archaeal replication show similarities to that of eukaryotes, excepting the DNA polymerase. Archaeal DNA polymerase PolD is mostly found in *Euryarchaeota* and not in *Eukarya*, whereas *Crenarchaeota* use a DNA polymerase of the eukaryal B-type family. Most archaeal genomes code for many variants of DNA polymerases, and if leading- and lagging strand synthesis are carried out by the same enzyme is not clear [33,34]. All other proteins of the archaeal replisome (replication elongation complex) are of eukaryal nature. The ring shaped sliding clamp for the DNA polymerase is a trimeric protein called proliferating cell nuclear antigen (PCNA), and is loaded onto the DNA by replication factor C (Rfc). PCNA encircles the DNA and prevents dissociation of the polymerase from the template. RNA primers for the synthesis of Okazaki fragments of the lagging strand are synthesized by DNA primase PriSL, a heterodimer. Archaeal and eukaryal Okazaki fragments have a length of about 100 nucleotides, whereas the bacterial ones have about 1000 nucleotides. The nuclease Fen1 and the DNA ligase Lig1 are responsible for removing the RNA primer and Okazaki fragment ligation. The minichromosome maintenance hexamer (Mcm) is a helicase that unwinds the DNA to generate a single stranded DNA template for the polymerase. Gins proteins interact with PriSL and Mcm through Gins-associated nuclease (Gan) and thereby assist to structural integrity of the replication complex. Single stranded DNA is protected by replication protein A (Rpa). Most *Crenarchaeota* contain a single stranded binding protein (Ssb) which is similar to the bacterial ones [33].

1.1.4.3. Chromatin

In eukaryotes, the chromosomal DNA is packed into the chromatin, which is composed of repeating nucleosome units. One unit consists of DNA that is wrapped around a histone protein core. This octameric histone protein core consists of two copies of the histones H2A, H2B, H3 and H4. The histones contain N- and C-terminal tails, which are sites for regulatory post-translational

modification. Prokaryotes have a single circular chromosomal DNA. Therefore, it was believed that they do not need such a complex machinery to make the DNA more compact. This is true for *Bacteria*, they have some small basic proteins that compact DNA. Surprisingly, genome sequencing has revealed that many archaeal species contain histone-like proteins that are homolog to eukaryal ones. They are common under *Euryarchaeota* but absent from *Crenarchaeota*. Archaeal histone-like proteins might build a tetrameric structure, which is similar to the eukaryotic H3/H4 tetrasome. Unlike eukaryal histones, archaeal histones lack the C- and N-terminal tails. A widespread chromatin protein under *Crenarchaeota* is Alba, which was characterized in *Sulfolobus*, and is also found in *Euryarchaeota*. In contrast to histones of *Euryarchaeota*, Alba proteins undergo post-translational modifications [12,35].

1.1.4.4. Polyploidy

Polyploid organisms contain multiple copies of the chromosome. Polyploidy is widespread under eukaryotes and found among plants, fish and amphibian. Prokaryotes are generally supposed to have a single copy of the chromosome per cell. However, some bacteria have been reported to be polyploid [36]. A well-known example is the radioresistant *Deinococcus radiodurans* with 8 copies of the chromosome [37], or *Azotobacter vinelandii* with about 80 copies [38]. Multiple copies of the genome have also been reported among the *Archaea*. For example, *Methanococcus janashii* is known to be polyploid [39], and the genome copy number of the halophiles *Halobacterium salinarum* and *Haloferax volcanii* has been determined. In exponential growth phase, *Hbt. salinarum* contains about 25 copies and in early stationary phase, polyploidy is down regulated to 15 copies of the genome. A similar scenario was found for *Hfx. volcanii*. During exponential growth 18 copies/cell were determined and 10 copies/cell at the beginning of stationary phase. It is considered that polyploidy is widespread under halophilic and haloalkaliphilic *Archaea* [36].

1.1.5. Halophilic and haloalkaliphilic *Archaea*

Hypersaline environments have salt concentrations higher compared to that of seawater with about 0.5M NaCl. Examples are saline lakes, saltern ponds and hypersaline soils; soda lakes, deep-sea brines and other habitats are characterized by high salt concentrations up to 5M NaCl. Many high-salt habitats are found in dry regions with high evaporation rates. So-called thalassohaline environments originate from evaporated seawater and have the same ionic composition of seawater where Na^+ and Cl^- are the predominant ions. Such environments have nearly neutral to slightly alkaline pH. In athalassohaline environments, the ionic composition is different to that of seawater.

One example is the Dead Sea with a high concentration of Mg^{2+} and Ca^{2+} and a low concentration of Na^{+} and a relatively low pH around 6. Even environments combining high salt with extremely high pH are home for microorganisms. Alkaline soda lakes, like Lake Magadi in Kenya have pH values of 11 and higher, and salt concentrations over 300g/L [40,41].

Microorganisms colonizing hypersaline environments are called halophiles and halotolerants. Moderate halophiles grow best in media containing 0.5 - 2.5M NaCl, whereas extreme halophiles need 2.5 - 5.2M NaCl for optimal growth and halotolerant microorganisms do not require high salt concentrations, but tolerate those [42]. Extreme halophiles adapted to the highest salt concentration are mostly found within the *Archaea*, in the class *Halobacteria*, order *Halobacteriales* within the single family the *Halobacteriaceae*. Classification is mainly based on polar lipid composition, 16S rRNA gene sequence and DNA-DNA hybridization [43], and to date 33 genera are listed (The list is based in part on *Bergey's Manual of Systematic Bacteriology*; www.the-icsp.org). These extremely halophilic, aerobic *Archaea* populate environments with saturated salt concentrations and they represent the major part of microorganisms that populate hypersaline soda lakes, the Dead Sea and saltern crystallizer ponds. Halophiles are also found among the methanogens of the *Euryarchaeota* in the family *Methanosarcinaceae* [42].

Most members of the *Halobacteriaceae* are well known for their pink or purple pigmentation. This is due to a C50 carotenoid pigments (α-bacterioruberin and derivates) in the membrane, which gives many salt lakes a red coloration, for example the hypersaline soda lake Lake Magadi in Kenya. Bacterioruberin provides UV light protection and therefore prevents DNA damages. This is an important feature, because hypersaline environments are mostly combined with strong sunlight [41,44].

1.1.5.1. Adaption to high salt concentrations - osmotic balance

Halophiles are able to withstand the osmotic pressure deriving from the high salt concentration of the environment. All halophilic microorganisms pump sodium ions out of the cytoplasm by using transport mechanisms based on Na^{+}/H^{+} antiporters and there exist different strategies to manage this osmotic stress. The so-called **"salt-in" strategy** is used by the *Halobacteriales*. They accumulate KCl in the cytoplasm to a concentration that is at least as high as the NaCl concentration of the surrounding medium. K^{+} is accumulated in the cytoplasm while Na^{+} is pumped out. As a consequence to the high KCl concentration, all enzymes and intracellular structures are adapted to the high salt environment [41,45].

Another strategy of adaption is the **"compatible-solute" strategy**. Here, Na^{+} is also extruded from the cytoplasm, and the osmotic pressure is balanced by the accumulation and/or synthesis of organic compatible solutes (zwitterionic organic molecules). Therefore the intracellular salt

concentration is low and intracellular components need no adaption to high salt concentrations. Examples for such osmotic solutes are glycerol, sucrose, trehalose, ectoine or glycine/betaine [45].

Both strategies, "salt-in" and "compatible-solute", enable the cell to reduce the water loss, to maintain cell turgor pressure by reducing the osmotic potential between the cell and the environment, and to protect enzymes from the low water activity [46]. Although members of the *Halobacteriales* use the "salt-in" strategy, an organic osmolyte (2-sulfotrehalose) has been detected together with high KCl concentrations in *Natronococcus occultus*, *Natronobacterium gregoryi*, *Natrialba magadii* and *Natronomonas pharaonis* [41].

1.1.5.2. Lipids and Membranes

The cellular membranes of extreme halophilic *Archaea* are adapted to the high salt concentrations of environments. It was demonstrated that membranes of halophilic, and also haloalkaliphilic *Archaea* have a low Na^+ and H^+ permeability [46], and the lipid composition is different to that of non-halophilic *Archaea*. Generally, the lipids base on a C20-C20 diether isoprenoid core. Phospholipids with head groups serine, inositol and ethanolamine are missing, and predominately, the membranes contain specific phosphatidyglycerol phospholipid. In particular, membranes of extreme halophilic *Archaea* contain a diacidic phospholipid - archaetidylglycerol methylphosphate (PGP-Me) that accounts 50-80% of the polar lipids in the membrane, and is an archaeal analogue of phosphatidylglycerol methylphosphate. It was demonstrated that such membranes are stable in high salt solutions whereas membranes of non-halophiles that lack PGP-Me become unstable. Therefore it is assumed that PGP-Me is significantly involved into membrane stability of extreme halophiles in hypersaline environments [47]. Furthermore, the membranes of haloalkaliphilic *Archaea* contain C20-C25 diether lipids in addition to the C20-C20 lipid core [48].

1.1.5.3. Halophilic proteins

As a consequence of the high intracellular salt concentrations due to accumulation of KCl, enzymes of extremely halophilic *Archaea* have to be adapted to stay fully stable and active. Under these high salt conditions, enzymes of mesophiles would denature immediately and lose their activities. Compared to enzymes of non-halophiles, halophilic enzymes are highly acidic. Proteins have a high content of acidic amino acids (glutamate and aspartate) whereas basic amino acids (histidine, lysine and arginine) are nearly missing. The amount of hydrophobic amino acids is low, in which amino acids with small residues (glycine, alanine and valine) dominate over amino acids with longer aliphatic residues [44,49]. Most proteins of halophiles have isoelectric points around 4.2. In the presence of 3-4M KCl or NaCl, most of the enzymes remain folded, and are fully active and stable,

although there are some exceptions [44]. One explanation on how enzymes stay stable would be that the salt in the cytoplasm has a protective effect because it shields the negative charges of the proteins. In a neutral environment, the negative charges would repel each other leading to unfolding and loss of activity. Another point is the low content of hydrophobic amino acids resulting in a low extent of hydrophobic interactions within the proteins. Therefore the high salt concentration in the cytoplasm is needed to enable and maintain hydrophobic interactions [44,50].

1.1.5.4. Haloalkaliphiles and adaption to high pH

The alkaliphilic members of the *Halobacteriaceae* require a high pH (between 8.5 and 11) in combination with high salt concentrations and very low Mg^{2+} concentrations (less than 10mM) for growth [51]. Stable highly alkaline environments in nature are so called soda lakes and soda deserts, with pH values of 10 and above, for example Lake Magadi in Kenya, Wadi Natrun in Egypt or Owens Lake in California. Such environments are nearly exclusively colonized by haloalkaliphilic *Archaea* that reach 10^7 to 10^8 per ml in these waters [52]. Soda lakes are characterized by large amounts of Na^+ (Na_2CO_3 or complexes of this salt), formed by evaporation. Additional high salt concentrations, like NaCl, form the alkaline hypersaline lakes [53].

As already mentioned, halophilic *Archaea* need to adapt all intracellular components to the high KCl concentration. Additionally, haloalkaliphilic *Archaea* have to deal with a second extreme, the high pH. Most intracellular enzymes are active at a neutral pH, so the pH of the cytoplasm needs to be maintained neutral. Internal pH was estimated by testing optimal enzyme activity of alkaliphile proteins. For example, it was demonstrated that α-galactosidase from an alkaliphile *Micrococcus* species has its optimal activity at a pH of 7.5. Nevertheless, there exist alkaline enzymes depending on a high pH value, for example the alkaline protease purified from an alkaliphilic *Bacillus* species shows optimal activity at a pH of 11.5. Many alkaline extracellular enzymes have been isolated from alkaliphilic *Bacteria* and are used for industrial applications [52].

Furthermore it was shown, that the protoplast of alkaliphilic *Bacillus* strains are unstable in alkaline environments. Therefore it was suggested that the cell wall has protective functions. Compared to *Bacillus* subtilis, the cell wall of several alkaliphilic *Bacillus* species additionally contains acidic polymers that build a kind of a negative charged matrix. It was suggested that the negative charges repulse hydroxide ions and adsorb Na^+ and H^+, and therefore contribute to growth in alkaline environments [52].

Alkaliphiles need Na^+ in the medium for growth, and it was demonstrated that Na^+ is necessary for the transport of various substrates through the membrane into the cell. Generally, energy

production is linked to the proton motive force. A proton motive force is established by excretion of H^+ and by the respiratory chain. This generates an electrochemical concentration gradient across the membrane that is finally used by the ATPase that is driven by protons. The transport of H^+ back into the cell is also coupled with co-transport of different substrates. For an alkaliphilic *Bacillus* species it was demonstrated that H^+ excretion is exchanged by Na^+ excretion. Na^+/H^+ antiporter systems pump Na^+ out of the cell combined with an influx of H^+. In this scenario, proton motive force can be called sodium motive force, and substrates are co-transported into the cell with Na^+ by Na^+ symporter [52]. These Na^+/H^+ antiporter systems in combination with ATPase-driven H^+ expulsion as well as K^+/H^+ antiporter may also contribute to maintain a low pH of about 8 on the surface of the membrane and to regulate the intracellular pH [46,52].

1.1.5.5. Extracellular proteases and proteolytical growth

Halophilic and haloalkaliphilic *Archaea* mainly obtain energy from the degradation of organic nitrogen compounds rather then from using other different carbon sources. Extracellular proteases are secreted to the surrounding medium, which enable the degradation of peptides for proteolytical growth. Extracellular proteases have been isolated from halophilic strains of *Halobacterium salinarum*, *Natrialba asiatica* and *Haloferax mediterranei*, and from the haloalkaliphiles *Natrialba magadii* and *Natronococcus occultus*. All these isolated enzymes are serine protease, and most of them depend on high salt concentrations for structural stability and are optimally active in high salt, basic pH and temperatures of 50°C and higher [54,55].

1.1.5.6. Lake Magadi - an alkaline soda lake

Lake Magadi is located in the Kenyan Rift Valley (Fig. 4), where tectonic activity leaded to the formation of closed basins with no water outflow and standing bodies of water. High evaporation rates exceed the water inflow leading to salt accumulation. The surrounding area of the lake is deficient in Ca^{2+} and Mg^{2+}, which is crucial for maintaining the alkaline pH of the lake. Evaporation leads to concentration of NaCl and HCO_3^-/CO_3^{2-} ions, which generate the alkaline pH. Significant amounts of Mg^{2+} and Ca^{2+} in the water would remove alkaline carbonates and neutralize the lake; an example is the Great Salt Lake in Utah. Much higher amounts of Mg^{2+} lead to slightly acid lakes due to reactions involving sepiolite precipitation; an example is the Dead Sea with a pH around 6. Lake Magadi has a pH of around 12, and salt concentrations of >30% (w/v) dominated by NaCl and Na_2CO_3 [53,56].

Figure 4: Soda crust of Lake Magadi in the Kenyan Rift Valley (Africa).
The pink/red color of the sea is due to carotenoid production of the haloalkaliphilic members of the *Halobacteriaceae*.
(Adapted from *Extremophiles Handbook*, 2011 [53])

Haloalkaliphilic archaeal species isolated from Lake Magadi: *Natronococcus occultus, Natronococcus amylolyticus, Natronobacterium gregoryi, Natronomonas pharaonis, Natrialba magadii* and *Halorubrum vacuolatum* [53]. Haloalkaliphilic archaeal species isolated from other soda lakes are: *Natrialba hulunbeirensis, Natrialba chahannaoensis, Natronolimnobius baerhuensis, Natronolimnobius innermongolicus, Natronorubrum bangense, Natronorubrum tibetense, Halorubrum alkaliphilum, Halorubrum luteum, Halorubrum tibetense, Halalkalicoccus tibetensis and Halobiforma nitratireducens* [53].

1.1.6. *Natrialba magadii*

Natrialba magadii is a haloalkaliphilic member of the family *Halobacteriaceae*, and was isolated from Lake Magadi in 1984 by Tindall and co-workers who initially placed *Nab. magadii* into the new genus - *Natronobacterium* [48]. Upon later sequence comparison of the 16S rRNA gene with 3 species of the genus *Natronobacterium*, *Natronobacterium magadii* was transferred to the genus *Natrialba* [51].

Nab. magadii cells are rod-shaped, 0.7-0.9 by 2-4μm in liquid media, and spherical on solid medium with 1-1.5μm in diameter. Cells are motile by polar flagella and colonies are colored orange-red, which is due to the carotenoid pigments in the membrane. Cells lyse in solution with NaCl concentrations below 1.5M. Optimal growth conditions are 3.5M NaCl and a pH of 9.5; sodium carbonate is required in the media as well as low Mg^{2+} concentrations. Optimal growth temperature are between 37-40°C. *Nab. magadii* is strict aerobe and chemoorganotroph, it grows proteolytically using peptides/amino acids as energy- and carbon source, carbohydrates are not utilized [48].

There are two strains of *Nab. magadii* available (Fig. 5). The lysogenic wild type strain called *Nab. magadii* L11 harbors the virus ϕCh1 that is integrated into the host chromosome as a so-called prophage. As the strain reaches stationary phase, lysis starts (Fig. 6). *Nab. magadii* is the only known host of ϕCh1. The wild type strain was cured from the virus by repeated sub-culturing leading to the cured strain *Nab. magadii* L13. The cured strain can be re-infected and is therefore used as an indicator strain for studying ϕCh1 [57].

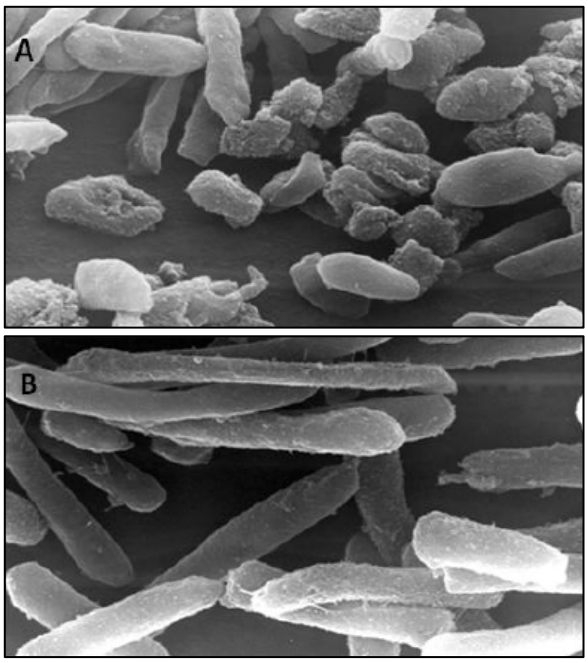

Figure 5: Electron micrographs of *Nab. magadii* L11, the wild type strain carrying the prophage **(A)** and the cured strain, *Nab. magadii* L13 **(B)**.

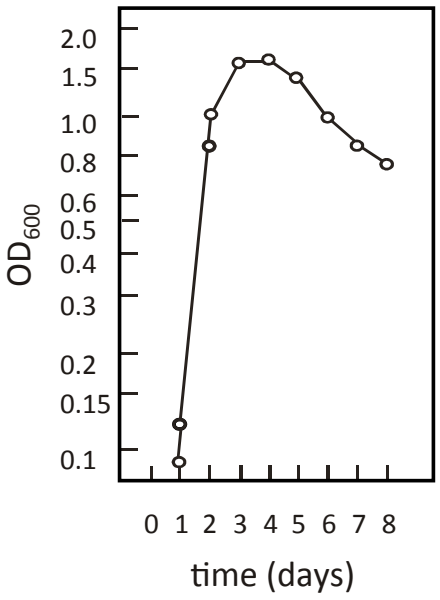

Figure 6: Growth and lysis behavior of the lysogenic wild type strain *Nab. magadii* L11. Doubling time is about 9 hours during exponential growth phase and lysis starts after 3 to 4 days.

1.1.6.1. Transformation of *Natrialba magadii*

Cline and Doolittle achieved the first efficient transformation of *Archaea* in 1986. They transfected *Halobacterium salinarum* with isolated ϕH DNA and analyzed transformation efficiency by plaque assays. The method is based on the generation of spheroblastic cells (which have lost the S-layer) by treatment with EDTA, and on PEG-mediated transfection of the ϕH DNA [58]. This method was adapted for several other archaeal species, and transformation methods for halophiles are published in the "Halohandbook", a collection of protocols for archaeal genetics [59]. This method was not successful for transformation of *Natrialba magadii* because the S-layer could not be removed by treatment with EDTA. In order to prepare spheroblasts, cells were first treated with bacitracin that inhibits

glycosylation of the S-layer, followed by incubation with proteinase K. The obtained spheroblasts were then successfully transfected with purified ϕCh1 DNA [60].

1.1.6.2. Shuttle vectors and selectable markers

After the successful transfection of *Nab. magadii* with ϕCh1 DNA, shuttle vectors were constructed that could be used for *Nab. magadii* and *E. coli*. Sequence analysis revealed that ORF53 and ORF54 of the ϕCh1 genome have similarities to the *rep*H gene. RepH is, together with an AT-rich region, required for the minimal replication origin of the plasmids of halophilic *Archaea* [61]. As selectable marker, the mutated *gyr*B gene was isolated from *Haloferax alicantei* and cloned into the pKSII+ vector, named pNov-1. As *Nab. magadii* lacks the mutated version of the *gyr*B gene, it provides resistance to novobiocin. Different parts of ORF53 and ORF54 were cloned into pNov-1, which resulted in the plasmids pRo-1 to pRo-11. The highest transformation efficiency was achieved with the vector pRo-5, which is used successfully ever since [60]. The second shuttle vector used for *Nab. magadii* is pNB102. This vector was developed from the plasmid pNB101 by inserting the ColE1 origin of replication of *E. coli* as well as antibiotic resistant genes that provide ampicillin and mevinolin resistance [62].

Mevinolin inhibits the HMG-CoA reductase of eukaryotes and halophilic *Archaea*. HMG-CoA reductase is involved in synthesis of mevalonate which is necessary for the isoprenoid lipids [63]. Novobiocin inhibits the DNA gyrase. It binds to the B subunit of DNA gyrase and blocks the ATP binding site. The mutated *gyr*B gene from *Haloferax* is not a target for novobiocin and has 3 pointmutations compared to wild type *gyr*B [64].

1.1.7. Promoters of halophilic *Archaea*

Gene expression systems that allow controlled expression of proteins by inducible and regulated promoters are nearly missing for halophilic *Archaea* [65]. Several constitutive promoters were analyzed in the studies of Gregor and Pfeifer in 2005 [29]. They compared promoter activities in *Haloferax volcanii* using the halophilic β-galactosidase *bga*H as a reporter gene. Therefore, different plasmid constructs were cloned, harboring transcriptional fusions of *bga*H with each of the analyzed promoters. One of the used promoters was that of the *fdx* gene, which is a typical housekeeping gene coding for ferredoxin in *Halobacterium salinarum*. The promoter of *fdx* (P*fdx*) is a strong and constitutive promoter [29]. Large amounts of BgaH activities were obtained from the P*fdx-bga*H fusion, especially from samples derived from exponential, as well as from stationary growth phase [29].

Due to these properties, P*fdx* of *Hbt. salinarum* was chosen to establish a vector system for overexpression of proteins in *Nab. magadii* [66]. However, very soon it turns out that this promoter is not functional in *Nab. magadii*: a construct was cloned harboring P*dfx* upstream of the ϕCh1 gene ORF34$_{52}$ lacking its own promoter; expression of gp34$_{52}$ controlled by P*dfx* was compared with gp34$_{52}$ expressed from its own promoter. Western blot analysis was performed and no differences in signal intensity for gp34$_{52}$ could be obtained [66].

Nevertheless, in order to achieve strong and controlled expression of proteins, a promoter is needed that has nearly no basal activity, and can simply be turned on and off, for example by changing growth conditions. Such a promoter was first characterized by Large *et al.* in 2007 for *Hfx. volcanii* [67]. Upon microarray analysis of *Hfx. volcanii* gene expression, the tryptophanase gene (*tna*) was identified which is strongly induced in the presence of tryptophan: upon addition of tryptophan to the culture, *tna* was the only differential regulated gene, and in the absence of tryptophan, the signal obtained for *tna* was very weak, meaning that the gene was controlled expressed [67]. The upstream region of *tna* was screened for promoter activity by using the *bga*H reporter gene. The promoter of *tna* could be isolated and by β-galactosidase assays it was demonstrated that expression is strongly induced by tryptophan [67]. This result was additionally confirmed using 2 other reporter genes (*pyr*E2, *cct*1) [67].

A gradually inducible expression system based on the *kdp* promoter (P*kdp*) was characterized by Kixmüller and Greie in 2012 [65]. Previous studies demonstrated, that the expression of the *kdpFABCQ* operon of *Hbt. salinarum* encoding the K^+ uptake system KdpFABC is regulated by K^+ concentrations in the culture medium [68]. The operon is expressed at concentrations below 20mM K^+ and expression increases with concentrations below 250 μM. Highest expression was detected at a concentration of 20μM K^+. Subsequently, the inducible expression vector pKIX harboring P*dkp* was constructed [65]. In order to verify if controlled expression can be achieved, *bga*H was cloned under the control of P*dkp*. The deletion strain *Hbt. salinarum* R1 (ΔkdpFABCQ) was transformed with the plasmid pKIX_*bga*H and the culture was exposed to different K^+ concentrations (3mM, 5mM and 100mM KCl). Expression of *bga*H was monitored by real time PCR. Highest expression was detected for the culture induced with 3mM KCl: due to K^+ depletion, *bga*H expression started to increase in the early exponential growth phase with a maximum in the early stationary phase. Compared to the un-induced culture, a 50-fold *bga*H over-expression was obtained [65].

The *tna* promoter of *Hfx. volcanii* and the *kdp* promoter of *Hbt. salinarum* are both inducible promoters that allow controlled expression. Since the *fdx* promoter of *Hbt. salinarum* was not functional in *Nab. magadii* [66], the search for an alternative promoter was continued and finally successful. Beatrix Alte established the tryptophanase inducible promoter of *Nab. magadii* in 2011

[69]: the genome was screened for homologs of the tryptophanase of *Hfx. volcanii*, leading to identification of the tryptophanase gene (*tna*A) of *Nab. magadii*. The upstream region was screened and promoter activity upon addition of different concentrations of tryptophan was quantified by using the halophilic *bga*H as a reporter gene. *Bga*H was cloned under control of the promoter of the *tna*A gene (p*tna*N). β-galactosidase assays were performed and it could be demonstrated that expression of *bga*H is induced by simply adding tryptophan to the medium [69].

1.2. Viruses of *Archaea*

1.2.1. From bacterial viruses to viruses infecting *Archaea* - An overview

Bacterial viruses were discovered 1915 by Frederick Twork, but unfortunately his work was not continued. Extensive scientific work on bacteriophages started 1917, when Felix D'Herelle isolated 'invisible microbes' of the Shiga bacillus from patients. He observed lysis of liquid bacterial cultures and clear areas on bacterial lawns on which the culture is non-existent and therefore supposed to be colonies of the invisible microbes [70]. D'Herelle called the invisible microbe bacteriophage, by using the term "phage" in sense of "developing at the expense of", which supported the idea of viruses being parasitizing particles [71,72]. Throughout history there was an ongoing debate on the definition of viruses. They were described as ultra-microscopic microbes, soluble molecules, toxins or enzymes that stimulate their own production [72]. 1935 Stanley was able to crystallize the tobacco mosaic virus showing that the obtained crystals retain their infectivity with the conclusion that viruses are chemical objects and no cellular organisms [73]. Nowadays viruses can be defined as obligate intracellular parasites made up of nucleic acid, proteins and sometimes lipids. They have no system for energy production and protein synthesis; therefore viruses depend on cellular mechanisms for reproduction. Viral genomes code, for example, for capsid (protective protein shell that harbors the viral genome) components, proteins for virus-host interaction or proteins for replication. Unlike cells, viruses do not reproduce by division, they are assembled from pre-formed components [74].

The vast majority (95%) of all reported bacteriophages belong to the order *Caudovirales* with the 3 families *Myoviridae*, *Siphoviridae* and *Podoviridae.* These phages carry a dsDNA genome and have a head-tail morphology: icosahedral heads containing the genome, and contractile or non-contractile tails with tail fibers attached, mediating host cell attachment and injection of the viral genome into the cell. Viewing the life cycles, bacteriophages can be either temperate or lytic. Generally, during a

lytic life cycle immediately after infection the viral genome replication and virion production starts ending up with lysis of the host cell and virus release. Temperate viruses are able to enter a lysogenic state after infection, meaning that a virus is able to co-exist with the host as a prophage while most of the viral genes are not expressed. The genome can integrate into the host chromosome or exist as a plasmid in the cytoplasm. In both cases, the prophage replicates in step with the host. Under certain conditions the lytic pathway is triggered, finally leading to virion release and lysis of the host cell [75].

The first archaeal virus, ϕH, was discovered 1974 and infects the archaeon *Halobacterium salinarum* [76]. As *Archaea* were not discovered at that time, this virus was described as a bacteriophage resembling members of the *Myoviridae*, having the typical head-tail morphology [77]. After *Archaea* were discovered as the third domain of life a couple more archaeal viruses resembling bacteriophages were reported all infecting members of the *Euryarchaeota.* Therefore it was believed that *Archaea* are mainly associated with viruses having this head-tail morphology [77]. However, subsequently numerous viruses were discovered with unique morphotypes not found among viruses of *Bacteria* or *Eukarya,* and it turns out that only a small part of archaeal viruses resembles bacteriophages. Such viruses with very unusual shapes are found among the hyperthermophilic *Crenarchaeota.* There is a huge morphological diversity of crenarchaeal viruses and moreover, most of the viral genes have no homologues in databases, they are unrelated to any other known viruses [78]. To date, all isolated archaeal viruses carry a dsDNA genome with one exception, *Haloracula hispanica* pleomorphic virus 1 (HRPV1), having a ssDNA genome [79].

The appearance of *Caudovirales* among the *Euryarchaeota* raises the reoccurring question about the origin of viruses. Earlier it was believed that viruses already existed before *Bacteria* and *Archaea* diverged. This view changed since archaeal *Caudovirales* are known to carry a high percentage of bacterial genes. It seems more likely that they entered *Archaea* by interdomain spreading, meaning archaeal *Caudovirales* might originate from *Bacteria* [77].

1.2.2. Viruses of the *Euryarchaeota*

As mentioned before, most known viruses of the *Euryarchaeota* resemble bacteriophages with the head-tail morphology. They infect extreme halophiles or methanogens that are mesophilic or moderately thermophilic, and belong to the bacteriophage families *Myoviridae* and *Siphoviridae*. Examples are ϕCh1 or ϕH. Viruses with other morphotypes, like the spherical virus SH1, or the spindle-shaped viruses His1 and His2, constitute only a small part of euryarchaeal viruses. Virus can

be either temperate or lytic. Not only the morphotype of bacteriophages and most viruses of the *Euryarchaeota* is similar, they also have homologous genes encoding for example proteins involved in capsid formation and virion assembly. The best characterized viruses are ϕH and the related virus ϕCh1, HF1 and HF2 all infecting Haloarchaea, and the siphovirus ΨM1 infecting *Methanothermobacter* [77,78,80].

1.2.3. Viruses of the *Crenarchaeota*

In contrast to viruses of the *Euryarchaeota*, most genes of crenarchaeal viruses have no homologs in databases. The vast majority of these viruses show exceptional morphotypes not found among bacterial or eukaryal viruses. There is a huge diversity of possible virion shapes, especially among viruses infecting the hyperthermophilic *Crenarchaeota*. Examples are the spindle-shaped virion of SSV1 (Fig. 7a), the bottle-shaped virion of ABV (Fig. 7c), or the two-tailed virion of ATV (Fig. 7b) with the unique feature that it develops the 2 tails independent and outside of the host cell [81]. Another example is the droplet virion structure of the *Guttaviridae* (Fig. 7d). Also to mention are the linear viruses of the *Lipothrixviridae* family showing a wide diversity in their terminal structures, which could be, for example claws [77,78,80].

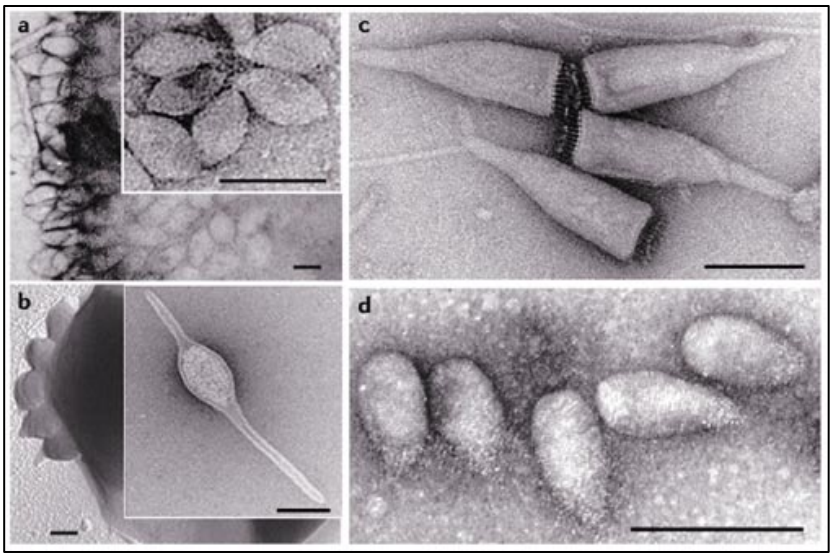

Figure 7: Electron micrographs of crenarchaeal viruses with unique morphotypes
a *Sulfolobus* spindle-shaped virus 1 (SSV1) **b** *Acidianus* two-tailed virus (ATV) and its extrusion from the host cell **c** *Acidianus* bottle-shaped viurs (ABV) **d** *Sulfolobus neozealandicus* droplet-shapedvirus (SNDV)
(Adapted from Prangishvilli *et al.*, 2006; Nature Reviews|Microbiology [77])

Also shown for various crenarchaeal viruses is the stable relationship with their host. This virus-host relationship is often referred to as the 'carrier state' meaning that virions are actively produced without lysing the host cell. However, only a few viruses have been reported to be purely lytic, for example *Sulfolobus* turreted icosahedral virus (STIV) [78,80]. Another unique feature shown for the 2 viruses STIV and *Sulfolobus islandicus* rod-shaped virus 2 (SIRV2), is their mechanism of virion release. They produce unique pyramidal lysis structures on the cell surface before lysis. These pyramids point outwards and open so that virions are released, leading to lysis of the cell [82–84].

Finally it has to be mentioned that only little is known about viruses infecting *Archaea*. Considering all these extraordinary characteristics ranging from the unique morphotypes of crenarchaeal viruses to the ATV tail development independent from a host cell, over to unique viral release mechanisms of STIV and SIRV2, it becomes quite clear that much more can be discovered.

1.2.4. Haloarchaeal viruses

Halorachaeal viruses infect halophilic *Archaea* living in hypersaline waters with extreme salt concentration close to saturation, or saturation. Members of the family *Halobacteriaceae* are dominant in such environments [85]. As mentioned before, the first archaeal virus, ϕH, was discovered in 1974 and infects the archaeon *Halobacterium salinarum* [76]. To date about 20 haloviruses have been isolated, most of them having the typical head and tail morphology with lysogenic or lytic life cycles. Examples are the viruses ϕH (Fig. 8a), ϕCh1 infecting *Natrialba magadii* or HF1 and HF2 (Fig. 8b) able to infect a wide range of Haloarchaea, including *Haloferax*, *Halobacterium*, *Haloarcula*, *Natrialba* and *Halorubrum.* HF1 and HF2 were the first haloviruses reported to be lytic. In 1993 they were isolated from the same lake and have identical virion morphology and genome sizes (about 77kb) which is 80% the same, however, they have a completely separate host range [85,86]. Despite the view that most haloviruses have a head-morphology, culture-independent analysis of hypersaline environments revealed a different picture. Direct electron microscopic analysis of such samples showed that the majority of found particles are non-tailed and spindle-shaped [87,88]. Isolated examples are His1 and His2 (Fig. 8c) or the spherical virus SH1 (Fig. 8d).

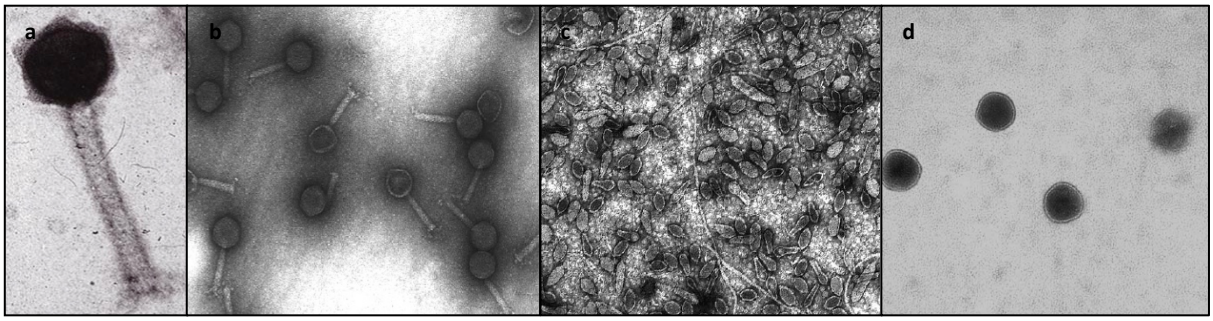

Figure 8: Electron micrographs of halovirues a ϕH [77] **b** the head-tail viurs HF2 **c** spindle-shaped virus His2, infecting species of *Haloarcula* **d** the spherical virus SH1 (Spherical halovirus 1) infecting species of *Haloarcula*, *Haloferax* and *Halorbrum* (Adepted from Dyall-Smith *et al.*, 2003 [86])

Among haloviruses, ϕH infecting *Halobacterium salinarum* is one of the best studied and the nearest relative to ϕCh1. As already mentioned the virus has a head-tail morphology with an icosahedral head and a contractile tail. It resembles bacteriophage P1 in morphology, replication and control of lysogeny [86]. For stability and infectivity, the virus depends on high salt concentration up to 3 M KCl or NaCl. ϕH is a temperate virus with a 59kb linear dsDNA genome and the prophage exists as a plasmid in the cytoplasm of the host cell. The linear genome is terminally redundant and partially circularly permuted. Six virus variants have been described. These variations are due to several insertions, a deletion and an inversion. Only 2 variants have two copies of the insertion element ISH1.8 in inverted orientation leading to inversion of an enclosed DNA segment, called the 'L - segment'. All other variants have only one copy of ISH1.8 and it also occurs in the host genome. The L-segment can also circularize to form a plasmid of 12kb called pϕHL that was isolated from the strain *H. salinarum* R_1-L. This strain has lost the ϕH DNA and is immune against infection [89,90].

1.2.5. ϕCh1

ϕCh1 was isolated in 1997 from the haloalkaliphilic archaeon *Natrialba magadii* upon spontaneously lysis [57]. It is the first and only virus reported to infect a member of haloalkaliphilic *Archaea*. The virus carries a linear dsDNA genome with a size of 58.498 bp and several RNA species, packed in the virus head. The morphology of ϕCh1 (Fig. 9) resembles that of other members of the *Myoviridae* infecting species of *Haloarchaea*, and as already mentioned, it's closest relative is ϕH [76]. All together the virus has a length of about 200nm - the icosahedral head carrying the genome has a length of 70nm, and the contractible tail is about 130nm long (Fig. 9).

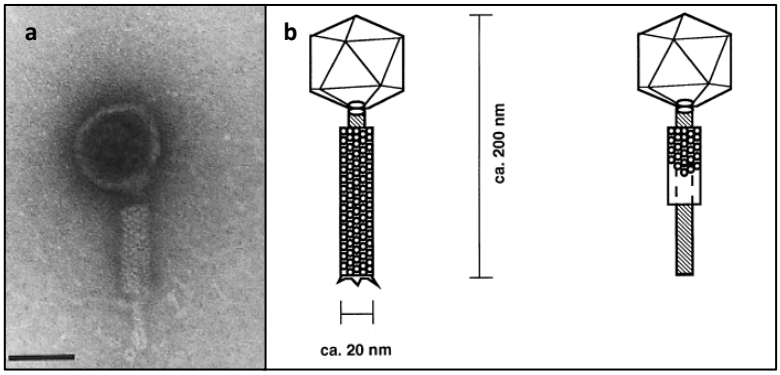

Figure 9: a Electron micrograph of ϕCh1 shows the typical morphology of members of the *myoviridae:* an icosahedral head and a contractile tail. The bar represents 50nm. **b Schematic drawing of the particle** structure shows the contracted and not contracted tail.
(Witte *et al.*, 1997 [57])

1.2.5.1. General characteristics

Since viruses infecting extremophiles are adapted to the environments of their host and are moreover only stable under these conditions, stability and infectivity of ϕCh1 were tested showing that concentrations below 2 M NaCl lead to a loss of infectivity. Accordingly the virus adapted to the high saline environment of the host *Nab. magadii*. The protein composition of the particle was determined by SDS-PAGE analysis. 4 major (proteins A, E, H and I) and five minor (proteins B, C, D, F and H) components were identified with sizes ranging from 15 - 80 kDa having low isoelectric points between pH 3.3 and pH 5.2, which is typical for halophilic proteins [57].

ϕCh1 is a temperate virus. The viral DNA integrates into the chromosome of *Nab. magadii* where the virus exists as a prophage that was confirmed by hybridization experiments using phage specific DNA probes. This is in contrast to ϕH, the viral DNA does not integrate into the chromosome but exists as an episomal prophage [89,90]. Growth analysis of *Nab. magadii* wild type strain shows that lysis starts when the culture reaches stationary phase, indicating a growth phase dependent lysis behavior. From the moment the optical density decreased (after 3 to 4 days), the number of virus particles in the medium increased. Attempts to infect other haloalkaliphilic *Archaea* then *Nab. magadii* with ϕCh1 failed [57].

It was shown that the ϕCh1 particle contains RNA, which is rather unusual for viruses. Several RNA species (80 - 700 nucleotides) were obtained from purified virus particles. They were mainly host derived, but also virus specific RNAs were detected [57]. The function of these RNAs is still unknown but they might be involved in DNA packaging as it was shown for the bacteriophage ϕ29 infecting *Bacillus subtilis*. The small RNA encoded by this phage plays an essential role during this packaging process [91,92].

Restriction analysis revealed that the ϕCh1 genome is partially dam-like methylated within 5'-GATC-3' and related sequences. Generally, a *dam* methylase (DNA adenine methylase) transfers methyl groups to the N6 position of adenine residues [93,94]. As the chromosomal DNA of *Nab. magadii* is not dam methylated, [95] it was considered that ϕCh1 codes for its own methylase. Genetic analysis led to

the identification of the *mtase* gene, with the gene product M.ϕCh1-I. The protein was heterologously expressed in *E. coli* in order to test the functional activity, and surprisingly expression resulted in an active protein that specifically methylated within 5'-GATC-3' sequences [57,96].

The gene coding for the major capsid protein of ϕCh1 could be identified and it was shown that it is processed during virus maturation. A proteolytical cleavage results in the protein E of the major viral capsid. Moreover, the sequence of the major capsid proteins revealed a 80% similarity to the capsid protein HP32 of ϕH [97].

1.2.5.2. Organization of the genome and sequence features

The genome sequence of ϕCh1 was published in 2002 [98]. It has a size of 58.498 bp and 98 open reading frames (ORFs) were predicted to be protein-coding genes starting with ATG, except four ORFs starting with GTG. Most ORFs are arranged in the same direction suggesting the formation of transcriptional units (Fig. 10). The linear genome is organized into three regions: The 5' region as well as the 3' region comprises rightward-transcribed genes (ORF1-34 and ORF56-98) whereas the middle part of the genome comprises transcription in both directions (ORF45-55). Organization and putative functions of ORFs are presented in Figure 10. Such a modular organization of the genome in functional genetic modules and conserved gene orders is typical for numerous head-tail dsDNA bacteriophages. The formation of neighboring genes with related functions in transcriptional units allows optimal timing of gene expression. Such genomes are usually organized in early, middle and late genes.

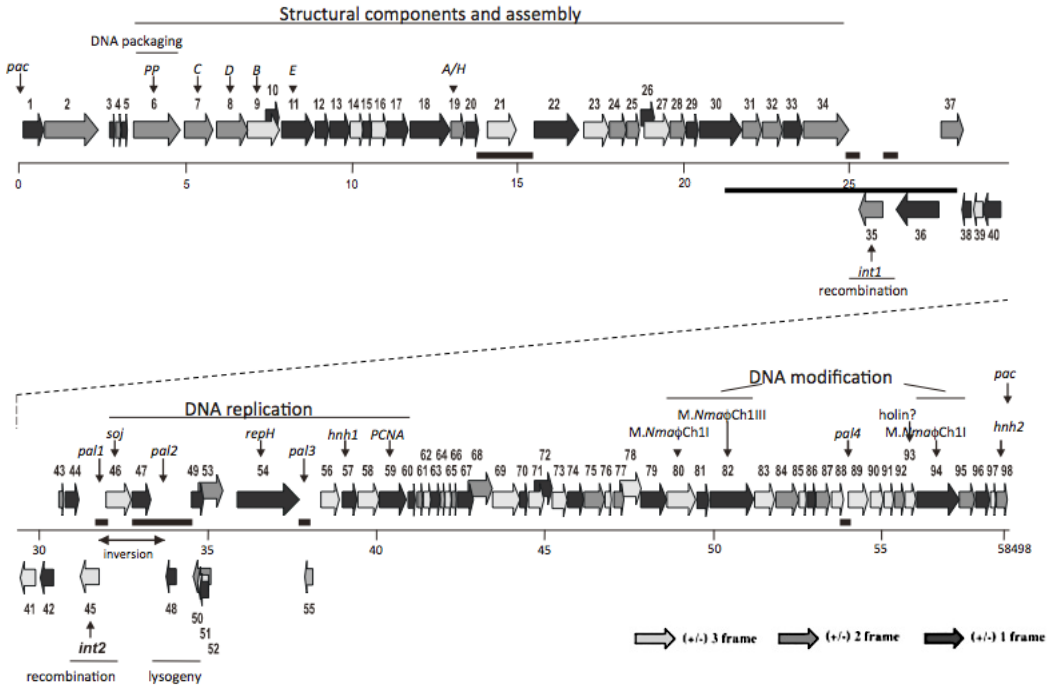

Figure 10 Organization of the linear ϕCh1 genome, and putative and verified functions of ORFs.
ORFs are represented by bars, which indicate the reading frame. The left part of the genome comprises genes coding for structural components and proteins involved in virion assembly. Most genes of the right part have unknown function excepting genes coding for DNA modification like the *mtase* gene. Genes involved in DNA replication, plasmid stabilization and regulation of gene expression are located in the middle part. (Klein *et al.*, 2002 [99])

The ϕCh1 DNA is terminally redundant and circularly permuted and therefore appears to be packaged by the so-called headful mechanism [98], which is also true for ϕH and other bacteriophages. Restriction analysis suggested the plasmid state during the reproduction cycle, which is also supported by the identification of homologs to proteins involved in plasmid regulation and stabilization. Using public databases to search for sequence similarities, 17 gene products were found that are similar to proteins with known functions and 31 were similar to hypothetical proteins of unknown functions. The majority of these ORFs with unknown function show only similarities to ϕH. Only part of the ϕH genome is sequenced [99]. The sequenced L-segment was used to find similarities with the central part of the ϕCh1 genome. The majority of the two compared genomic regions turned out to be remarkable similar. The relation between these two viruses is surprisingly since their hosts are adapted to two different environments. Halophilic *Halobacterium salinarum* populates habitats with neutral pH whereas *Natrialba magadii* depends on high pH [98].

The ϕCh1 genome does not harbor a virus-encoded DNA polymerase but interestingly a homolog to the eukaryal and archaeal PCNA proteins could be identified, which serve as a docking platform for proteins involved in replication and repair [98]. Two site-specific recombinases of the λ integrase (*int*)

type could be identified in the genome: ORF35 (*int1*) and ORF45 (*int2*). *Int1* is flanked by ORF34 and ORF36. These 2 ORFs contain several direct repeats of 30bp length, and are orientated in an inverted direction. Int1 is involved in the inversion of the two flanking ORFs with the consequence that the C-terminal parts of the structural proteins encoded by ORF34 and 36 are exchanged leading to different gene products. One inverted gene product of ORF34 termed $gp34_{52}$ is supposed to be the tail fiber protein of ϕCh1 responsible for attachment to the host cell [98,100].

1.2.5.3. Gene regulation of lysogenic state and the lytic life cycle

As mentioned before, ϕCh1 is a temperate virus that integrates into the chromosome of *Nab. magadii* and rests there as a so-called prophage until the lytic life cycle is triggered. Apparently temperate viruses need a control system to enter, and hold the lysogenic state and to switch to the lytic life cycle. Many bacteriophages regulate lysogenic and lytic life cycle with transcriptional repressors. Such a regulation is best described for the bacteriophage λ. The repressor proteins Cro and CI are crucial for the decision between lysogenic or lytic cycle. The two corresponding genes are organized head to head and are transcribed leftwards and rightwards. The operator region (O_R) in between contains 3 repressor binding sites (O_{R1}, O_{R2}, O_{R3}) as well as the promoters of cI (P_{RM}) and cro (P_R). This overlap of repressor- and RNA polymerase binding sites allows decision between lysogenic and lytic life cycle and stabilization of the respective state. Cro and CI bind to the 3 binding sites within the operator with different affinity order. Lysogeny is maintained by transcription of cI only. CI regulates and controls its own expression and inhibits transcription of Cro and early lytic genes by blocking the promoter P_R and the second promoter P_L. On the other hand, Cro is crucial for the lytic life cycle. It blocks the promoter P_{RM} and thereby it prevents expression of CI [101–103].

The close relative of ϕCh1, ϕH, shows a similar regulation strategy of lysogenic state and lytic life cycle. The proteins Rep and T4 are involved in regulation. The two respective genes are organized head to head similar to *cro* and *cI* of bacteriophage λ. The repressor, Rep, is transcribed during lysogeny and blocks transcription of the early lytic genes from the promoter for T4. T4 is produced during the lytic life cycle and seems to block transcription of Rep [104]. Rep contains a helix-turn-helix motif for DNA binding, which is typical for most repressors of bacteriophages [105].

Two putative repressor molecules could be identified in the ϕCh1 genome: ORF48 (*rep*) and ORF49 are arranged head to head with an intergenic region (Fig. 11B) containing promoter consensus sequences that are also found under halophilic *Archaea* [106].

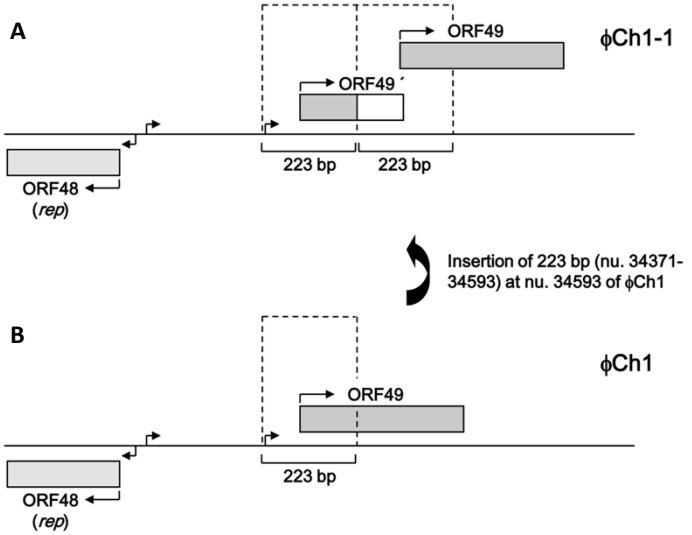

Figure 11: Organization of the lysogenic region of ϕCh1.
A shows the schematic representation of the 223bp insertion resulting in the additional ORF49' of ϕCh1-1. **B** represents the lysogenic region of the wild type ϕCh1. ORF48 and ORF49 are orientated head to head flanking the intergenic region, which has promoter function.

The gene product of ORF48, Rep, contains an amino acid pair Ala^{73}-Gly^{74} in the C-terminus, which is conserved among repressors of numerous bacteriophages. Rep has similarities to the repressor of ϕH but predicted structural features indicate that the Rep has no helix-turn-helix motif [98]. In the lysogenic strain *Nab. magadii* L11, *rep* is expressed during the lysogenic and the lytic life cycle (Fig. 12) whereas most known repressors of other temperate viruses are only expressed during lysogeny. Therefore Rep seems not to be the protein holding the lysogenic state [106].

Another ORF was identified as a putative repressor molecule - ORF49. Like Rep, the gene product of ORF49 lacks a helix-turn-helix motif. Its putative regulatory function was revealed when a mutant virus, called ϕCh1-1, was isolated from the lysogenic strain L11-1. The strain showed a different lysis behavior compared to the wild type (Fig. 13). An earlier onset of lysis could be observed and ϕCh1-1 produces larger plaques compared to the wild type virus. Sequence analysis revealed a duplication of 223bp comprising a part of ORF49 resulting in a new ORF called ORF49' (Fig. 11A). After passaging of the strain L11-1 the insertion was lost and the wild type situation regained, indicating that ORF49 has a regulatory function during virus development. Expression of ORF49 in the wild type strain L11 is delayed compared to the expression of ORF48. Transcription was first detected 32h after infection (Fig. 12) and increases over the time of particle development [106].

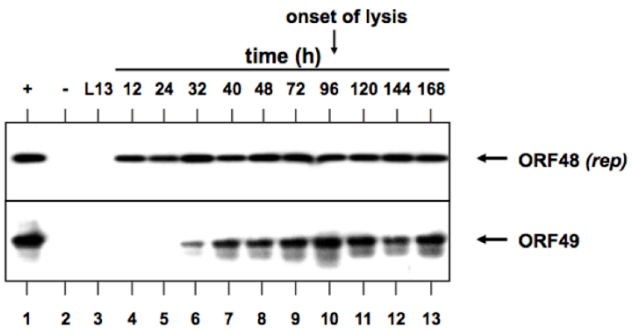

Figure 12: Transcriptional analysis of ORF48 and ORF49 by RT-PCR. ORF48 seems to be expressed constitutively during lysogenic state and lytic life cycle. ORF49 expression starts 32 hours after infection and increases over the time.
(Iro et al. 2007 [106])

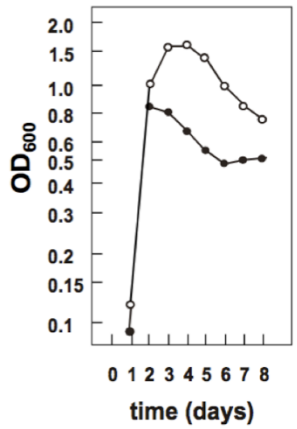

Figure 13: Growth curve analysis of *Nab. magadii* L11-1. Compared to the wild type strain L11 (o) the mutant strain L11-1 shows an earlier onset of lysis. (Iro et al. 2007 [102])

Furthermore the influence of ORF49 on infectivity of ϕCh1 was tested by phage titer analysis. A *Nab. magadii* L13 strain carrying a plasmid expressing ORF49 was infected with ϕCh1. Expression of ORF49 leads to a reduced infectivity of the virus indicating repressor activity. Moreover it was tested if gp49 is able to bind to ϕCh1 DNA by EMSA, actually gp49 binds to DNA but rather unspecific [107].

As mentioned before, the intergenic region of ORF48 and ORF49 contains promoter consensus sequences typical for halophilic *Archaea*. To analyze this region, *Haloferax volcanii* was used to perform BgaH assays, where expression of the *bgaH* gene from the intergenic region was determined. It was demonstrated that the region actually has promoter function, and that Rep alone is able to repress transcription from this region: Rep blocks transcription from the ORF49 promoter, which indicates that ORF48 acts as a transcriptional repressor [106].

ORF48 and ORF49 do not belong to the class of helix-turn-helix proteins, which raises the question on how these proteins do bind to the DNA. It is possible that these proteins have other domains that allow binding under high salt conditions. Another possibility is the action of enhancing elements that facilitate DNA binding. Two ORFs could be identified as putative co-operative elements. ORF43-44 show high identities to the co-operative element of the ϕH repressor - the transcripts T9/T10 [106].

2. Material and Methods

2.1. Material

2.1.1. Bacterial and Archaeal strains

E.coli	**Genotype**	**Source**
XL1-Blue	*endA1, gyrA96, hsdR17* ($r_{k-}m_{K+}$), *lac, recA1, relA1, supE44, thi,* (F´, *lacI*^{q}, *lacZ*Dlac*, proAB*$^{+}$*, tet*)	Novagen
Rosetta(DE3)pLysS	F^{-}*ompT hsdS*$_{B}$(R_B^- m_B^-) *gal dcm λ(DE3 [lacI lacUV5-T7 gene 1 ind1 sam7 nin5])* pLysS RARE *(Cam*^{R}*)*	Novagen

Archaea	**Characteristics**	**Source**
Nab. magadii L11	wild type strain; integrated provirus ϕCh1	Witte et al., 1997
Nab. magadii L13	cured strain; ϕCh1 not integrated	Witte et al., 1997
Nab. magadii L13Δ*tna*A	tryptophanase deletion mutant	this thesis

2.1.2. Media

1L LB medium for *E. coli*

Peptone	10 g
Yeast Extract	5 g
NaCl	5 g

pH 7,0

add dH_2O to a final volume of 1L, add 15g agar/1L for agar plates, autoclave;

1L NVM$^+$ rich medium for haloalkaliphilic *Archaea*

Casamino acids	8.8 g
Yeast extract	11.7 g
Tri-Na citrate	0.8 g
KCl	2.35 g
NaCl	235 g

pH 9 to 9,5, add dH_2O to a volume of 935ml, 8g agar/1L for plates, 4g agar/1L for softagar, autoclave;

After autoclaving, 1L medium or agar is complemented with:

0,57 M Na_2CO_3 (dissolved in steriledH_2O) 63 ml
1 M $MgSO_4$ (dissolved in sterile dH_2O) 1 ml
20 mM $FeSO_4$ (dissolved in steriledH_2O) 1 ml

1L NMMb$^+$ mineral medium for *Natrialba magadii*

NaCl	205 g	3,5 M
KCl	2 g	27 mM
Na_2HPO_4	0.28 g	2 mM
NaH_2PO_4	0.28 g	2 mM
Alanin	2.23 g	25 mM
Leucin	0.66 g	5 mM
Arginin	0.81 g	5 mM
Histidin	0.778 g	5 mM
Lysin	0.731 g	5 mM
Tri-Natriumcitrat	0.8 g	2,7 mM
Natriumacetat	1.66 g	20 mM
Natriumpyruvat	1.1 g	10 mM

pH 9 to 9,5, add dH_2O to a volume of 900ml, 8g agar/1L for plates, 4g agar/1L for softagar, autoclave;

After autoclaving, 1L medium or agar is complemented with:

1.75 M Na_2CO_3 (dissolved in sterile dH_2O)	100 ml
1 M $MgSO_4$ (dissolved in sterile dH_2O)	1 ml
20 mM $FeSO_4$ (dissolved in sterile dH_2O)	250 µl
1000x trace elements	1 ml

1000x trace elements 100ml:

$MnCl_3$ 93 mg (4 mM)
$CaCl_2$ 44 mg (3 mM)
$CuSO_4$ 64 mg (4 mM)
$ZnSO_4$ 86 mg (3 mM)
add dH_2O to a volume of 100 ml

2.1.3. Antibiotics and other additives

2.1.3.1. *E.coli*

Compound	Stock concentration	Final concentration	Preparation and storage
Ampicillin	20mg/ml	100µg/ml	powder dissolved in ddH_2O, filtered, stored at 4°C
Tetracylin	10mg/ml	10µg/ml	powder dissolved in half volume ddH_2O half volume 96%EtOH, stored at -20°C, light protection
Chloramphenicol	40mg/ml	20µg/ml	powder dissolved in 96%EtOH, stored at -20°C
IPTG	1M	0.5-1mM	powder dissolved in ddH_2O, filtered, stored at -20°C

2.1.3.2. *Natrialba magadii*

Compound	Stock concentration	Final concentration	Preparation and storage
Novobiocin	3mg/ml	3µg/ml	powder dissolved in ddH_2O, filtered, stored at 4°C
Mevinolin	10mg/ml	7.5µg/ml	prepared from tablets *), dissolved in 96% EtOH, stored at -20°C, light protection
Tryptophan	0.6M	2mM	powder dissolved in 1M NaOH, aliquotes stored at -20°C, light protection

*) 6 tablets (20mg each) get powdered and dissolved in 12ml 96% EtOH (15-20min gently stirring, on a magnetic stirrer), spin down 15min at 4°C and collect the supernatant (10mg/ml).

2.1.4. Restriction Enzymes, DNA-Polymerases and other DNA-modifying Enzymes

Restriction Enzymes	Thermo, NEB	Enzymes are supplied with the suitable reaction buffers. Single and double digests were performed according to the manufactures protocols.

Pwo-DNA polymerase	PeqLab	• purified from *Pyrococcus woesei* • 3'-5' exonuclease activity (proofreading function) • used in cloning
Pfu-DNA polymerase	Promega	• purified from *Pyrococcus furiosus* • 3'-5' exonuclease activity (proofreading function) • used in cloning
GoTaq® -DNA polymerase	Promega	• purified from *Thermus aquaticus* • no proofreading function • used for analytic PCRs

Klenow fragment, exo-	Thermo	• large fragment of DNA Polymerase I from *E. coli* • 5'-3' polymerase activity • no 3'-5' / 5'-3' exonuclease activity • used for blunting of DNA by fill-in 5' overhangs(cloning)
T4-DNA ligase	Promega	• active in the supplied reaction buffer • used for ligation of blunt end DNA fragments as well as DNA fragments with overhangs (cloning)
Fast Alkaline Phosphatase	Thermo	• used for removal of 5' phosphate groups from linear DNA (cloning)

2.1.5. Marker

2.1.5.1. DNA ladders

Ladder	Description
λ/*Bst*EII	λDNA (Thermo) digested with *Bst*EII (Thermo) Fragments (bp): 8454, 7242, 6369, 5687, 4822, 4324, 3675, 2323, 1929, 1371, 1264, 702
pUC19/*Bsu*RI(*Hae*III)	Plasmid digested with *Hae*III (Thermo) Fragments (bp): 174, 257, 298, 434, 458, 587
pUC19/*Hpa*II	Plasmid digested with *Hpa*II (Thermo) Fragments (bp): 501, 489, 404, 331, 242, 190, 147, 111, 110, 67, 34
1kb DNA ladder (Thermo #SM0311)	size range: 250 to 10.000bp
2-Log DNA ladder biotinylated(NEB)	size range: 100 to 10.000bp

2.1.5.2. Protein ladders

Description	Remarks
Unstained protein marker (Thermo #26610)	standard bands: 14.4, 18.4,25.0, 35.0, 45.0, 66.2, 116.0 kDa
Prestained protein marker (Thermo #26616)	size range: 10, 15, 25, 35, 40, 55, 70, 100, 130, 170 kDa

2.1.6. Buffers and Solutions

2.1.6.1. DNA gel electrophoresis

50X TAE

2M	Tris-HCl pH 8.2
1M	Acetic Acid
0.1M	EDTA

10X TBE

108g	Tris base
55g	Boric acid
0,5M	EDTA

pH 8
adjust pH with boric acid

0.8 - 1.5% Agarose gel

Agarose melted in 1X TAE

30% Acrylamide

29%	Acrylamide
1%	N,N'-methylenebisacrylamide

5X DNA loading dye

50mM	Tris-HCl pH 8.2
0,1%	SDS
0,05%	Bromphenol blue
0,05%	Xylene Cyanol

autoclave, and add:

25%	Sucrose (sterile filtered)

6% Acrylamide gel

30% AA	1.2ml
1X TBE	4.8ml
10% APS	100µl
TEMED	10µl

PAA Gel elution buffer

10mM	EDTA
10mM	$MgAc.4H_2O$
0.5M	NH_4OAc

2.1.6.2. SDS PAGE and Western blot

1M Sodium phosphate buffer pH 6.8

1M Na_2HPO_4	46.3ml
1M NaH_2PO_4	53.7ml
	100ml

Separating gel buffer

1.5 M	Tris-HCl pH 8.8
0.4 %	SDS

ad 250 ml ddH_20

2X Laemmli sample buffer

0.12mM	Tris-HCl pH 6.8
4%	SDS
17.4%	Glycerol
2%	β-mercaptoethanol
0.02%	Bromphenol blue

Stacking gel buffer

0.5 M	Tris-HCl pH 6.8
0.4 %	SDS

ad 250 ml ddH_20

10X SDS Running buffer

0.25M	Tris-base
1.92M	Glycin
1%	SDS

30% Acrylamide

29%	Acrylamide
1%	N,N'-methylenebisacrylamide

Coomassie staining solution

25%	Methanol
10%	Acetic acid
0.15%	Coomassie Brilliant Blue R-250

Coomassie destaining solution

10% Acetic acid

10X TBS

0.25M	Tris-HCl pH8
1.37M	NaCl
27mM	KCl

Transblot buffer

48mM	Tris-base
39mM	Glycine
0.037%	SDS
20%	Methanol

Ponceau-S Staining solution

0.5%	Ponceau-S
3%	TCA

Blocking solution

5% milkpowder in 1X TBS

2.1.6.3. Antibodies

Primary Antibodies

- Penta His Antibody from mouse (QIAGEN)
- RGS His Antibody from mouse (QIAGEN)
- α-E from rabbit (Protein E of ϕCh1, Greineder, s. a.)
- α-34 from rabbit (gp34 of ϕCh1, Till, 2011)

Secondary Antibodies

- ECL mouse IgG, horse raddish peroxidase linked (GE Healthcare Life Science)
- ECL rabbit IgG, horse raddish peroxidase linked (GE Healthcare Life Science)

2.1.6.4. Protein purification under denaturing conditions

Buffer B (Lysis Buffer)

100mM	NaH_2PO_4
10mM	Tris-base
8M	Urea

adjust pH to 8 with NaOH every time before usage

Buffer C (Wash Buffer)

100mM	NaH_2PO_4
10mM	Tris-base
8M	Urea

adjust pH to 6.3 with HCl every time before usage

Buffer D (Elution Buffer)

100mM	NaH_2PO_4
10mM	Tris-base
8M	Urea

adjust pH to 5.9 with HCl every time before usage

Buffer E (Elution Buffer)

100mM	NaH_2PO_4
10mM	Tris-base
8M	Urea

adjust pH to 4.5 with HCl every time before usage

10X PBS

1.37M	NaCl
27mM	KCl
81mM	Na_2HPO_4
14.7mM	NaH_2PO_4

pH 7.4

2.1.6.5. Southern blot

20X SSC

3M	NaCl
0.3M	Na-citrate

pH 7.2

50X Denhardt's solution

Ficoll 400	1g
Polyvinylpyrolidone	1g
BSA	1g

ad ddH_2O 100ml

10X Wash Solution

100mM	Tris-base
100mM	NaCl
10mM	$MgCl_2$ Hexahydrat

pH 9.5

Blocking solution

125mM	NaCl
17mM	Na_2HPO_4
8mM	NaH_2PO_4
0,5%	SDS

pH 7.2

Hybridization buffer

20x SSC	25ml
50x Denhardt´s Sol.	10ml
10% BSA	5ml
1M Na_2HPO_4	5ml
20% SDS	500µl
0.5M EDTA	200µl

1X Wash Solution I

1:10 dilution of the blocking solution

2.1.6.6. Competent cells - *E. coli* (XL1-Blue, Rosetta)

MOPS I

100mM	MOPS
10mM	KCl
10mM	RbCl

adjust pH 7 with KOH

MOPSII

100mM	MOPS
70mM	KCl
10mM	RbCl

adjust pH 6.2 with KOH

MOPSIIa

100mM	MOPS
10mM	KCl
10mM	RbCl
15%	Glycerol

adjust pH 6.2 with KOH

2.1.6.7. Competent cells and transformation of *Nab. magadii*

Buffered high salt spheroblasting solution

50mM	Tris-HCl pH 8.0
2M	NaCl
27mM	KCl

autoclave, and add

15%	Sucrose (sterile filtered)

Buffered high salt spheroblasting solution with glycerol

50mM	Tris-HCl pH 9.5
2M	NaCl
27mM	KCl
15%	Glycerol

autoclave, and add

15%	Sucrose (sterile filtered)

Unbuffered high salt spheroblasting solution

2M	NaCl
27mM	KCl

autoclave, and add

15%	Sucrose

60% PEG 600 in unbuffered spheroblasting solution

PEG-600 aliquotes are stored at -80°C

Proteinase K (Quiagen)

0.5M EDTA

2.1.6.8. Isolation of chromosomal DNA of *Nab. magadii*

High alkaline salt solution		Other reagents see methods
4M	NaCl	
50mM	Tris-HCl pH 9.5	

2.1.6.9. Isolation of ϕCh1 virus particles

High alkaline salt solution		**Solution 1.1**	
4M	NaCl	2M	NaCl
50mM	Tris-HCl pH 9.5	50mM	Tris-HCl pH 8.5 - 9
		0.6M	CsCl

Solution 1.3		**Solution 1.5**	
2M	NaCl	2M	NaCl
50mM	Tris-HCl pH 8.5 - 9	50mM	Tris-HCl pH 8.5 - 9
3.7M	CsCl	4M	CsCl

2.1.7. Plasmids

Construct	*Features*	*Source*
pBlueScript II KS(+)	*bla*, ColE1 ori, mcs, *lac*Zaa lac promoter	Stratagene
pUC19	*bla*, pMB1 ori, mcs, *lac*Za	Yanish-Perron *et al.*1985
pQE60	*bla*, ColE1 ori, lac operator element, mcs, C-terminal 6x His-tag	Quiagen
pRSET-A	*bla*, pUC ori, T7 promoter, N-terminal 6x His-tag	Invitrogen
pRo-5	*bla*, gyrB (Nov^R), ColE1 ori, ϕCh1 ori	M. Mayrhofer-Iro *et al*., 2013
pNB102	*bla*, *hmg* (MevR), ColE1 ori, pNB101 ori	Zhou *et al*., 2004
pBAD24	*bla*, pBR322 ori, araC, mcs	Guzman *et al.,* 1995
pQE60-ORF56	pQE60 with ϕCh1 ORF56	this thesis
pQE60-ORF79	pQE60 with ϕCh1 ORF79	this thesis
pRSET-A-tnaA	pRSET-A with 3' end of the tryptophanase gene (*tna*A) of *Nab. magadii*	this thesis
pRSET-A-ORF79	pRSET-A with ϕCh1 ORF79	Beraha, 2013
pBAD24-tnaN	pBAD24 with the tryptophanase promoter of *Nab. magadii* (*tna*N)	Alte, 2011
pRo5-tnaN-ORF79	pRo-5 with ϕCh1 ORF79 under control of *tna*N	Witte, 2012
pNB102-$ORF34_{52}$	pNB102 with the ϕCh1 $ORF34_{52}$	Till, 2011
pRo-5-ORF55	pRo-5 with ϕCh1 ORF55	this thesis
pRo-5-ORF56	pRo-5 with ϕCh1 ORF56	this thesis
pRo-5-ORF21	pRo-5 with ϕCh1 ORF21	this thesis
pNB102-ORF55	pNB102 with ϕCh1 ORF55	this thesis
pNB102-ORF56	pNB102 with ϕCh1 ORF56	this thesis
pNB102-ORF21	pNB102 with ϕCh1 ORF21	this thesis
pNB102-p49-ORF79	pNB102 with ϕCh1 ORF79 under control of the promoter of ORF49 (ϕCh1)	Alte, 2011
pKSII+/ΔTrp	pKSII+ with *tna*A up- and downstream region with the Nov^R -cassette in between	this thesis
pΔTrp12/11	pKSII+ with *tna*A up- and downstream region with the Nov^R -cassette in between	this thesis
pΔTrp11/11	pKSII+ with *tna*A up- and downstream region with the Nov^R -cassette in between	this thesis

2.1.8. Primers

Sequence is written from 5' to 3' direction, restriction sites underlined;

Trp-1-X	GATCTCTAGAATCTCCGTCGACGAACTGC	*Xba*I
Trp-2-SH	GATCAAGCTTCCCGGGCCAATAGGTGTTGTATGT	*Hind*III/*Sma*I
Trp-3-H	GATCAAGCTTGTTTCGGTTTCCCGTTTCG	*Hind*III
Trp-4-K	GTACGG TACCCCTCGCCCTGCCAGC	*Kpn*I
Trp-12-X	GATCTCTAGACCGCTTGTGACAACCGTC	*Xba*I
Trp-11-X	GATCTCTAGAAGTTGACGCAGGATCTGTTCTG	*Xba*I
Trp-21-SH	GATCAAGCTTCCCGGGTAGCAACTCGAGAACGCCAC	*Hind*III/*Sma*I
21-Xba	CAGCTCTAGACGGAAGCCATCGGACTGGA	*Xba*I
21-Kpn	GATCGGTACCTCAACCCCGAACTTCTACTC	*Kpn*I
21-Hind-2	CAGCAAGCTTCGGAAGCCATCGGACTGGA	*Hind*III
55-Hind	CAGCAAGCTTCGGCCCTTTGATGTTTGA	*Kpn*I
55-Kpn	GATCGGTACCTGCTCTGGGCCTCTTTGC	*Kpn*I
56-3	CAGCGTCTAGACTGCAGTCACTGCTGACCACCGG	*Xba*I/*Pst*I
56-Kpn	GATCGGTACCGATTAATTTCAAACCATCGATGAC	*Kpn*I
56-Bgl	GAACAGATCTCTGCTGACCACCGGCT	*Bgl*II
56-Nco	GATTCCATGGGAGAGAACAATCCCAA	*Nco*I
79-Nco-1	GATCCATGGTCGAAGTGACGAACC	*Nco*I
79-Bgl-C	GATCAGATCTAGCATCGGTCGAGTCACC	*Bgl*II
Tna-B2	GTCAGGATCCATGAGCGGCAAGAAGGACG	*Bam*HI
Tna-H	GACTAAGCTTACTGTGAGGACGGGACCG	*Hind*III
RSET-Nde	GACGCATATGCGGGGTTCTCATCATC	*Nde*I
79-KB	GACGAGATCTGGTACCTC AAGCATCGGTCGAGTCA	*Bgl*II/*Kpn*I
Nov-9	GATGTCGGTCATCGCGG	
Nov-11	GCATGTCGTGGCTGTTCG	
UF4	GTTGTCGGCATCGTGGAC	
Trp-del5	GAACATCCTCCACCGC	
Soj-3	CAGCAGCTGCAGCAGCAGTCAGCCATGGAATCCCT	
Soj-5	GCAGCAAGATCTATCGGAGTTACCAACCAGAAA	
Ori-1	GATCATCGATACGCGCCCTGTAGCG	
Ori-4	CAGCAGATCGATCGCGTTAAATTTTTGTTAAATCAG	

2.2. Methodes

2.2.1. DNA electrophoresis

2.2.1.1. Agarose gel

Agarose gels were prepared by melting the acquired amount of agarose in 1X TAE. The liquid gel was then poured into an electrophoresis equipment and after cooling, the gel was covered with 1X TAE separating buffer. DNA was separated based on size by using an electric field. Dependent on the size of the DNA fragment of interest different concentrations of agarose in 1X TAE were used, ranging from 0.8 to 1.5%. Generally, for DNA fragments of sizes below 700bp, a 6% polyacrylamid gel was used instead of agarose gels in order to get a distinct separation of the DNA fragments.

2.2.1.2. 6% Polyacrylamid gel

The components were mixed (listed in 2.1.6.1.) and the gel poured between 2 glass plates by using the Bio-Rad Mini-Protean® equipment. The polymerized gel was placed in the apparatus for electrophoresis and covered with 1X TBE running buffer. A power of 20mA/gel was applied with a running time of 20 to 26 minutes, depending on the size of the fragment.

2.2.1.3. Staining of DNA

DNA was visualized by using ethidium bromide staining. After electrophoresis the gel was incubated in an ethidium bromide bath with a concentration of about 10µg/ml and the DNA visualized with an UV-transilluminator.

2.2.2. Polymerase chain reaction

Preparative and analytical PCR

2 different polymerases were used for the preparative PCR, the *Pwo* DNA polymerase from PeqLab and preferentially the *Pfu* DNA polymerase from Promega. Both enzymes have a 3'-5' exonuclease activity (proofreading function) which makes these enzymes an important tool during cloning procedures. The *GoTaq*® DNA polymerase from Promega was used for analytical PCR in order to verify specific DNA sequences in a sample. It lacks the 3'-5' exonuclease activity which makes the enzyme faster in incorporating nucleotides. *GoTaq*® DNA polymerase is able to incorporate 1000

nucleotides per minute during amplification whereas *Pfu* DNA polymerase manages about 500 nucleotides per minute (which also is due to the proofreading activity).

All used primers were obtained from the company VBC genomics. Stocks were prepared by solving the lyophilized primers with ddH_2O to a final concentration of 1µg/µl. From this stock solution 1:10 dilutions were prepared and used for the PCR mixtures. Annealing temperatures (T_A) were calculated with the program Gene Runner (Hastings Software).

As templates different kinds of DNA samples were used during this work which could be purified ϕCh1 DNA, chromosomal DNA of *Nab. magadii* as well as plasmid DNA. Also crude extracts of *Nab. magadii* served as templates.

Template preparation of *Nab. magadii*

Therefore 50 - 100µl culture (depending on the denseness) were centrifuged 3 min at 13.000rpm, the pellet was dissolved in ddH_2O (80-100µl) and could then be used as a template. This was a useful help when screening for positive transformants of *Nab. magadii* (described in 2.2.8.2.).

100µl PCR mixtures were used for the*Pfu* DNA polymerase

Component	Final volume	Final concentration
10X reaction buffer	10µl	1X
2mM dNTP mixture	10µl	0.2mM
primer 1	5µl	500ng
primer 2	5µl	500ng
template	1µl	< 500ng
sterile ddH_2O	67µl	
Pfu polymerase (2-3U/µl)	2µl	
	100µl	

PCR program for *Pfu* DNA polymerase

Step	Minutes	Temperature	Number of cycles
1. Initial Denaturation	5'	95°C	1
2. Denaturation	1'	95°C	
3. Annealing	1'	T_A	35
4. Extension	1'/500bp	72°C	
5. Final Extension	3x extension time	72°C	1
6. Soak	indefinite	4°C	

30-50µl PCR mixtures were used for the *GoTaq*® DNA polymerase

Component	Final volume	Final concentration
5X reaction buffer	10µl	1X
2mM dNTP mixture	5µl	0.2mM
primer 1	2.5µl	500ng
primer 2	2.5µl	500ng
template	1µl	< 500ng
sterile ddH_2O	28.75µl	
GoTaq® polymerase (5U/µl)	0.25µl	
	50µl	

PCR program for *GoTaq*® DNA polymerase

Step	Minutes	Temperature	Number of cycles
1. Initial Denaturation	5'	95°C	1
2. Denaturation	1'	95°C	
3. Annealing	1'	T_A	35
4. Extension	1'/1kb	72°C	
5. Final Extension	3x extension time	72°C	1
6. Soak	indefinite	4°C	

In every case, PCR products were analysed using agarose or 6% PAA gels (depending on the size of the DNA fragment) in order to control the quality of the product and to decide how to proceed. Generally, preparative PCR products were purified by using the QIAquick PCR Purification Kit from Qiagen, but it could also be necessary to use the QIAquick Gel Extraction Kit (Quiagen) when there is not only one distinct band visible on the gel.

2.2.3. DNA purification

2.2.3.1. Purfication of DNA samples

The QIAquick PCR Purification Kit (Qiagen) was used for cleaning PCR products in order to get rid of all unwanted components still present in the PCR mixture like nucleotides, primers or buffer ingredients. The Kit could also be used for cleaning other DNA samples. Purification was performed as described in the manufactures protocol and the final elution step was done with ddH_2O.

2.2.3.2. Gel elution

Gel elution was performed to clean a PCR product and also other DNA samples from unwanted bigger or smaller DNA fragments. Therefore the specific DNA fragment was excised from an agarose or a 6% PAA gel under 70% UV light after staining with ethidium bromide. When gel elution was done using an agarose gel, the QIAquick Gel Extraction Kit (Qiagen) was used for the purification according to the protocol and elution of the purified DNA was done with ddH_2O.

6% PAA gels were used for elution of smaller DNA fragments. The excised fragment was incubated with a sufficient amount of PAA Gel elution buffer that solves the DNA out of the gel. Incubation was done at 37°C gently shaking, over night or at least 5 hours. Afterwards the sample was centrifuged 5 min at 13.200 rpm and the supernatant transferred into a new tube and purified according to the QIAquick PCR Purification Kit's protocol. Again, the final elution step was done with ddH_2O.

2.2.4. Restriction

Almost all DNA restrictions were performed using restriction enzymes and buffers from Thermo Scientific. Enzymes were used according to the suggested buffer conditions and temperatures (most enzymes cut best at 37°C). For conventional restriction enzymes the incubation time was 3 hours or overnight. Also fast digest enzymes were available which need much shorter incubation time. All of these fast digest enzymes work in the same reaction buffer, which makes them attractive for double digests.

2.2.5. DNA modifications

2.2.5.1. Fill-in 5' overhangs

The Klenow fragment (exo-) from Thermo Scientific was used for blunt ending of 5' overhangs. The enzyme has a 5'-3' polymerase activity filling in 5' overhangs. Klenow could be used with the supplied reaction buffer as well as with buffers from most other enzymes from Thermo Scientific. Reactions were set up according to the manufactures protocol.

2.2.5.2. Dephosphorylation

Fast Alkaline Phosphatase was used for dephosphorylation of linear plasmids. The enzyme removes 5' phosphate groups from linear DNA and it is also active in buffers from other enzymes from Thermo Scientific. This removal of the phosphate group is important for ligation of blunt ends. Reactions were set up as suggested in the manufactures protocol.

2.2.5.3. Ligation

T4-DNA ligase from Promega was used for the ligation of digested DNA with 5' or 3' overhangs as well as blunt end DNA. The enzyme is active in the supplied reaction buffer. Incubation was performed 3 hours at room temperature or over night at 16°C. Ligation was mixed with an insert:vector ratio of 3:1 to increase the chance for successful ligation.

Ligation mixture:	11.5µl	insert DNA
	1µl	plasmid DNA
	1.5µl	reaction buffer
	1µl	T4-DNA ligase

After ligation the whole batch was used for transformation of competent *E. coli* cells.

2.2.6. Transformation of *E. coli*

2.2.6.1. Generation of competent *E. coli* cells

100ml LB Medium (supplemented with suitable antibiotics) were incubated with the desired *E. coli* strain to a starting OD_{600} of 0.1 at 37°C, shaking, until the culture reached an OD_{600} of 0.6 (logarithmic growth phase). At this time point, the cells were harvested by a centrifugation step - 10min, 16250 x g at 4°C. The resulted pellet was then resuspended in 40ml MOPS I and then incubated on ice for 10min. A second centrifugation step was done, again 10min, 16250 x g at 4°C. The pellet was resuspended in 40ml MOPS II and incubated on ice for 30 min, before the last centrifugation step was done, again 10min, 16250 x g at 4°C. Finally the pellet was resuspended in 2ml MOPS IIa and 100µl aliquots were prepared in pre-cooled eppendorf tubes. The aliquots were then stored at -80°C and are ready to use for transformation procedure whenever they are needed.

2.2.6.2. Transformation of competent *E. coli* cells

100µl of competent *E. coli* cells from -80°C has been thawed about 10 min on ice. DNA was added and the cells were incubated 30min on ice. For transformation with a ligation product, the whole batch was added to the competent cells. For transformation with purified plasmid DNA, the suitable concentration was added dependent on the used *E. coli* strain because of different transformation efficiency. After the incubation a heat shock was done, 2 min at 42°C followed by a quick cooling step on ice. 300µl of LB medium were added and the cell regenerated at 37°C for 30 min without shaking. Finally the samples were plated on selective media (LB) plates and incubated at 37°C over night until single colonies appeared.

2.2.6.3. Quick-prep for screening transformants

In order to find positive clones, after transformation with a ligation product first of all single colonies were inoculated in 5ml LB medium containing the required antibiotics for selection. After incubation at 37°C over night, a quick-prep screening was done to identify positive clones. Therefore 300µl of the *E. coli* over night cultures deriving from the single colonies were centrifuged 3 min at 13.200 rpm at room temperature. The supernatant was discarded and the pellet completely resuspended in 30µl 5X DNA loading dye. 14µl of Phenol/Chloroform 1:1 were added to the samples followed by strong vortexing, at least 30 seconds. Again the samples were centrifuged for 5 minutes at 13.200 rpm and immediately after that, 12µl of the liquid phases were applied to a 0.8% agarose gel. Afterwards staining was done with ethidium bromide.

Plasmid DNA of the transformants could be compared and putative positive clones could be identified because of the different running behavior of plasmids with different sizes. (Plasmids containing an insert run higher in an agarose gel then the respective empty plasmids.) Plasmids of putative positive clones were then isolated using the Fermentas/Thermo GeneJET^{TM} Kit and verified by restriction analysis and PCR.

2.2.7. Plasmid isolation from *E. coli*

The Fermentas/Thermo GeneJET^{TM} Kit was used for plasmid preperations. A fresh over night culture harboring the plasmid of interest was used for isolation. Steps were done as described in the manufactures protocol excepting the final elution step here sterile ddH_2O was used instead of the provided elution buffer.

2.2.8. Transformation of *Natrialba magadii*

2.2.8.1. Generation of competent *Nab. magadii* cells

Competent cells of *Nab. magadii* have to be prepared fresh for each transformation. Therefore, three 500ml baffled Erlenmeyer flasks containing 60ml NVM+ rich medium and bacitracin with a concentration of 70µg/ml were inoculated with a fresh and dense culture of *Nab. magadii*. An increasing volume of the culture was added to the three flasks filled with 60ml NVM+, preferentially 3ml, 5ml and 8ml culture. The cells were grown at 37°C shaking at 165 rpm over night, until one of the three cultures reached an OD_{600} of 0.5 - 0.6. This culture was then used for the next steps in generating competent cells. Therefore the cells were harvested by a centrifugation step 15 min at 6.000 rpm at room temperature. The pellet was resuspended in 30 ml high salt buffered spheroblasting solution with glycerol and Proteinase K (Quiagen) was added to a final concentration of 20µg/ml. In a 100 ml flask, the batch was incubated at 42°C shaking at 133 rpm. Proteinase K digests the instable S-layer and after 1 - 2 days cells were usually spheroblasts (controlled by microscope analysis).

These competent spheroblast cells were immediately used for transformation. Competent cells could also be stored at -80°C for at least one week. Therefore 1.5 ml of this cell suspension was centrifuged 3 min at 10.000 rpm and the pellet resuspended in high salt buffered spheroblasting solution containing glycerol. Preferentially fresh competent cells were used for transformation.

2.2.8.2. Transformation of competent *Nab. magadii* cells

Per transformation batch, 1.5 ml suspension of the spheroblasts were centrifuged 3 min at 10.000 rpm and the pellet resuspended in 150 µl high salt buffered spheroblasting solution. Frozen spheroblasts from -80°C have been thawed at RT or 37°C for 10 min, centrifuged and resuspended in 150 µl high salt buffered spheroblasting solution.

The cells were incubated with 15µl 0.5 M EDTA 10 min at room temperature. Afterward the DNA (about 3µg) was added and incubated for 5 min. Not more than 10µl should be added in order to keep the NaCl concentration of the high salt buffered spheroblasting solution. 150µl of 60% PEG-600 in high salt unbuffered spheroblasting solution were added and the batch incubated 30 min at room temperature. PEG-600 aliquots from -80°C were thaw at 65°C and 60% PEG-600 in high salt unbuffered spheroblasting solution. (This was prepared before starting with the transformation). In order to wash the cells the batch was carefully mixed with 1 ml NVM+ medium and centrifuged at 10.000 rpm for 5 min. This wash step was repeated with another 1 ml medium. Afterwards the pellet

was resuspended in 1 ml rich medium for regeneration - shaking at 37°C until the cells regained rod shape (controlled by microscope analysis).
Finally, all of the regenerated cells were plated on selective NVM+ agar plates 100 - 120 µl per plate. Additionally, a 1 ml 1:10 dilution with NVM+ medium was prepared from the regenerated cells; this whole 1 ml was plated too. When plating cells after transformation with a suicide vector for homologous recombination no dilution was prepared and 120µl from the regenerated cells were plated per plate. The plates were incubated at 37°C in sealed plastic bags and after at least 2 weeks, single colonies started to appear.

2.2.8.3. Screening the transformants

Single colonies were inoculated in 700 - 1000 µl selective rich medium in Eppendorf tubes and incubated at 42°C shaking at 133 rpm for growth. For faster growth the tubes could be opened from time to time in order to keep the aerobic conditions. Generally after about 7 days templates could be prepared (as described in 2.2.2.), and the cultures were tested by analytic PCR in order to identify positive transformants.

2.2.9. Homozygation of a *Natrialba magadii* deletion mutant

After successful recombination confirmed by PCR, the culture has to be passaged in order to get a homozygous mutant since *Nab. magadii* has up to 50 copies of chromosomal DNA. Positive identified transformants were grown in NVM+ rich medium supplemented with novobiocin until the culture was dense. Afterwards passaging starts. Therefore 20 ml NVM+ rich medium supplemented with novobiocin was inoculated with 100 µl of the culture and incubated at 37°C, shaking, until stationary phase was reached. This culture was the pre-culture for the next passage; again 20 ml rich medium with novobiocin was inoculated with 100 µl of this pre-culture and incubated at 37°C to stationary phase. PCR was used to test for homozygous mutant during passaging.

2.2.10. Isolation of chromosomal DNA of *Nab. magadii*

200 - 500 ml of a *Nab. magadii* culture was incubated at 37°C to an OD_{600} of 0.6 to 0.8. Afterwards the cells were harvested by centrifugation 20 min at room temperature and the pellet was carefully resuspended in 5 ml 4 M NaCl/50mM Tris-HCl pH 9.5 (avoid foaming). The suspension was then transferred into a 50 ml falcon tube. After adding 5 ml 14 mM desoxycholat the tube was rotated

carefully until the cell suspension was completely mixed. 15 ml ddH_2O were added and again the sample was mixed carefully. 25 ml Phenol/Chloroform 1:1 were added to the suspension and centrifuged 30 min at 10.000 rpm at 4°C.

The supernatant was transferred into a 100 ml Erlenmeyer flask and overlaid with the 0.6x volume isopropanol. With a sterile Pasteur pipette the precipitated DNA was fished and washed in 70% Ethanol and solved in 5 ml sterile ddH_2O (more ddH_2O if necessary).

1 g CsCl per ml of solved DNA were added and dissolved at room temperature and Ethidium bromide was added.

After transferring the sample into a Quick-seal centrifugation tube it was centrifuged for 16 hours at 60.000 rpm at room temperature. The pink DNA band was collected carefully with a syringe and ethidium bromide was removed by extraction with water-saturated butyl alcohol. Finally, the chromosomal DNA was dialysed against ddH_2O to get rid of the CsCl, 4 hours, and the H_2O was changed for dialysis over night. DNA could be stored at 4°C. For control a sample of the chromosomal DNA was applied on a 0.8% agarose gel.

2.2.11. Southern blot

This method is used to find a specific DNA sequence in a DNA sample. Generally, the particular DNA was applied on an agarose gel together with a biotinylated DNA marker. After separation and denaturation the ssDNA was blotted on a nylon membrane. The membrane was then incubated with a biotinylated probe binding the sequence of interest, and finally the blot was developed using the Phototope® -Star Detection Kit (New England Biolabs).

1. Probe synthesis - PCR

Biotinylated probes were generated by PCR using biotinylated dUTP (Bio-11-dUTP, GeneON) in the dNTP mixture with a dTTP/dUTP ratio of 50:50. *GoTaq*® DNA polymerase was used for synthesis. The probe was purified by gel extraction using the QIAquick Gel Extraction Kit(Qiagen) and controlled on an agarose gel to be sure that the sample is cleaned of any other DNA fragments (eventually the purification step has to be continued), and to estimate the concentration. Finally the probe is ready for use.

For preparing a 1mM dNTP mixture sufficient for one PCR batch, dATP, dGTP, dCTP, dTTP (Thermo Scientific) and dUTP were pre-mixed as followed:

1mM dNTP mixture containing biotinylated dUTP:

5 µl	1mM	dATP	
5 µl	1mM	dGTP	
5 µl	1mM	dCTP	
2.5 µl	1mM	dTTP	50:50
2.5 µl	1mM	dUTP	
20 µl			

The whole 20 µl were used for the PCR.

100 µl PCR batch:

Component	Final volume	Final concentration
5X reaction buffer	20µl	1X
1mM dNTP mixture	20µl	0.2mM
primer 1	5µl	500ng
primer 2	5µl	500ng
template	1µl	< 500ng
sterile ddH_2O	48.5µl	
GoTaq® polymerase (5U/µl)	0.5µl	
	100µl	

2. Separation of DNA fragments and blotting of the DNA to a membrane

The DNA sample and a biotinylated DNA marker were applied to an agarose gel (with the respective concentration of agarose) and DNA fragments separated. The DNA was visualized using ethidium bromide for staining. Afterwards the gel was incubated in 0.25 M HCl for 30 min, which helps transferring bigger DNA fragments to the nylon membrane. The gel was then incubated in 0.4 M NaOH/0.6 M NaCl for 30 min denaturing the DNA followed by neutralization - the gel was incubated in 1.5 M NaCl/0.5 M Tris-HCl pH 7.5 or 30 min.

Amersham $Hybond_{TM}$ nylon membrane (GE Healthcare) was used for blotting the DNA. A capillary transfer blot was built up over night using 10X SSC buffer. On the next day the membrane was incubated 1 min in 0.4 M NaOH and 1 min in 0.2 M Tris-HCl pH7.5 and afterwards the blotted DNA was fixed by UV-crosslinking (Stratalink cross - linker obtained from Stratagene).

3. Blocking and Hybridization

Before hybridization could be done, the membrane has to be blocked to prevent unspecific binding of the probe. Therefore the membrane was placed into a hybridization tube and 12 ml of hybridization buffer were added together with 120 µl salmon sperm DNA (10mg/ml). The tube was

placed in a hybridization oven and rotated at 65°C where the membrane was blocked for 3 hours. After blocking the probe was denatured for 5 min at 95°C and added to the membrane. Hybridization took place over night at 65°C.

The next day the membrane was washed: 2x with 2X SSC/0.1% SDS 5 min at room temperature and 2x with 0.1X SSC/0.1% SDS (pre-warmed at 65°C) 15 min at 65°C;

4. Blot development using the Phototope® -Star Detection Kit (New England Biolabs)

Detection is based on chemiluminescence. In principle streptavidin binds to the biotinylated targets on the membrane. Biotinylated alkaline phosphatase is added which also binds to the bound streptavidin. CDP-Star Reagent reacts with the alkaline phosphatase and emitted light is captured on x-ray film.

Steps in developing the blot:

The membrane was incubated in blocking solution 1x 5 min followed by incubation with streptavidin solution (7 ml blocking-solution + 7 µl streptavidin) for 5 min. Afterwards the blot was washed 3x 5 min with wash solution I followed by incubation with biotinylated alkaline phosphatase solution (7 ml blocking-solution + 7 µl alkaline phosphatase). The membrane was then washed 1x 5 min with blocking solution and 3x 5 min with wash solution II. Finally the membrane was incubated with 3ml 1X dilution buffer and 6 µl CDP Star reagent for 5 min. Afterwards the membrane was carefully dried using a soft paper and an x-ray film (Amersham Biosciences) was exposed.

2.2.12. Isolation of ϕCh1 virus particles

A fresh and well growing *Nab. magadii* L11 culture was inoculated in 4.5 - 5 L NVM+ rich medium and the culture was incubated at 37°C. OD_{600} was measured daily until complete lysis of the culture could be observed. At this time point the culture was centrifuged 20 min at 8.000 rpm at room temperature to get rid of cellular debris. The supernatant containing ϕCh1 particles was transferred into large Erlenmeyer flasks and 10% PEG-6000 was added. PEG-6000 was dissolved by gently stirring over night using a magnetic stirrer. Virus particles bind to PEG-6000 so that after a centrifugation step, 30 min at 8.000 rpm, the pellet contains ϕCh1 particles. This pellet was resuspended in 30 - 50 ml high salt alkaline solution (4 M NaCl/50mM Tris/ HCL pH 9.5).

A discontinuous CsCl gradient was performed in order to purify the virus particles from the sample. The gradient was established by filling 2 ml CsCl solution 1.5 into an ultracentrifugation tube (Beckman). This was covered with 4 ml CsCl solution 1.3 followed by 5 ml of the sample containing the virus particles, which was covered with approximately 1 ml CsCl solution 1.1. Centrifugation of the gradient was performed at 30.000 rpm for 20 hours at room temperature. The ϕCh1 virus particles could be identified as light band in the gradient. The band was carefully collected using a pipette. Afterwards a continuous CsCl gradient was established for purification of the virus particles. Therefore the sample was mixed with CsCl solution 1.3 and was centrifuged at 30.000 rpm for 20 hours and the band containing the virus particles could then be collected using a pipette. Finally the samples containing the virus particles were dialysed against high salt alkaline solution to get rid of the CsCl. The quantity of the ϕCh1 particles in the sample was analyzed by a phage titer.

2.2.13. Virus titer analysis

A dilution series from purified ϕCh1 particles was prepared using NVM+ rich medium (usually 10^{-2}, 10^{-4}, 10^{-6}, 10^{-8}). 100 µl of the dilution was mixed with 300 - 500µl of well growing *Nab. magadii* cells and 5 ml soft-agar (NVM+ rich medium). Everything was then poured onto NVM+ agar plates (dependent on the used strain also plates supplemented with antibiotics should be used). The plates were stored one day at room temperature and afterward they were incubated at 37°C for 1 - 10 days in sealed plastic bags, until plaques get visible. By counting the plaques on the plate the plaque forming units per ml (pfu/ml) could be calculated.

During this diploma work virus titer analysis was performed to test the infectivity of ϕCh1 from two strains: *Nab. magadii* L11 (pro-5/ORF56) and *Nab. magadii* L11 (pNB102/ORF79). During growth curve analysis samples of the supernatant were taken which were used to perform the virus titer analysis. The supernatant was used instead of the purified ϕCh1 particles. To 1 ml supernatant, 10 µl Chloroform was added and the samples were stored at room temperature. Dilutions of the samples were prepared and the titer performed.

2.2.14. Isolation of ϕCh1 DNA

100 µl purified ϕCh1 particles were mixed with 300 µl ddH_2O leading to lysis of the virus. For extraction of the DNA 200 µl of phenol/chloroform (1:1) was added followed by strong vortexing.

The sample was centrifuged 5 min at 13.200 rpm and the upper phase containing the DNA was isolated. Adding 2x volume 96% ethanol the DNA was precipitated and the sample centrifuged 30 min at 16.400 rpm at 4°C. The supernatant was removed carefully and the resulting DNA pellet washed twice with 70% ethanol and dried at 65°C. The DNA was then resolved in 10 µl ddH_2O and an aliquot loaded on an 0.8% agarose gel for control.

2.2.15. Protein methodes

2.2.15.1. Preparation of crude protein extracts

1.5 ml of a growing culture (*E. coli* or *Nab. magadii*), were centrifuged 3 min at 13.200 rpm. The supernatant was removed and if necessary a second quick spin was performed in order to separate the supernatant completely from the pellet. The pellet was resuspended in x µl (x = OD_{600} x 75) 5 mM sodium phosphate buffer pH 6.8. The same volume (x µl) of 2X Laemmli buffer was added to the batch and the sample cooked for 10 min at 95°C.

Since cell pellets of *Nab. magadii* could hardly be resuspended in the sodium phosphate buffer an additional incubation step at 37°C for 24 hours was performed, making the resuspension of the pellet much easier. Therefore the 5mM Sodium Phosphate buffer and 2X Laemmli buffer were added to the cell pellet without any pipetting, the pellet was just carefully detached from the tube wall. Afterwards the sample was incubated at 37°C for one day, cooked and then resuspended.
After boiling, the crude extracts can be loaded on a protein gel and stored at -20°C.

2.2.15.2. SDS-PAGE

Crude protein extracts were prepared and analyzed by SDS-PAGE (sodium dodecyl sulfate polyacrylamide gel elektrophoresis). SDS denatures proteins and applies a negative charge by masking their own charge. So in an electric field proteins are separated according to their size. A 12% polyacrylamid gel was used to separate proteins, and the gel was prepared using the equipment of Bio-Rad Mini-Protean®. The separation gel was mixed on ice, casted between 2 glass plates and covered immediately with isopropanol to achieve a clear straight line. After polymerization isopropanol was removed. The ingredients of the stacking gel were mixed on ice and poured on top of the separation gel and the comb was inserted in the stacking gel. The polymerized gel was placed in the gel apparatus for electrophoresis and covered with 1X SDS Running buffer.

12% Separation gel		4% Stacking gel	
1.75 ml	ddH_2O	1.233 ml	ddH_2O
1.25 ml	4X Separation gel buffer	500 µl	4X Stacking gel buffer
2 ml	30% PAA	267 µl	30% PAA
60 µl	10% APS	20 µl	10% APS
10µl	TEMED	5 µl	TEMED

The prepared protein samples were loaded on the gel together with a protein marker. Starting with 40V the proteins accumulate in the slots and migrate into the stacking gel until the bromphenol blue color has reached the border of stacking- and separation gel. At this time point the electric potential was increased to 100V and the proteins separated in the separation gel. When working with crude extracts from *Nab. magadii*, 60V were applied instead of 100V.

2.2.15.3. Staining with Coomassie

The stacking gel was removed from the separation gel, overlaid with Coomassie staining solution and incubated. Afterwards the staining solution was removed and the gel incubated with the destaining solution until clear protein bands get visible.

2.2.15.4. Western blot

Generally, this method allows the detection of a certain protein in a protein mixture using specific antibodies binding to the particular protein. Often, a labeled secondary antibody binding to the primary antibody is used for detection.

1. Transfer (Blotting)

The protein samples used for Western blot were prepared as described in 2.2.15.1.,and loaded onto a SDS PAGE polyacrylamid gel together with a protein marker. Six Whatman filter papers and a nitrocellulose membrane (Whatman) were used for the blotting. Filter paper and the membrane were incubated in transblot buffer and the blot was build up and placed in the semi-dry blotting apparatus. Conditions for one blot were 20 min at 20V and for two blots, 30 min at 20V.

After blotting the membrane was stained with Ponceau S solution to make sure that the blotting procedure was successful and to mark the bands of the protein marker. Destaining was done with H_2O.

2. Blocking

The membrane was blocked using 5% milk powder in 1X TBS at 4°C over night to prevent interaction of antibodies with membrane parts free from blotted proteins.

3. Blot development

After blocking, the membrane was washed in 1X TBS for 10 min at room temperature on a shaking table followed by incubation with the primary antibody. Primary Antibodies were prepared in 1X TBS and 0.3 % BSA with different dilutions of the used antiserum:

Antibody	Dilution in 1X TBS/0.3% BSA
Penta His Antibody from mouse	1:1000
RGS His Antibody from mouse	1:1000
α-E from rabbit	1:5000
α-34 from rabbit	1:5000

Incubation was done 1 hour at room temperature. Afterwards the membrane was washed, 3 times for 10 min with 1X TBS followed by incubation with the secondary antibody again for 1 hour, room temperature. The used secondary antibodies are listed in 2.1.6.3., and were prepared in 1X TBS in a dilution of 1:5000. The membrane was washed again 3 times for 10 min with 1X TBS.

4. Detection (ECL - enhanced chemiluminescence)

The used secondary antibodies were linked with horse raddish peroxidase and detection was done with the SuperSignal West Pico Chemiluminescent Substrate (Pierce) according to the manufactures protocol. With this ECL substrate the activity of the HRP could be detected by emission of light. After incubation with the substrate, emitted light is captured on x-ray film (Amersham Biosciences).

2.2.16. Expression of recombinant proteins and protein purification

During this diploma thesis, purification of recombinant His-tagged proteins was done with the ϕCh1 gene products of ORF56 and ORF79 and the gene product of the 3' end of *tnaA* of *Nab. magadii* for antibody production. 2 different plasmids were used for the overexpression. His-tagged gp56 and gp79 were expressed by the vector pQE60 providing a C-terminal 6x His-tag and the *E. coli* strain XL1-blue was used for the overexpression. The *tnaA* gene product was expressed using the vector pRSET-A providing an N-terminal 6x His-tag and the strain Rosetta was used for expression. The

recombinant proteins were then purified under denaturing conditions and prepared for antibody production.

2.2.16.1. Overexpression of His-tagged proteins

A fresh over night culture of an *E. coli* strain harboring the expression vector carrying the desired gene for protein expression was used to inoculate LB media to an OD_{600} of 0.1. The culture was grown at 37°C up to an OD of 0.3 - 0.4. At this time-point gene expression was induced adding IPTG (final concentration of 0.5 mM). After 3 - 4 hours the culture was centrifuged 15 min at 6.000 rpm at 4°C and the resulted pellet was frozen at -20°C.

During the protein expression samples were taken before induction with IPTG and after the expression period. Crude protein extracts were prepared and the samples analyzed by SDS-PAGE.

2.2.16.2. Protein purification under denaturing conditions

The frozen pellet from protein expression has been thawed on ice for about 10 min and was resuspended in buffer B (lysis buffer) and stirred at room temperature for a couple of hours or overnight. Successful lysis was controlled by microscope analysis. If necessary, the cells were additionally lysed by sonication.

Afterwards the lysate was centrifuged for 30 min at 10.000 x g at room temperature. The supernatant was transferred into a flask and incubated with the necessary amount of Ni-NTA (Qiagen). The mixture was stirred on a magnetic table over night at room temperature. The next day, the solution was loaded onto a chromatography column with a closed outlet.

The flow-through was collected and the proteins on the column material washed twice with 4 ml buffer C. Afterwards the his-tagged protein was eluted with buffer D - 4 times with 500 - 700 µl followed by elution with buffer E - 4 times with 500 - 700 µl. Samples were prepared from each step and the same volume of 2X Laemmli buffer was added. After cooking for 10 min at 95°C the protein samples were analyzed by SDS-PAGE.

Dialysis

Fractions containing the overexpressed protein were pooled and dialysed against 1X PBS for antibody production. Dialysis was done 1 hour at room temperature and over night. The dialysis step was also controlled by SDS-PAGE and the protein prepared for antibody production.

2.2.17. Cloning strategies

Cloning of a construct for the deletion of the tryptophanase gene of Nab. magadii L13

The tryptophanase gene (*tna*A) within the chromosome of *Nab. magadii* L13 was deleted by the introduction of a novobiocin resistant cassette replacing *tna*A via homologous recombination. Therefore up- and downstream regions of the gene were used as homologous flanks with the Nov^R -cassette in between. To increase the chance of successful recombination, 3 different constructs were cloned and used for transformation of *Nab. magadii* L13.

1. pKSII+/ΔTrp

The upstream and downstream region of *tna*A were amplified from the template chromosomal DNA of *Nab. magadii* using the following primer: *upstream flank: Trp-11-X/Trp-2-SH (956 bp), downstream flank: Trp-3-H/Trp-4-K (997 bp)*

First of all, the upstream flank was cloned into pKSII+. Therefore vector and PCR product were restricted using *Xba*I and *Hind*III and ligated. Afterwards the downstream flank was cloned into pKSII+ already carrying the upstream flank - both were digested with *Hind*III and *Kpn*I and ligated. In the last cloning step, up- and downstream flanks on pKSII+ were separated by the Nov^R -cassette. The Nov^R -cassette has a size of 2453 bp and was isolated from pMDS11 by restriction of the plasmid with *Hind*III and *Sma*I. Finally pKSII+ carrying up- and downstream flank was also digested with *Hind*III and *Sma*I, leading to the separation of up- and downstream sequence, and ligated with the Nov^R -cassette.

2. pΔTrp12/11 and pΔtnaA::nov^R

pKSII+/ΔTrp was used as starting point- the upstream flank of this construct was replaced by a new sequence. The new upstream flank for pΔTrp12/11 was amplified using the primer Trp-21-SH and Trp-12-X (fragment: 1905bp) and for pΔ*tna*A::nov^R the primer Trp-11-X and Trp-21-SH were used(fragment: 550bp). pKSII+/ΔTrp was digested with *Xba*I and *Sma*I in order to isolate the rest vector carrying the Nov^R -cassette + downstream flank from the upstream flank. The PCR products were digested with *Xba*I and *Sma*I too and cloned into the pKSII+ rest vector.

Cloning of three ORFs of ϕCh1: ORF21, ORF55, ORF56

All three open reading frames were cloned into the shuttle vectors pRo-5 and pNB102 and transformed into *Nab. magadii* L11 and L13. By PCR the ORFs were amplified using the following primers: (template = ϕCh1 DNA)

ORF	*Primer (pRo-5)*	*Primer (pNB102)*	*Fragment size*
ORF21	*21-Hind-2 / 21-Kpn*	*21-Xba / 21-Kpn*	*1183 bp*
ORF55	*55-Hind / 55-Kpn*	*55-Hind / 55-Kpn*	*459 bp*
ORF56	*56-3 / 56-Kpn*	*56-3 / 56-Kpn*	*745 bp*

- **pRo-5-ORF21, pNB102-ORF21**

The PCR product and the vector pRo-5 were restricted with the enzymes *HindIII* and *KpnI* and ORF21 was cloned into pRo-5. For cloning into pNB102, the PCR product and the vector were digested with *Xba*I and *Kpn*I and ligated.

- **pRo-5-ORF55, pNB102-ORF55**

PCR product and the vector pRo-5 were restricted with *HindIII* and *KpnI* and ORF55 cloned into pRo-5. For cloning into pNB102, first of all the vector was digested with *XbaI* followed by blunt ending using the Klenow fragment. Blunt ended pNB102 was then digested with *Kpn*I. The PCR product was digested with *Kpn*I and cloned into pNB102.

- **pRo-5-ORF56, pNB102-ORF56**

The PCR product was digested using *KpnI*. pRo-5 was first digested with *HindIII*, the linear vector blunt ended by using the Klenow fragment and digested again using *KpnI* and ligated with the PCR product. For cloning into pNB102, PCR product and vector pNB102 were both digested with *KpnI* and *XbaI* and ligated.

Cloning of ORF56 and ORF79 into the plasmid pQE-60

ORF56 was amplified by PCR with the primer 56-Bgl and 56-Nco using ϕCh1 DNA as a template. The product had a size of 519bp and was digested with the restriction enzymes *Bgl*II and *Nco*I. The fragment was ligated into the *E. coli* expression vector pQE60, also digested with *Bgl*II and *Nco*I. ORF79 was amplified with the primer 79-Nco-1 and 79-Bgl-C using the ϕCh1 DNA as a template. The product had a size of 785bp and was digested with *Bgl*II and *Nco*I and ligated in the expression vector pQE-60.

Cloning of tnaA into the plasmid pRSET-A

The 3' end of the tryptophanase gene was amplified using the primer Tna-B2 and Tna-H and template DNA of *Nab. magadii* L13. The product had a size of 627bp and both, PCR product and the *E. coli* expression vector pRSET-A were restricted with *BamH*I and *Hind*III and ligated. The construct pRSET-A/tnaA was finally transformed into the *E. coli* strain Rosetta.

3. Results and Discussion

3.1. *Natrialba magadii* L13Δ*tna*A - a tryptophanase deletion mutant

3.1.1. The inducible promoter of *Natrialba magadii* - p*tna*N

In order to achieve controlled expression of certain proteins and to examine protein functions, a suitable promoter is needed that has nearly no basal activity, and can simply be turned on and off by changing growth conditions. For halophilic *Archaea*, such a promoter was first characterized in *Haloferax volcanii* by Large *et al*. in 2007 [67]. Upon microarray analysis the tryptophanase gene (*tna*) could be identified that it is strongly induced in the presence of tryptophan. The upstream region was screened for promoter activity, resulting in the identification of the strong, tightly controlled and tryptophan inducible promoter of the *tna* gene [67].

So far, a promoter having these properties was not described for *Nab. magadii*. Therefore Beatrix Alte established the tryptophan inducible promoter for *Nab. magadii*, called p*tna*N [69]. The genome of *Nab. magadii* was screened for homologs of the tryptophanase of *Hfx. volcanii*, which was successful. A tryptophanase gene (*tna*A) could be identified and the upstream region of the gene was analyzed. Promoter activity was quantified by using the halophilic β-galactosidase as a reporter gene [108].

First of all, growth behavior of *Nab. magadii* L13 upon adding different concentrations of tryptophan to the media was tested. Therefore the strain *Nab. magadii* L13 was cultivated in mineral medium NMMb+ lacking tryptophan. To test the effect of different tryptophan concentrations on the growth behavior, 1mM, 2mM and 4mM dissolved in 1M NaOH were added to the cultures at an OD_{600} of 0.3. A concentration of 2mM tryptophan was used for β-galactosidase assays.

Induction of BgaH under the control of p*tna*N

In order to test the promoter activity of both, the *tna* promoter (p*tna*H) of *Hfx. volcanii* and the putative promoter region of *tna*A (p*tna*N) of *Nab. magadii*, BgaH assays were performed. Therefore 2 different constructs were used; p*tna*H and p*tna*N were cloned upstream the reporter gene β-galactosidase and the plasmids were transformed into *Nab. magadii* L13. Induction of BgaH was done at an OD_{600} of 0.3 with 2mM tryptophan and BgaH assays were performed. The results are illustrated in Figure 14. It could be demonstrated that the upstream region of the *tna*A gene (p*tna*N)

has promoter activity. Both promoters, p*tna*H and p*tna*N are inducible with tryptophan in *Nab. magadii* L13, and promoter activity of p*tna*N is stronger than that of p*tna*H.

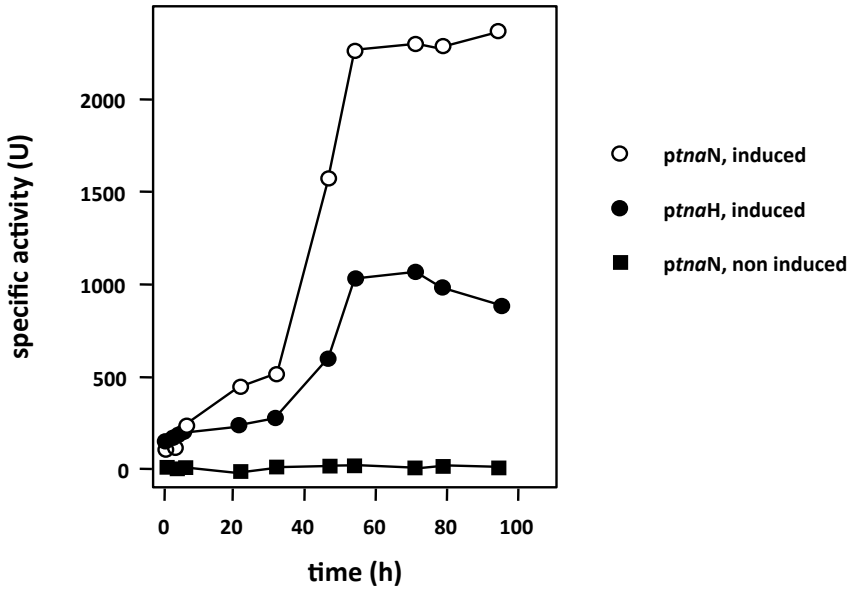

Figure 14: Induction of *bgaH* under the control of p*tna*N.
The promoter activity of p*tna*H and p*tna*N was quantified by BgaH assays. Both promoters are active in *Nab. magadii* and moreover, p*tna*N seems to be a strong inducible promoter. Expression of BgaH could first be detected 2 hours after induction with a maximum activity after about 60 hours for both, p*tna*H and p*tna*N.

However, trials to express different genes of ϕCh1 under the control of p*tna*N failed so far (data not shown). One possible explanation could be the degradation of the inducer. Every time expression is induced, the promoter of the tryptophanase gene *tna*A located on the chromosome is induced too and leads to expression of the gene. As already mentioned, *tna*A encodes the tryptophanase, and this enzyme is responsible for the degradation of tryptophan. Therefore, the inducer has to be added daily to achieve nearly constant expression. For overexpression of proteins a system is needed in which the inducer is not degraded and therefore does not has to be added daily. To overcome this problem the *tna*A gene was deleted in course of this thesis.

3.1.2. Construction of the tryptophanase deletion mutant *Nab. magadii* L13Δ*tna*A

The first deletion mutant of *Nab. magadii* was achieved by Christian Derntl in 2009 [109]. He constructed a Nep deficient strain called P3, in which the gene coding for the extracellular protease Nep is disrupted by a novobiocin resistant cassette. A suicide plasmid containing the required sequences was used for homologues recombination.

The aim of this study was to replace the *tna*A gene (genome position: 1970129-1971481/F) together with its promoter p*tna*N in the chromosome by a novobiocin resistant cassette (Nov^R) via homologous recombination. The resistant cassette allows positive selection for the mutant. A suicide plasmid, which is not able to replicate in *Archaea* was used to introduce the relevant sequences into cells of *Nab. magadii* L13. The used construct harbors upstream- and downstream regions of the *tna*A gene that serve as homologous flanks for recombination, with the Nov^R cassette in between. Three different constructs were cloned, all with the same sequence for the downstream flank, and three different sequences for the upstream flank (details on the cloning procedure are described in "Material and Methods"). All three plasmids were transformed in *Nab. magadii* L13, but successful recombination with a proper double crossover could only be detected for transformants derived from transformation with the plasmid pΔ*tna*A::nov^R, which is represented in Figure 15.

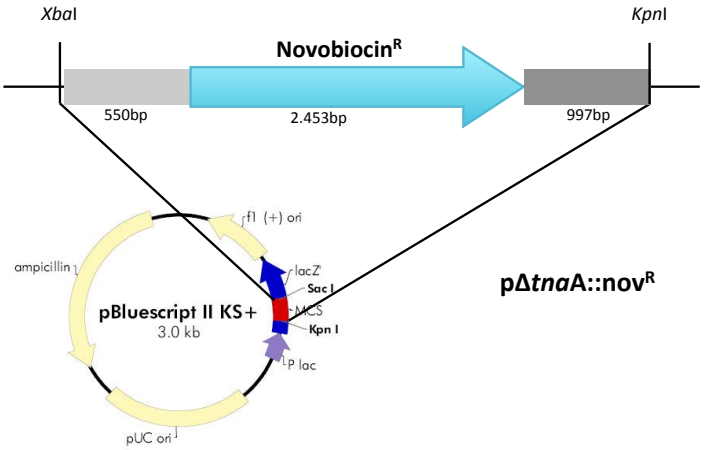

Figure 15: Schematic representation of the plasmid pΔ*tna*A::nov^R.
The grey boxes represent the upstream (5') and downstream (3') regions of the *tna*A gene, which are needed for homologous recombination. The sequences flank the novobiocin resistant cassette that is supposed to replace *tna*A in the chromosome by double crossover.

After transformation of pΔ*tna*A::nov^R in *Nab. magadii* L13 and incubation on selective agar plates supplemented with novobiocin (protocols in "Material and Methods"), transformants were tested for successful recombination. Different possible outcomes could be expected:

1. A single crossover involves only one of the flanks, either up- or downstream flank, resulting in incorporation of the whole plasmid pΔ*tna*A::nov^R into the chromosome. In this scenario the intact *tna*A gene in the genome is not affected and the plasmid with the resistant cassette exists in its linear form next to *tna*A, conferring novobiocin resistance (Fig. 16a and b).

2. A proper double crossover would lead to replacement of *tna*A including p*tna*N by the Nov^R cassette, and the wild type gene replaces the Nov^R cassette on the plasmid (Fig. 16c). As the plasmid has no origin of replication, it is assumed that it is simply lost over the time.

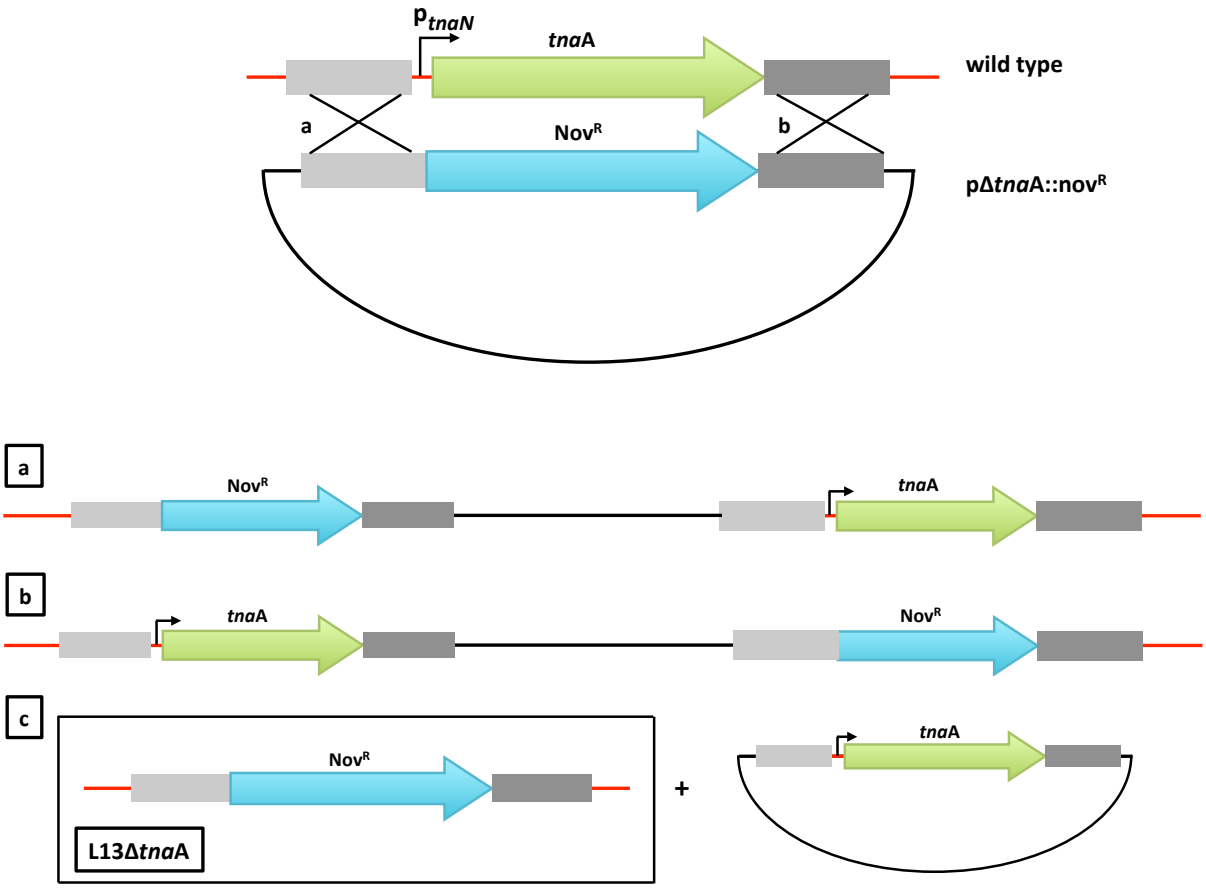

Figure 16: Homologous recombination

The up- and downstream regions (grey boxes) of the *tna*A gene serve as sequences for homologous recombination. Recombination is indicated by the crossed lines, black lines indicate plasmid DNA (pΔ*tna*A::nov^R) and red lines chromosomal DNA of *Nab. magadii* L13 (wild type). Three different outcomes are possible. **a** and **b** outline the possible single crossovers. In situation **a**, only the upstream flank is involved in homologous recombination, leading to incorporation of the whole plasmid DNA into the chromosome. In situation **b**, only the downstream flank is involved in the recombination event and similar to a, the whole plasmid DNA gets integrated into the chromosome, but downstream of *tna*A. The *tna*A gene is not affected and is still present in the genome. Transformants deriving from a single crossover cannot be sorted out just by a selective medium supplemented with novobiocin as the incorporated plasmid DNA confers novobiocin resistance too. A proper double crossover involves both homologous flanks (a+b) leading to replacement of the *tna*A gene and the promoter p*tna*N in the chromosome by the Nov^R cassette, which is outlined in **c**. The *tna*A gene (+p*tna*N) is transferred onto the plasmid while the Nov^R cassette replaces *tna*A/p*tna*N in the chromosome. The plasmid harboring *tna*A is not propagated in the cell and is therefore supposed to be simply lost and the wild type gene is no longer existent in the cell. In order to test whether a single- or double crossover was achieved, transformants are screened by PCR.

To test for recombination deriving from either single- or double crossover, transformants were screened by PCR using the primer Trp-4-K binding to the sequence of the downstream flank, and Nov-9 that binds within the Nov^R cassette (primer binding sites Fig 17A). As a positive control, the plasmid pΔ*tna*A::nov^R was used, and chromosomal DNA of *Nab. magadii* L13 serves as a template for the negative control (Fig. 17B). A PCR product was obtained from all tested transformants, implying that recombination was successful. In order to verify whether a single- or a double crossover was

achieved, the transformants were further analyzed by PCR using different primer sets. A double crossover can only be detected by using primers binding upstream/outside of the 5' homologous region and downstream/outside of the 3' region respectively in combination with primers that bind within the Nov^R cassette (Fig. 17A). In case of a single crossover, either upstream- or downstream flank are involved in the recombination event, and not both. Therefore, only a PCR product obtained from both, Trp-12-X/Nov-11 and UF4/Nov-9 indicate that a proper double crossover was achieved. A scheme of the integrated Nov^R cassette into the chromosome and the binding sites of the used primers for the screening is illustrated in Figure 17A. All transfomants that were tested positive for recombination (Fig. 17B) were also tested positive for a double crossover (data not shown, compare with Fig. 18). Homozygation was performed with 5 transformants.

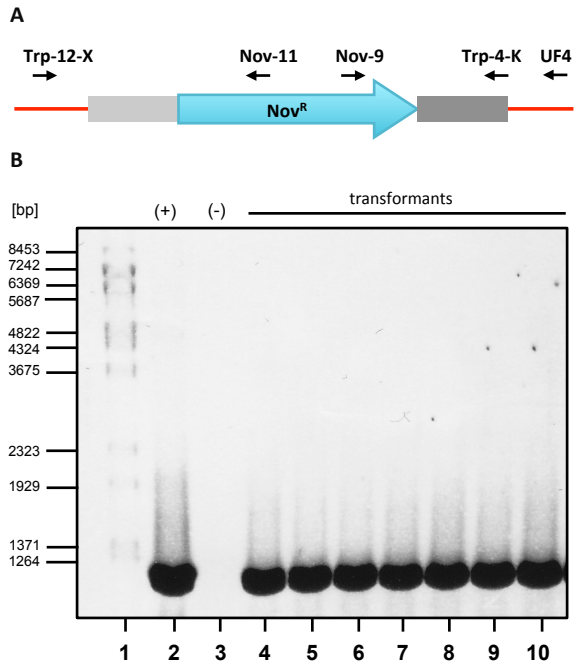

Figure 17 A: Schematic illustration of binding sites of the used primer to screen transformants for recombination. Using primers Trp-4-K/Nov-9, clones where recombination occurred could be identified. Positive clones were further analyzed in order to test whether a single or double crossover was achieved. Primers Trp-12-X/Nov-11 were used to verify recombination of the upstream flank, and Nov-9/UF4 for the downstream flank. If a PCR product is obtained from both primer combinations, a double crossover is indicated.

Figure 17 B: PCR analysis - Test for recombination using the primers Trp-4-K/Nov-9. The obtained product has a size of 1087bp. pΔ*tna*A::nov^R serves as positive control (+), chromosomal L13 DNA as negative control (-). All transformants were positively tested for recombination (lane 4-10).
Lane 1: Marker λ*Bst*EII; 0.8% agarose gel

3.1.3. Homozygation of *Nab. magadii* L13Δ*tna*A

Nab. magadii is polyploid and suspected to have up to 50 copies of chromosomal DNA in exponential growth phase. Therefore, transformants that are tested positively for a double crossover still harbor several copies of the intact *tna*A gene. To achieve a homozygous mutant, the derived cultures have to be passaged, meaning that a culture is prepared in media that is supplemented with novobiocin, and every time the culture reaches stationary phase the next passage is prepared. 5 transformants that were tested positive for a double crossover were used for

homozygation. Passaging is performed until *tna*A is no longer detectable by PCR analysis. By using the primers Tna-B2 and Tna-H the wild type *tna*A gene can be detected. During passaging, 3 of the 5 strains regained the wild type situation and have lost the Nov^R cassette in the chromosome, and in one strain, the wild type signal for the *tna*A gene did not disappear. Homozygation could be achieved only for one of the 5 strains. In this mutant strain the wild type *tna*A gene could no longer be detected by PCR after 17 passages. This strain was further analyzed by PCR to ensure proper incorporation of the Nov^R cassette. PCR analysis is demonstrated in Figure 18. As a result, the mutant strain *Nab. magadii* L13Δ*tna*A appeared to be homozygous for the deleted *tna*A gene.

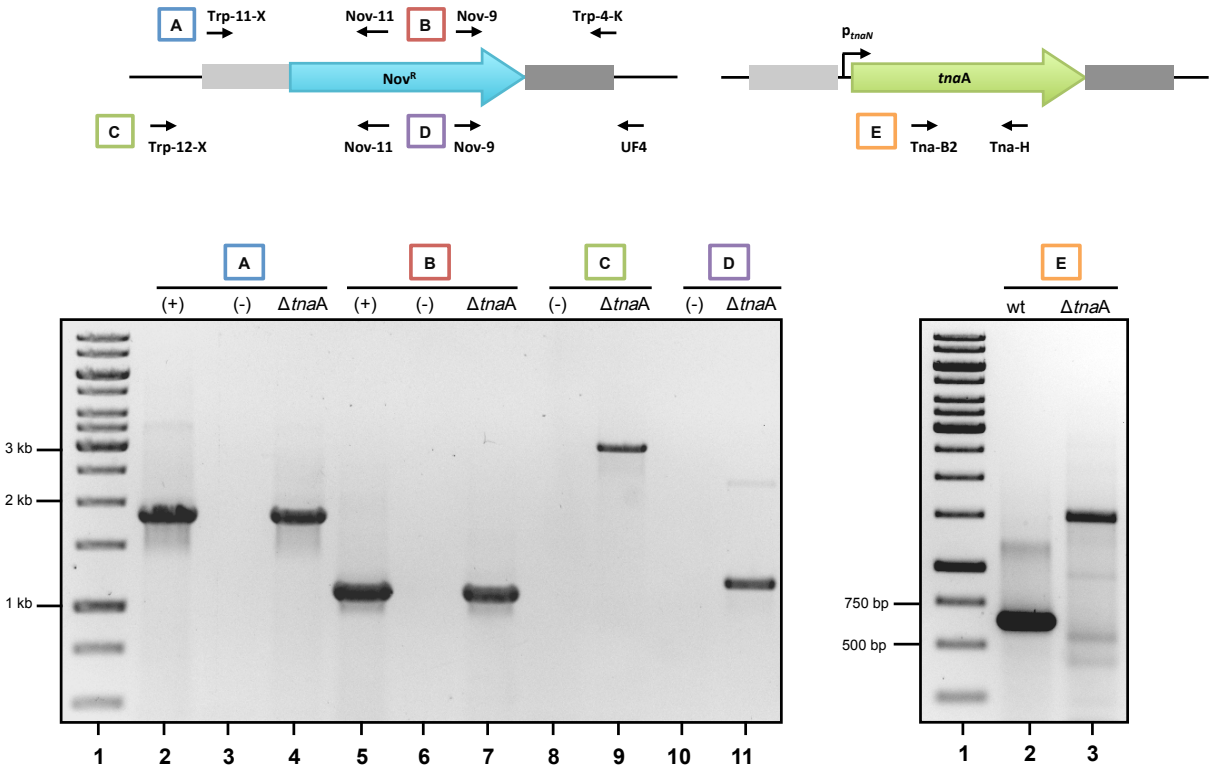

Figure 18: Verification of the mutant strain *Nab. magadii* L13Δ*tna*A after 17 passages

The primers Tna-B2 and Tna-H bind to the wild type *tna*A gene resulting in a PCR product of 629bp. The wild type (wt) gene could not be detected in the mutant strain L13Δ*tna*A, even after 50 PCR cycles no signal was obtained, which is demonstrated in E. As a positive control (wt) L13 chromosomal DNA was used. In order to ensure integration of the Nov^R cassette, PCR analysis to verify a proper double crossover was repeated, demonstrated in A-D (compare with Fig. 17). Primer binding sites are illustrated. The plasmid pΔ*tna*A::nov^R serves as positive control (+) for A+B, L13 chromosomal DNA as negative control (-) for A-D. A: Trp-11-X binds to the upstream flank, Nov-11 binds inside the Nov^R cassette, resulting in a PCR product of 1.804bp (lane 2-4). B: Trp-4-K binds to the downstream flank, Nov-9 inside the NovR cassette, the PCR product has a size of 1.087bp (lane 5-7). C+D demonstrate PCR analysis that ensures the double crossover. C: Trp-12-X binds 5' to the upstream flank, in combination with Nov-11 a PCR product of 3.159bp was obtained (lane 8, 9). UF4 binds 3' to the downstream flank, in combination with Nov-9 a PCR product of 1.239bp was obtained (lane 10, 11).
Lane 1: 1kb DNA ladder; A-D 0.8% agarose gel, E: 1% agarose gel;

3.1.4. Confirmation of the homozygous *Nab. magadii* L13Δ*tna*A

Southern blot analysis

Solely on the basis of PCR analysis it cannot be excluded that intact copies of the *tna*A gene are still present in the chromosome. Therefore an additional approach was carried out. The putative homozygous mutant strain was confirmed by southern blot analysis. The chromosomal DNA of *Nab. magadii* L13 and *Nab. magadii* L13Δ*tna*A was isolated as described in "Material and Methods". The purified DNA was restricted with *Cla*I and the resulted fragments were separated by using a 0.8% agarose gel. Biotinylated hybridization probes have been synthesized by PCR as described in "Material and Methods". Using the primers Trp-del5 and Trp-2-SH the 5' region of *tna*A was amplified yielding a PCR product of 629bp - the hybridization probe 1. For synthesis of the hybridization probe 2 with a size of 1.117bp, the 3' region was isolated using the primers Trp-3-H and Trp-4-K. Chromosomal DNA of *Nab. magadii* L13 was used as a template for the PCR reaction. The hybridization scheme is outlined in Figure 19.

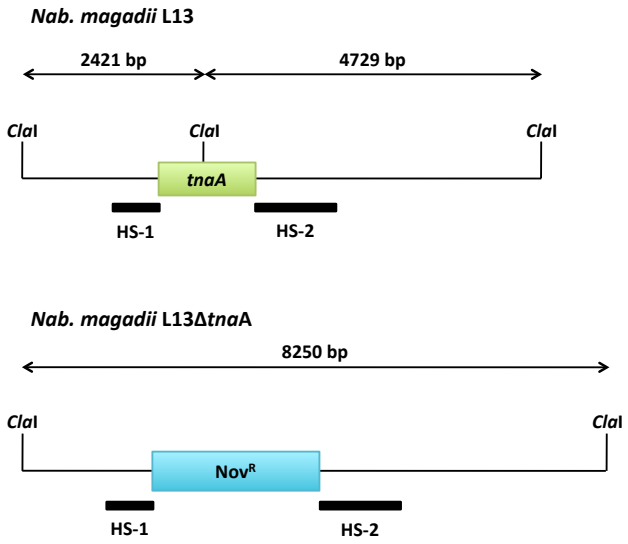

Figure 19: Hybridization scheme
Chromosomal DNA of *Nab. magadii* L13 and *Nab. magadii* L13Δ*tna*A was restricted with *Cla*I. A restriction site exists within the sequence of *tna*A but not in the Nov^R cassette. Therefore, digestion with *Cla*I results in different fragments in this genomic region of *Nab. magadii* L13. HS-1 hybridizes upstream of *tna*A and detects the 2421 bp fragment of the wild type. HS-2 hybridizes downstream of *tna*A and detects the fragment with 4729 bp. As Nov^R does not contain a restriction site for *Cla*I, HS-1 as well as HS-2 detect the same fragment with a size of 8250 bp in *Nab. magadii* L13Δ*tna*A. (HS: hybridization probe)

Results of the southern blot analysis are illustrated in Figure 20. A wild type signal could not be detected for the mutant strain *Nab. magadii* L13Δ*tna*A, neither with the hybridization probe-1 or hybridization probe-2. Unfortunately, all signals of the southern blot are shifted. The whole southern blot procedure was repeated several times, always leading to the same result. The reason for the shifted DNA could not be clarified, but nevertheless, it could be clearly demonstrated that *Nab. magadii* L13Δ*tna*A is homozygous for the deleted *tna*A gene.

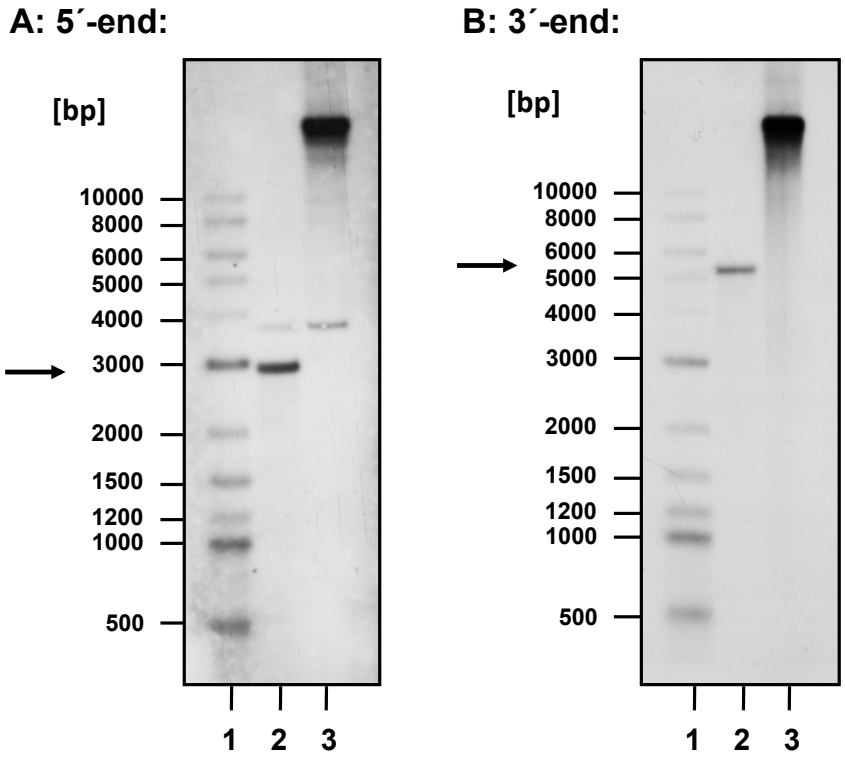

Figure 20: Southern blot analysis of *Nab. magadii* L13Δ*tna*A

As described in Figure 19, different signals are expected for the wild type and mutant strain, arrows indicate the wild type signals. **A** illustrates the blot using HS-1 that hybridizes with the upstream region of *tna*A. A signal of about 3000 bp could be detected for the wild type (*Nab. magadii* L13), which is represented in lane 2. Lane 3 shows, that this wild type signal was not detectable in the deletion mutant *Nab. magadii* L13Δ*tna*A. The additional signal of about 4000 bp is most likely due to unspecific binding of the hybridization probe. Southern blot **B** shows the obtained signals by using HS-2. The probe hybridizes with the downstream region of *tna*A. A wild type signal of about 5000 bp was detected for *Nab. magadii* L13, represented in lane 2. Similar to A, the wild type signal could not be detected in *Nab. magadii* L13Δ*tna*A (lane 3).
Lane 1, A+B: biotinylated 2-log DNA ladder

3.1.5. Discussion

The inducible promoter p*tna*N for *Natrialba magadii* was established by Beatrix Alte in 2011. The promoter can be induced with tryptophan by simply adding tryptophan dissolved in 1M NaOH to the medium. Unfortunately, expression of proteins cannot be controlled as the inducer tryptophan is degraded continuously by the enzyme tryptophanase encoded by the *tna*A gene. Every time expression is induced, the *tna*A gene is expressed too. For controlled overexpression of proteins, a system is needed in which the inducer is not degraded. To overcome this problem, the tryptophanase deletion mutant *Nab. magadii* L13Δ*tna*A was constructed in this study. The plasmid

pΔ*tna*A::nov^R harbors up- and downstream region of the *tna*A gene, which are interrupted by a novobiocin resistant cassette (Nov^R) (Fig. 15). The plasmid was used for homologous recombination that leads to replacement of the *tna*A gene in the chromosome by Nov^R (Fig. 16). A proper double crossover was achieved and the strain having the deletion in the chromosome was passaged in order to get a homozygous mutant. Homozygation of *Nab. magadii* L13Δ*tna*A was achieved after 17 passages, which was confirmed by southern blot analysis (Fig. 20).

Next, the phenotype of *Nab. magadii* L13Δ*tna*A has to be analyzed: growth behavior should be compared to the wild type strain *Nab. magadii* L13 in rich medium NVM+ as well as in mineral medium NMMb+ - with and without adding tryptophan. Furthermore, western blot analysis using an antibody that detects the tryptophanase should be performed in order to make finally clear that the deletion mutant does not express and contain copies of wild type *tna*A gene. Therefore, antibody production is currently in progress. In order to test, whether overexpression of proteins is successful in *Nab. magadii* L13Δ*tna*A upon induction with tryptophan, the strain will be transformed with plasmids harboring different proteins under control of p*tna*N. The proteins gpE or $gp34_{52}$ would be a good choice, as antibodies already exist in the laboratory.

Hopefully, with *Nab. magadii* L13Δ*tna*A a system could be established that enables overexpression and purification of proteins from ϕCh1 as well as from *Nab. magadii*. As these proteins are adapted to the high salt intracellular environment of *Nab. magadii*, purification under native conditions will provide proper folded proteins, a property that cannot be achieved by heterologous expression using for example the well-established over-expression strains of *E. coli*.

3.2. ϕCh1 ORF79 - a putative regulator of gene expression

At the beginning of studying ORF79 nothing was known about the putative function. The open reading frame has a size of 791bp, and the translated protein a size of 28.7 kDa. Alignment studies couldn't reveal similarities to other sequences or genes with known function [98]. Investigation of ORF79 started with the construction of the deletion mutant *Nab. magadii* L11Δ79 by Regina Selb in 2010. Growth and lysis behavior of the mutant strain have been compared to the wild type strain *Nab. magadii* L11. Lysis of the mutant strain occurred 24 hours earlier than in the wild type, which was the first indicator of a putative regulatory function of ORF79 [110]. Later, the mutant strain was complemented with a plasmid that provides an intact version of ORF79 under control of the constitutive promoter 49. This promoter was chosen due to lack of information of the ORF79 promoter. Complementation was successful as the growth and lysis behavior of the wild type strain L11 could be restored in the complemented strain *Nab. magadii* L11Δ79 (pNB102-p49-ORF79) [69]. Growth curve analysis of the 3 strains is illustrated in Figure 21.

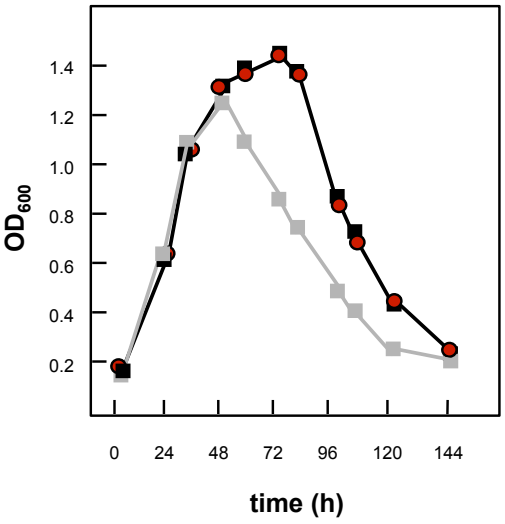

Figure 21: Growth curve analysis of *Nab. magadii* L11Δ79
The grey line represents growth of L11Δ79, the black line indicates the wild type L11. An altered growth and lysis behavior of L11Δ79 compared to L11 could be observed, lysis occurred earlier in the mutant strain. The complemented strain *Nab. magadii* L11Δ79 (pNB102-p49-ORF79) is represented by the red dots. The intact version of ORF79 on the plasmid is under control of the promoter 49, leading to constitutive expression of ORF79. The growth and lysis behavior of wild type strain L11 could be restored by complementation.

In order to investigate possible changes in the expression of different genes of ϕCh1, western blot analysis of the mutant and the complemented strain were performed. It was demonstrated, that certain proteins are differentially expressed in the strain *Nab. magadii* L11Δ79 and the wild type strain *Nab. magadii* L11. Expression of the major capsid protein E and the putative tail fiber protein $gp34_{52}$ were monitored during growth curve analysis. The corresponding genes ($ORF34_{52}$ and ORF11) are located upstream of ORF79. In the wild type, expression of protein E starts after about 52 hours whereas in the mutant strain, protein expression starts earlier. Expression of $gp34_{52}$ seemed to be

completely de-regulated. The protein was detectable in all samples of the mutant strain, which indicates that ORF79 has an influence on the expression of $gp34_{52}$. The complemented strain shows a comparable pattern of protein expression with the wild type, indicating that complementation was successful regarding $ORF34_{52}$ and ORF11 [69,111]. Results of the western blot analysis are summarized in Figure 22.

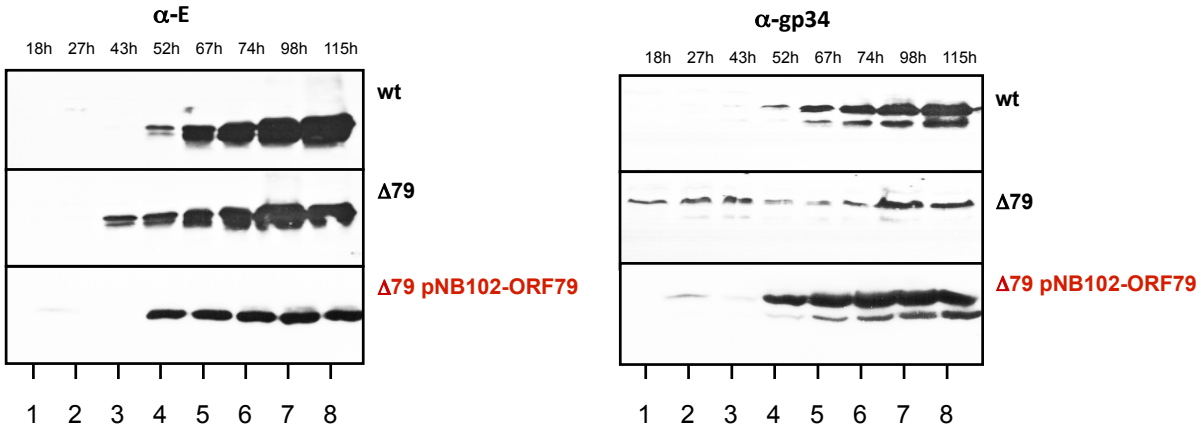

Figure 22: Western blot analysis of *Nab. magadii* L11, L11Δ79 and L11Δ79 (pNB102-p49-ORF79)
αE: Expression of the major capsid protein E could first be detected 52h (lane 4) after inoculation in the wild type strain L11 whereas in the mutant strain L11Δ79, protein E was detected already 43h (lane 3) after inoculation. **αgp34**: The expression of $gp34_{52}$ seemed to be completely de-regulated. In the wild type strain, expression of the protein was first detected 52h after inoculation. In the mutant strain, $gp34_{52}$ could be detected in all samples (lane 1-8). The complemented strain L11Δ79 (pNB102-p49-ORF79) shows nearly the same pattern of protein expression, which reflects the obtained results of the growth curve analysis.

In order to investigate the role of ORF79 in regulation, virus titer was performed using purified wild type ϕCh1, and particles isolated from the mutant strain, ϕCh1-Δ79 (Fig. 23). Two strains have been infected: *Nab. magadii* L13 (pNB102-p49-ORF79) and *Nab. magadii* L13 (pNB102). Successful infection would lead to plaque formation but infection of the strain *Nab. magadii* L13 expressing ORF79 failed. Neither ϕCh1 nor ϕCh1-Δ79 leaded to relevant plaque formation when plated on *Nab. magadii* L13 (pNB102-prom49-ORF79). This reduced infectivity further supports the putative regulatory function of ORF79. The plaque formation rate of *Nab. magadii* L13 (pNB102) infected with ϕCh1-Δ79 exceeds the plaque formation rate obtained from infection with wild type ϕCh1, which also indicates a regulator function of ORF79 [69].

Strain	ϕCh1 wt (pfu/ml)	ϕCh1-Δ79 (pfu/ml)
Nab. magadii L13 (pNB102)	1 x 10^8	3 x 10^7
Nab. magadii L13 (pNB102-ORF79)	<1 x 10^1	<1 x 10^1

Figure 23: Plaque forming units obtained from infection of *Nab. magadii* L13 (pNB102) and *Nab. magadii* L13 (pNB102-p49-ORF79) with wild type ϕCh1 and ϕCh1-Δ79.
The plaque formation rate of *Nab. magadii* L13 (pNB102) infected with ϕCh1 reflects infection rate of an infected L13 wild type strain. The pfu/ml obtained from infection with ϕCh1-Δ79 exceeds the pfu/ml value obtained from infection with ϕCh1. Infection of the strain *Nab. magadii* L13 (pNB102-p49-ORF79) failed. No relevant plaque formation was obtained from the infection with ϕCh1 wild type and ϕCh1-Δ79.

3.2.1. Influence of the gene product of ORF79 on expression of $ORF34_{52}$

By western blot analysis, it was demonstrated that expression of the putative tail fiber protein $gp34_{52}$ is altered in the deletion mutant *Nab. magadii* L11Δ79 (Fig. 22). A de-regulation is indicated as the protein could be detected during the whole life cycle of the mutant strain, whereas in the wild type strain *Nab. magadii* L11, expression starts about 52 hours after inoculation. The putative regulatory effect of gp79 on the expression of $ORF34_{52}$ was further analyzed in this study.

Co-expression of ORF79 and $ORF34_{52}$ in *Nab. magadii* L13 and Western blot analysis

In order to examine a regulatory function of gp79 on the expression of $ORF34_{52}$, both reading frames were co-expressed in *Nab. magadii* L13. Therefore, two plasmids were constructed and transformed in *Nab. magadii* L13 as described in "Material and Methods". The plasmid pRo-5 provides the sequence of ORF79 that is under control of the inducible promoter p*tna*N (pRo5-p*tna*N-ORF79). The plasmid pNB102 harbors the sequence of $ORF34_{52}$ including its own promoter (pNB102-$ORF34_{52}$). Figure 24 illustrates the plasmid configuration.

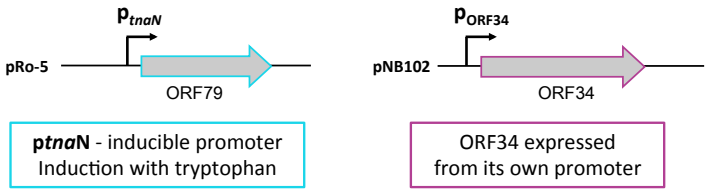

Figure 24: pRo5-p*tna*N-ORF79 and pNB102-$ORF34_{52}$
ORF79 is under control of the inducible promoter p*tna*N, expression of ORF79 can be induced with tryptophan. $ORF34_{52}$ is expressed from its own promoter in order to examine whether ORF79 influences the expression.

The strain *Nab. magadii* L13 (pRo5-p*tna*N-ORF79, pNB102-ORF34$_{52}$) was grown in mineral medium NMMb+, which is free of tryptophan. In mineral medium, cells produce huge amounts of carotenoid pigments. This becomes visible by the pink color of the culture in the colorless medium, and the color becomes more and more intense the denser the culture gets. Upon adding tryptophan to the medium, cultures developed different colors depending on the period of exposure to tryptophan, shown in Figure 25. The left flask contains an un-induced culture, having a pink color. The flask in the middle was induced with tryptophan only once during growth analysis, leading to an orange color of the culture. The right flask contains culture that was induced daily leading to a brownish color. Measurement of the optical density was done at 700nm instead of 600nm because the pigments are supposed to have a maximum of absorption between 500 and 650nm.

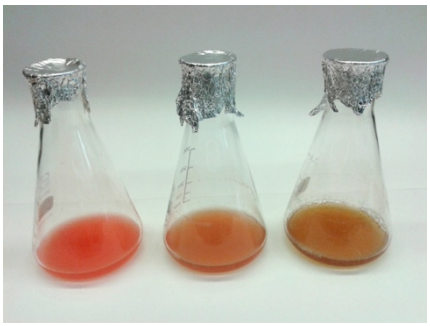

Figure 25 *Nab. magadii* L13 grown in minimal medium

Induced expression of ORF79 leads to a decrease in the production of gp34$_{52}$

A pre-culture of *Nab. magadii* L13 (pRo5-p*tna*N-ORF79, pNB102-ORF34$_{52}$) was prepared and used to inoculate NMMb+ medium to an OD_{700} of 0.1. This culture was split into three in order to set up three different situations for the experimental procedure. One culture was induced daily with 2mM tryptophan and the second culture was induced only once, at the beginning of the analysis. By adding tryptophan to the medium the promoter p*tna*N is induced and expression of ORF79 starts: ORF79 and ORF34$_{52}$ are co-expressed in the cell. The third culture served as a control: expression of ORF79 was not induced with tryptophan and only ORF34$_{52}$ is expressed. Incubation of the three cultures was done at 37°C with agitation. The optical density (OD_{700}) of the cultures was measured daily and protein samples for western blot analysis were taken and prepared as described in "Material and Methods". The α-gp34 antibody was used for detection (preparation and dilution of α-gp34 see "Material and Methods"). The results are illustrated in Figure 26. It could be demonstrated that gp79 has an influence on the expression of gp34$_{52}$.

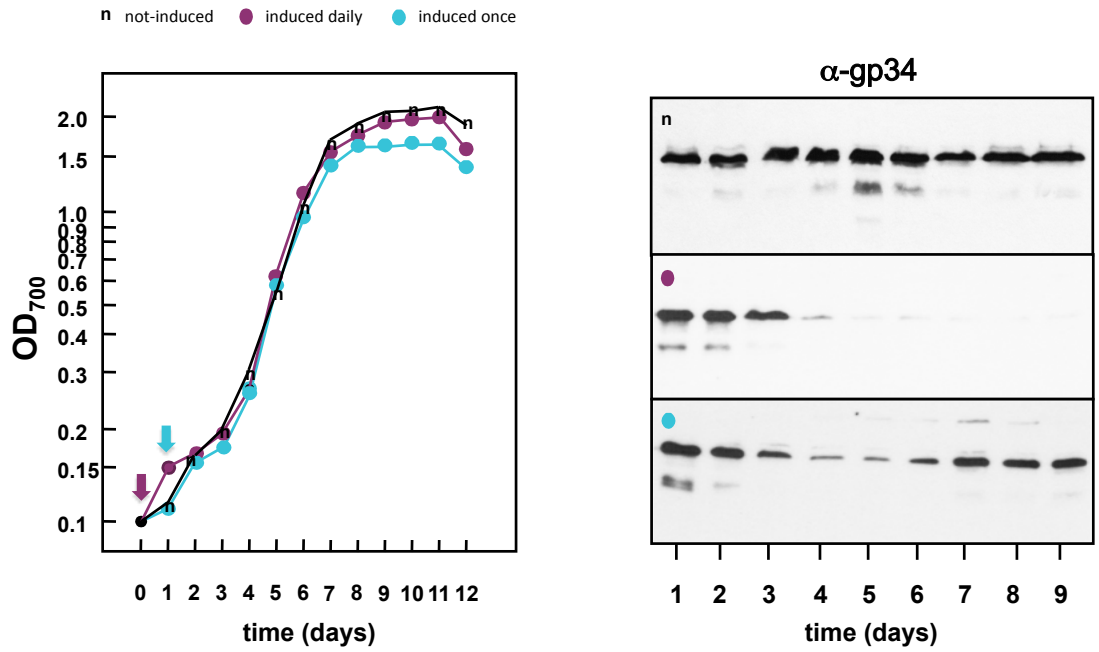

Figure 26: Growth kinetics and Western blot analysis of *Nab. magadii* L13 (pRo5-p*tna*N-ORF79, pNB102-ORF34$_{52}$)
Nab. magadii L13 (pRo5-p*tna*N-ORF79, pNB102-ORF34$_{52}$) was inoculated to an OD_{700} of 0.1. The culture was split into three: an un-induced culture served as a control, one culture was induced with tryptophan only once on day one and the third culture was induced daily. Incubation was done at 37°C, with agitation. The arrows at the growth curve indicate the time-point of induction. Growth kinetics of the 3 cultures are similar. Protein samples for western blot analysis were taken at each time-point. Samples 1-9 (lane 1-9) were further analyzed by western blot using the α-gp34 antibody. For the un-induced culture, a constitutive expression of gp34$_{52}$ could be detected which is demonstrated by the uppermost blot. The middle blot demonstrates the expression of gp34$_{52}$ in the culture that was induced daily. At the beginning of induction gp34$_{52}$ could be detected, but the signal started to get weaker on day 3 and disappeared for the subsequent samples. The lowermost western blot shows gp34$_{52}$ expression in the culture induced solely on day one. Expression of gp34$_{52}$ could be detected in all samples, but upon induction of ORF79 the signal started to get weaker on day 3 and finally came up again after 3 days. (For western blot analysis, same amounts of protein were applied, control via coomassie staining.)

3.2.2. Expression of ORF79 in the wild type strain *Nab. magadii* L11

Another attempt to demonstrate that ORF79 has a regulatory effect, the open reading frame was expressed in the lysogenic wild type strain *Nab. magadii* L11. The plasmid pNB102-p49-ORF79 was transformed into the strain L11 and growth curve analysis was performed. A pre-culture of the strains *Nab. magadii* L11 (pNB102-p49-ORF79) and Nab. *magadii* L11 (pNB102) in rich medium were used to inoculate NVM+ to an OD_{600} of 0.1. Incubation was done at 37°C with agitation, the optical density (OD_{600}) was measured daily, samples for western blot analysis were taken daily and prepared as described in "Material and Methods". Protein expression of the major capsid protein E and the putative tail fiber protein gp34$_{52}$ were monitored; the α-E and α-gp34 antibodies were used for

detection (preparation of antibodies see "Material and Methods"). The results are summarized in Figure 27. The obtained results further indicate the putative repressor function of ORF79.

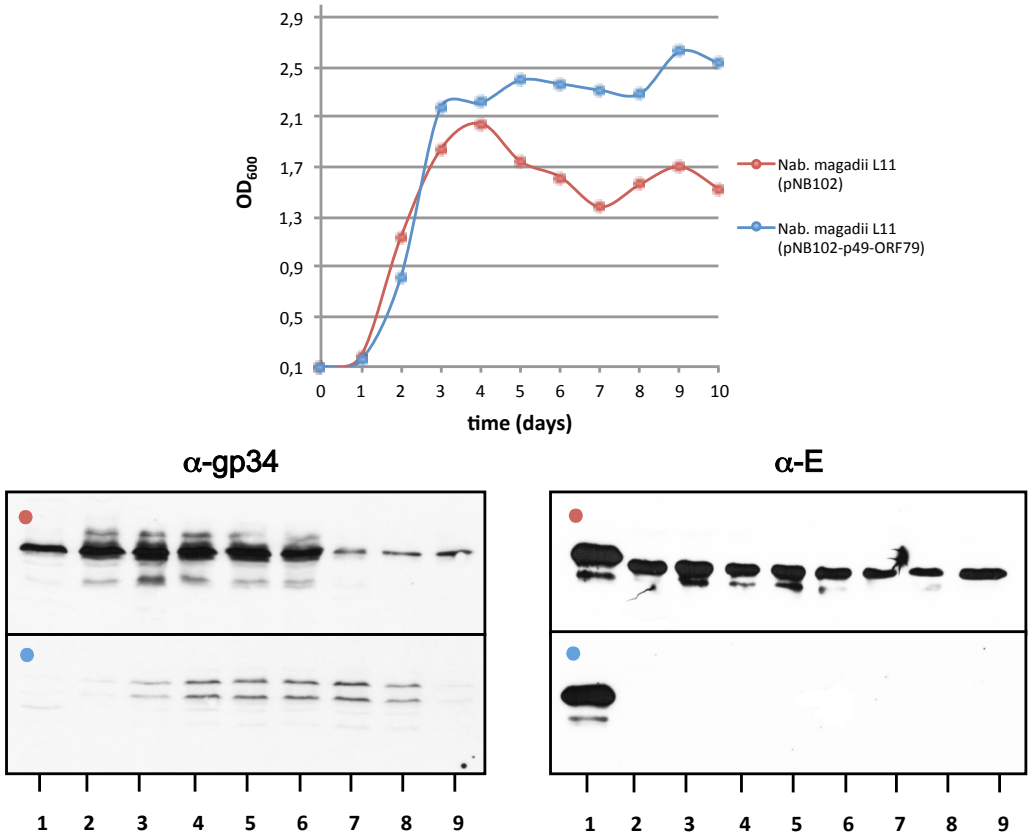

Figure 27: Growth kinetics and Western blot analysis of the strain *Nab. magadii* L11 (pNB102-p49-ORF79)
On the plasmid pNB102-p49-ORF79, ORF79 is under control of the promoter 49, leading to a constitutive expression of the protein. As a consequence, lysis of the strain *Nab. magadii* L11 (pNB102-p49-ORF79) is reduced compared to *Nab. magadii* L11 (pNB102). Protein samples were prepared during growth curve analysis, and samples of day 1-9 were used for western blot analysis of $gp34_{52}$ expression. The according blot shows that compared to *Nab. magadii* L11 (pNB102), expression of $gp34_{52}$ is reduced in *Nab. magadii* L11 (pNB102-p49-ORF79). For the western blot using the α-E antibody, samples of day 1-8 were used (lane 2-9). Lane 1 shows the positive control - purified protein E. No expression of the major capsid protein could be detected in the strain *Nab. magadii* L11 (pNB102-p49-ORF79).
(For western blot analysis, same amounts of protein were applied, control via coomassie staining.)

3.2.3. Discussion

The deletion mutant *Nab. magadii* L11Δ79 provided first indications for a regulatory function of ORF79. Compared to the lysogenic wild type strain *Nab. magadii* L11, the mutant strain showed an earlier onset of lysis (Fig. 21). Furthermore it was demonstrated that the deletion of ORF79 has an effect on expression of certain ϕCh1 proteins. Western blot analysis showed that expression of

$gp34_{52}$ is de-regulated in the deletion mutant, and the expression of the major capsid protein E starts earlier (Fig. 22). *Nab. magadii* L11Δ79 was complemented with the plasmid pNB102-p49-ORF79 that provides an intact version of ORF79 under control of the constitutive promoter of ORF49. The phenotype of the wild type strain *Nab. magadii* L11 could be restored: the complemented strain *Nab. magadii* L11 (pNB102-p49-ORF79) showed a comparable pattern of protein expression as well as the growth and lysis behavior of the wild type L11 (Fig. 21 and 22). Virus titer assays were performed in order to investigate the influence of ORF79 on regulatory processes. Wild type ϕCh1 and mutant ϕCh1-Δ79 particles were used for the infection and it could be demonstrated that the ORF79 has a dramatic effect on ϕCh1 development (Fig. 23). All these data indicate that ϕCh1 ORF79 actually has a putative regulatory function in the lysogenic life cycle of ϕCh1.

In course of this study, co-expression of ORF79 and $ORF34_{52}$ was performed in *Nab. magadii* L13 whereby it could be demonstrated that induced expression of gp79 has an influence on the expression of $gp34_{52}$. Upon induction of ORF79 expression, the production of $gp34_{52}$ decreased, which was demonstrated by western blot analysis (Figure 26). By daily induction of ORF79 expression, expression of $gp34_{52}$ decreased at the beginning of growth and was no longer detectable in the latest samples. The culture, which was induced only once, on day one, showed a decreased expression of $gp34_{52}$ about two days after induction. Tryptophan is degraded in the cell and therefore it is assumed that expression of ORF79 stops. Thereby, the signal for $gp34_{52}$ expression appears again after app. 3 days. The co-expression of ORF79 and $ORF34_{52}$ was performed in *Nab. magadii* L13 meaning that only the two ϕCh1 reading frames ORF79 and $ORF34_{52}$ are present in the cells. Therefore it could be demonstrated that no other open reading frame of ϕCh1 has an influence on the function of gp79. Nevertheless, by using the host strain as an expression system, it could not be answered if factors of *Nab. magadii* L13 itself have an influence on the putative repressor function of the protein. The results of this experiment provide one more indication for the regulatory function of ORF79. Nevertheless, an additional experiment is needed for the analysis by co-expression to investigate the specificity of ORF79. An ORF of ϕCh1 that is not affected by the expression of ORF79 should serve as control in this experiment.

The regulatory effect of ORF79 on $gp34_{52}$ was also shown by constitutive expression of ORF79 in the lysogenic strain *Nab. magadii* L11. The strain harbors the provirus, meaning that ϕCh1 is integrated into the host chromosome. It could be demonstrated that expression of ORF79 leads to a reduced infectivity of ϕCh1 as lysis of the strain *Nab. magadii* L11 (pNB102-p49-ORF79) is reduced (Fig. 27).

Western blot analysis showed, that in this strain the expression of $gp34_{52}$ is reduced compared to the wild type, and moreover, expression of gpE could not be detected for the strain expressing ORF79 (Fig.27). These results further indicate the putative repressor function of ORF79.

All the obtained data provide good evidence that the gene product ORF79 is a putative repressor of ϕCh1 and that it has regulatory function during the lysogenic life cycle of the virus. Further experiments should provide insights into the DNA binding capacity of gp79. Most repressor molecules of bacteriophages contain a helix-turn-helix domain for DNA binding. The sequence of ORF79 lacks such a motif. To find out more about the DNA binding property of gp79 electrophoretic mobility shift assays should be performed. Unfortunately, purification of gp79 under native conditions failed, as over-expression in *Nab. magadii* L13 could not be achieved until now. Purification under native conditions was hardly achieved with *E. coli* and all attempts to perform band shift assays with purified gp79 failed. Therefore, the *Nab. magadii* deletion mutant L13Δ*tna*A was developed in course of this master thesis which hopefully provides a tool for over-expressing proteins of ϕCh1 as well as of *Natrialba magadii* under native conditions. Another future attempt should be to analyze when expression of ORF79 actually starts during the lysogenic life cycle of ϕCh1. Protein expression can be monitored by western blot analysis, which could not be performed until now because antibodies detecting gp79 were not available. Antibody development is currently in progress, therefore analysis could be performed soon. Another approach to analyze expression of ORF79 is reverse transcription PCR. Gene expression could be monitored during a growth curve analysis by preparing RNA samples for RT-PCR.

3.3. ϕCh1 ORF56 - Indications for a regulatory function

3.3.1. Characterization of ORFs of ϕCh1 with indications for regulators

ORF21, ORF55 and ORF56 of ϕCh1, that are predicted to have regulatory function, were analyzed in this study. Upon sequence alignment studies all three ORFs are predicted to be transcriptional regulators. Furthermore, ORF55 and ORF21 contain a helix-turn-helix motif for DNA binding, which is a typical domain for the majority of repressor molecules of bacteriophages. Therefore, these two ORFs seemed to be good candidates for putative regulators of gene expression. All three ORFs have been cloned into the plasmids pNB102 and pRo-5 (for details on the cloning strategy see "Material and Methods") and transformed into the wild type strain *Nab. magadii* L11 and the cured strain *Nab. magadii* L13 in order to examine if expression of the respective ORF has an influence on growth and lysis behavior. Transformation was successful for all constructs, excepting for pNB102-ORF56. The plasmid could hardly be transformed into *Nab. magadii* L13, and several attempts to transform *Nab. magadii* L11 failed. Growth curve analysis has been performed with the transformed strains expressing the three ORFs. Pre-cultures of the strains *Nab. magadii* L13/L11 (pRo-5-ORF21 or pNB102-ORF21), *Nab. magadii* L13/L11 (pRo-5-ORF55 or pNB102-ORF55), *Nab. magadii* L13/L11 (pRo-5-ORF56 or pNB102-ORF56) and *Nab. magadii* L13/L11 (pRo-5 or pNB102) in rich medium have been used to inoculate NVM+ to an OD_{600} of 0.1. Incubation was done at 37°C with agitation and the optical density (OD_{600}) was measured daily. Growth curve analysis has been performed with at least 4 clones of each strain. With regard to the used plasmid, no differences in growth behavior could be detected. Selected data obtained from growth curve analysis with the strains harboring the pRo-5 constructs are presented in Figure 28 and Figure 29.

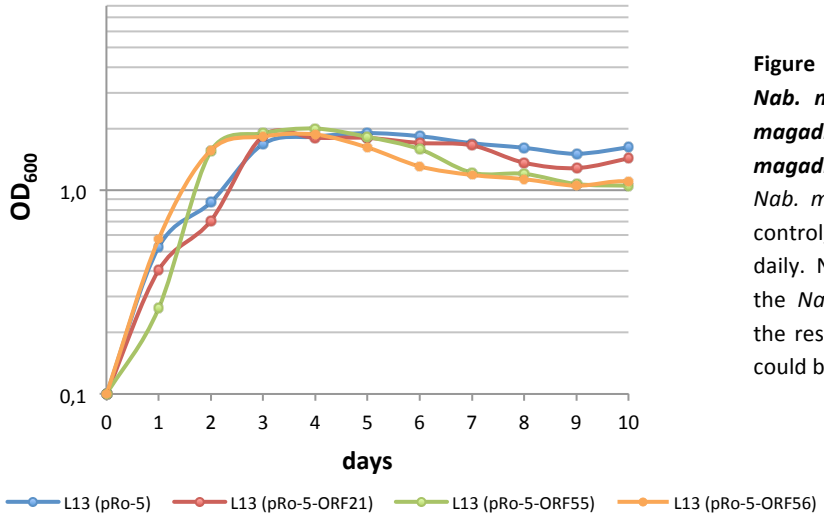

Figure 28: Growth kinetics of the strains *Nab. magadii* L13 (pRo-5-ORF21), *Nab. magadii* L13 (pRo-5-ORF55) and *Nab. magadii* L13 (pRo-5-ORF56).
Nab. magadii L13 (pRo-5) served as the control, the optical density was measured daily. No differences in growth between the *Nab. magadii* L13 strains expressing the respective ORF and the control strain could be detected.

Figure 28 illustrates, that with regard to growth, the *Nab. magadii* L13 strains expressing ORF21, ORF55 and ORF56 behave similar to the control strain *Nab. magadii* L13 harboring the empty plasmids.

Expression of the 3 ORFs in the wild type strain *Nab. magadii* L11 revealed that the expression of one ORF has an effect on growth and lysis behavior. Whereas the strains *Nab. magadii* L11 (pRo-5-ORF21) and L11 (pRo-5-ORF55) show the growth and lysis behavior of the wild type strain L11 (data not shown), for the strain expressing ORF56 nearly no lysis could be observed. The growth curve analysis is demonstrated in Figure 29. Analysis was repeated with 4 different clones, and for each, the same growth and lysis behavior could be observed. Expression of ORF56 in the wild type strain *Nab. magadii* L11 reduces the lysis characteristics, which was the first indication for a putative regulatory function of this open reading frame. Therefore all following experiments were solely done with *Nab. magadii* L11 (pRo-5-ORF56).

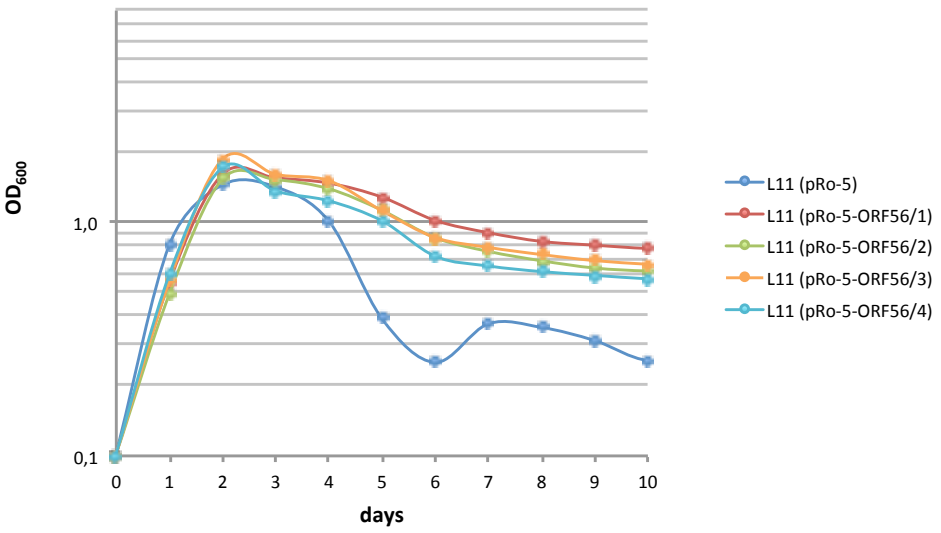

Figure 29: Growth kinetics of *Nab. magadii* L11 (pRo-5-ORF56)
Nab. magadii L11 harboring the empty plasmid pRo-5 served as a control. 4 different clones of *Nab. magadii* L11 (pRo-5-ORF56) were analyzed, all showing the same growth behavior. After 2-3 days, lysis of the wild type strain starts. Compared to the control, nearly no lysis could be observed for the 4 different clones.

3.3.2. Virus titer and Western blot analysis

Growth curve analysis of *Nab. magadii* L11 (pRo-5-ORF56) was repeated and performed as described above. Samples for western blot analysis were taken daily, and prepared as described in "Material and Methods". Additionally, every day 1ml of the supernatant was taken. Chloroform was added to

the 1ml and the sample was stored at room temperature. The supernatant was used to infect *Nab. magadii* L13 - virus titer analysis has been performed as described in "Material and Methods". Growth curve and results of the virus plaque assay are summarized in Figure 30.

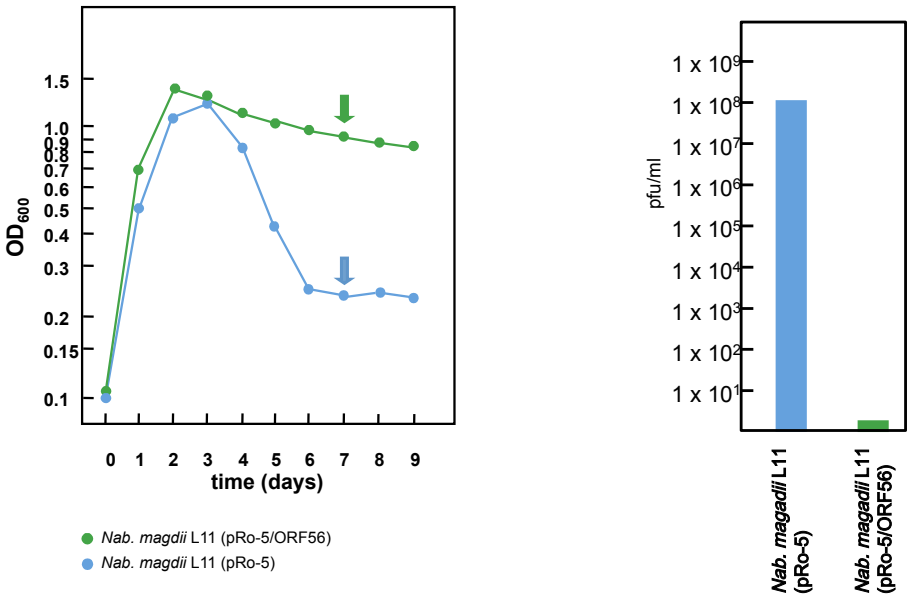

Figure 30: Growth kinetics and Virus titer analysis of *Nab. magadii* L11 (pRo-5/ORF56)
The strain *Nab. magadii* L11 (pRo-5) starts with lysis after about 3 days. The strain *Nab. magadii* L11 (pRo-5/ORF56) shows nearly no lysis behavior, at best there is only reduced lysis, as it was already demonstrated in Fig. 29. The arrows indicate the time point of which samples of the supernatant that were used to infect *Nab. magadii* L13 in course of the plaque assay. As expected, no relevant plaque formation rate was obtained from the supernatant sample of *Nab. magadii* L11 (pRo-5/ORF56), which reflects the reduced infectivity of ϕCh1. The pfu/ml obtained from the supernatant of L11 (pRo-5) reflects an infection rate obtained for the wild type strain L11.

Virus titer analysis demonstrated the reduced development of ϕCh1 when ORF56 is expressed in the wild type strain *Nab. magadii* L11. In order to visualize this phenotype on the protein level, western blot analysis was performed. Expression of the major capsid protein E and the putative tail fiber protein $gp34_{52}$ was monitored during growth curve analysis. The α-gp34 and α-E antibodies were used for detection (preparation of the used antibodies see "Material and Methods"). The results are illustrated in Figure 31.

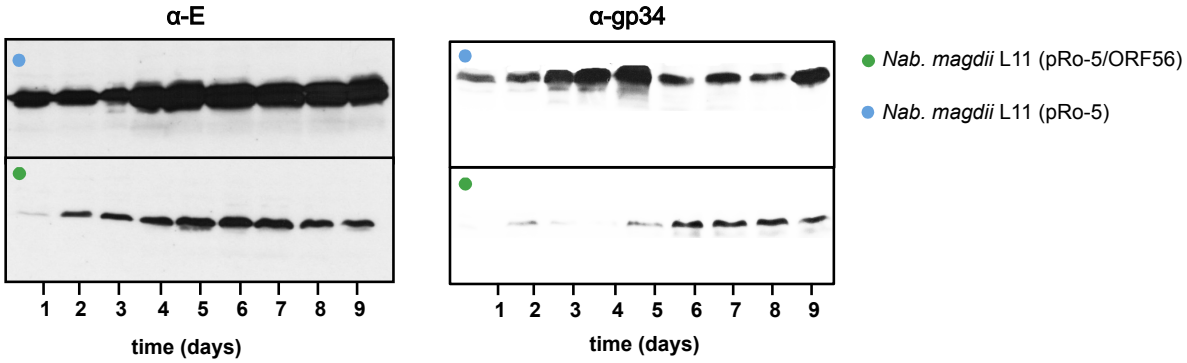

Figure 31: Western blot analysis of *Nab. magadii* L11 (pRo-5) *and Nab. magadii* L11 (pRo-5/ORF56)
Compared to the strain *Nab. magadii* L11 (pRo-5), expression of the viral proteins gpE and $gp34_{52}$ is reduced in the strain *Nab. magadii* L11 (pRo-5/ORF56) which further reflects the reduced infectivity of ϕCh1. (For western blot analysis, same amounts of protein were applied, control via coomassie staining.)

According to the weak lysis behavior of *Nab. magadii* L11 (pRo-5/ORF56) a reduced number of virus plaques in the virus titer assay was obtained, and the expression of viral proteins is reduced as it could be demonstrated for the major capsid protein E and $gp34_{52}$. Expression of ORF56 seemed to reduce the infectivity. But it is also possible that this reduced infectivity is a consequence of a lost provirus. Therefore it was also necessary to demonstrate that the provirus still exists in the strain *Nab. magadii* L11 (pRo-5/ORF56) by southern blot analysis.

3.3.3. Southern blot analysis

The chromosomal DNA of *Nab. magadii* L11 (pRo-5) and *Nab. magadii* L11 (pRo-5/ORF56) was isolated as described in "Material and Methods". The DNA was digested with *Bgl*II and the resulted fragments were separated using a 0.8% agarose gel. Biotinylated hybridization probes have been synthesized by PCR using the primers Soj-5 and Soj-3. Purified ϕCh1 DNA was used as a template. The probe has a size of 764bp and detects the DNA fragment of 3.130bp. First of all, concentration of the used chromosomal DNA had to be adjusted. Before the agarose gel was used for the blotting procedure, the DNA was visualized using ethidium bromide for staining to ensure a similar concentration of chromosomal DNA (Figure 32, left panel). Results of the southern blot are shown in Figure 32. It could be demonstrated that the provirus is integrated into the chromosome of *Nab. magadii* L11 (pRo-5/ORF56).

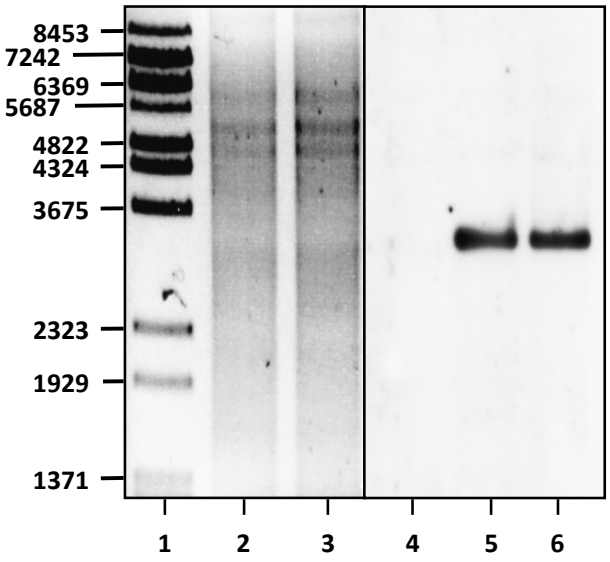

Figure 32: Southern blot analysis of *Nab. magadii* L11 (pRo-5/ORF56)
Left panel: the concentration of the restricted chromosomal DNA of *Nab. magadii* L11 (pRo-5) and *Nab. magadii* L11 (pRo-5/ORF56) was adjusted, which is demonstrated in lane 2 (L11/pRo-5) and lane 3 (L11/pRo-5-ORF56). The right panel shows the southern blot: a signal of nearly same intensity could be detected for *Nab. magadii* L11 (pRo-5) (lane 5) *and Nab. magadii* L11 (pRo-5/ORF56) (lane 6).
0.8% agarose gel, lane 1, 4: Marker λ*Bst*EII

3.3.4. Discussion

Three open reading frames of ϕCh1 with unknown function were analyzed in this study. Upon bioinformatical predictions ORF21, ORF55 and ORF56 are suggested to be putative transcriptional regulators. ORF21 and ORF55 were supposed to be good candidates as they contain a helix-turn-helix motif. This DNA-binding domain is found in the majority of repressor molecules of bacteriophages. Therefore it was surprisingly that ORF56, that lacks the helix-turn-helix motif, was the only ORF that shows an influence on the lysogenic life cycle of ϕCh1. ORF56 has a size of 521bp and the gene product a size of 19.6kDa. Growth curve analysis demonstrated that compared to the lysogenic wild type strain *Nab. magadii* L11, the strain expressing ORF56 on a plasmid shows a different growth behavior: nearly no lysis could be observed for *Nab. magadii* L11 (pRo-6/ORF56) (Fig. 30). Furthermore, plaque assays were performed, demonstrating that plaque formation obtained from infection of *Nab. magadii* L13 with lysate samples of *Nab. magadii* L11 (pRo-6/ORF56) was reduced (Fig. 30). Western blot analysis demonstrated that expression of viral proteins is reduced in *Nab. magadii* L11 (pRo-6/ORF56) (Fig. 31). In order to exclude that the reduced infectivity is due to a lost provirus of the strain *Nab. magadii* L11 (pRo-6/ORF56), southern blot analysis was performed.

All the obtained data demonstrated that ORF56 reduces the infectivity of ϕCh1, indicating a putative regulatory function of this open reading frame. Next steps in analyzing ORF56 should identify when expression of the protein starts during the lysogenic life cycle. Antibody production for gp56 is currently in progress, whereby western blot analysis should be performed in order to monitor gp56

expression. As already mentioned, the sequence of ORF56 lacks a helix-turn-helix motif mediating DNA binding. Band shift assay should be performed in order to demonstrate a putative DNA binding function of gp56. The problem of protein purification was also discussed for ORF79. As it is not possible to purify these proteins under native conditions, a *Nab. magadii* L13Δ*tna*A deletion mutant was constructed in this thesis with the aim to enable over-expression of proteins and their purification under native conditions.

4. References

1. Scamardella, J. M. Not plants or animals: a brief history of the origin of Kingdoms Protozoa, Protista and Protoctista. *Int. Microbiol.* **2,** 207–16 (1999).

2. Chatton, E. *Titres et Travoux Scientifiques (1906-1937)*. (E. Sottano, Sete, France, 1938).

3. Woese, C. & Fox, G. Phylogenetic structure of the prokaryotic domain: the primary kingdoms. *… Natl. Acad. Sci.* **74,** 5088–5090 (1977).

4. Woese, C. R., Kandlert, O. & Wheelis, M. L. Towards a natural system of organisms: Proposal for the domains. *… Natl. Acad. Sci.* **87,** 4576–4579 (1990).

5. Huber, H. *et al.* A new phylum of Archaea represented by a nanosized hyperthermophilic symbiont. *Nature* **417,** 63–67 (2002).

6. Barns, S. M., Delwiche, C. F., Palmer, J. D. & Pace, N. R. Perspectives on archaeal diversity, thermophily and monophyly from environmental rRNA sequences. *Proc. Natl. Acad. Sci.* **93 ,** 9188–9193 (1996).

7. Farlow, W. On the nature of the peculiar reddening of salted codfish during the summer season. *U.S. Fish Comm. Rep. 1878* 969–973 (1880).

8. Rothschild, L. J. & Mancinelli, R. L. Life in extreme environments. *Nature* **409,** 1092–101 (2001).

9. Forterre, P., Brochier, C. & Philippe, H. Evolution of the Archaea. *Theor. Popul. Biol.* **61,** 409–422 (2002).

10. DeLong, E. Everything in moderation: Archaea as “non-extremophiles.”*Curr. Opin. Genet. Dev.* (1998).

11. Cavicchioli, R. Archaea--timeline of the third domain. *Nat. Rev. Microbiol.* **9,** 51–61 (2011).

12. Allers, T. & Mevarech, M. Archaeal genetics - the third way. *Nat. Rev. Genet.* **6,** 58–73 (2005).

13. DeLong, E. F. & Pace, N. R. Environmental diversity of bacteria and archaea. *Syst. Biol.* **50,** 470–8 (2001).

14. Cavicchioli, R. Cold-adapted archaea. *Nat. Rev. Microbiol.* **4,** 331–43 (2006).

15. Marteinsson, V. T. *et al.* Thermococcus barophilus sp. nov., a new barophilic and hyperthermophilic archaeon isolated under high hydrostatic pressure from a deep-sea hydrothermal vent. *Int. J. Syst. Bacteriol.* **49 ,** 351–359 (1999).

16. Pikuta, E. V., Hoover, R. B. & Tang, J. Microbial Extremophiles at the Limits of Life. *Crit. Rev. Microbiol.* **33,** 183–209 (2007).

17. Jolivet, E. Thermococcus gammatolerans sp. nov., a hyperthermophilic archaeon from a deep-sea hydrothermal vent that resists ionizing radiation. *Int. J. Syst. Evol. Microbiol.* **53,** 847–851 (2003).

18. Gribaldo, S. & Brochier-Armanet, C. The origin and evolution of Archaea: a state of the art. *Philos. Trans. R. Soc. Lond. B. Biol. Sci.* **361,** 1007–22 (2006).

19. Jarrell, K. F. *et al.* Major players on the microbial stage: why archaea are important. *Microbiology* **157,** 919–936 (2011).

20. Van de Vossenberg, J. L., Driessen, a J. & Konings, W. N. The essence of being extremophilic: the role of the unique archaeal membrane lipids. *Extremophiles* **2,** 163–70 (1998).

21. Matsumi, R., Atomi, H., Driessen, A. J. M. & van der Oost, J. Isoprenoid biosynthesis in Archaea--biochemical and evolutionary implications. *Res. Microbiol.* **162,** 39–52 (2011).

22. Sa, M. & Sleytr, U. W. E. B. S-Layer Proteins. *J. Bacteriol.* **182,** 859–868 (2000).

23. Albers, S.-V. & Meyer, B. H. The archaeal cell envelope. *Nat. Rev. Microbiol.* **9,** 414–26 (2011).

24. Kandler, O. & König, H. Cell wall polymers in Archaea (Archaebacteria). *Cell. Mol. Life Sci.* **54,** 305–8 (1998).

25. Brown, J. R. & Doolittle, W. F. Archaea and the prokaryote-to-eukaryote transition. *Microbiol. Mol. Biol. Rev.* **61,** 456–502 (1997).

26. Huet, J., Schnabel, R., Sentenac, A. & Zillig, W. Archaebacteria and eukaryotes possess DNA-dependent RNA polymerases of a common type. *EMBO J.* **2,** 1291–4 (1983).

27. De Koning, B., Blombach, F., Brouns, S. J. J. & van der Oost, J. Fidelity in archaeal information processing. *Archaea* **2010,** (2010).

28. Bell, S. D. & Jackson, S. P. Transcription and translation in Archaea: a mosaic of eukaryal and bacterial features. *Trends Microbiol.* **6,** 222–228 (1998).

29. Gregor, D. & Pfeifer, F. In vivo analyses of constitutive and regulated promoters in halophilic archaea. *Microbiology* **151,** 25–33 (2005).

30. Bell, S. D. Archaeal transcriptional regulation--variation on a bacterial theme? *Trends Microbiol.* **13,** 262–5 (2005).

31. Barry, E. R. & Bell, S. D. DNA replication in the archaea. *Microbiol. Mol. Biol. Rev.* **70,** 876–87 (2006).

32. Lundgren, M., Andersson, A., Chen, L., Nilsson, P. & Bernander, R. Three replication origins in Sulfolobus species: Synchronous initiation of chromosome replication and asynchronous termination. *Proc. Natl. Acad. Sci. United States Am.* **101 ,** 7046–7051 (2004).

33. Lindås, A.-C. & Bernander, R. The cell cycle of archaea. *Nat. Rev. Microbiol.* **11,** 627–638 (2013).

34. Ishino, Y. & Ishino, S. Rapid progress of DNA replication studies in Archaea, the third domain of life. *Sci. China. Life Sci.* **55,** 386–403 (2012).

35. White, M. F. & Bell, S. D. Holding it together: chromatin in the Archaea. *Trends Genet.* **18,** 621–6 (2002).

36. Breuert, S., Allers, T., Spohn, G. & Soppa, J. Regulated polyploidy in halophilic archaea. *PLoS One* **1,** e92 (2006).

37. Hansen, M. T. Multiplicity of Genome Equivalents in the Radiation-Resistant Bacterium Micrococcus Radiodurans. *J. Bacteriol.* **134,** 71–75 (1978).

38. Nagpal, P., Jafri, S., Reddy, M. A. & Das, H. K. Multiple chromosomes of Azotobacter vinelandii. *J. Bacteriol.* **171 ,** 3133–3138 (1989).

39. Malandrin, L., Huber, H. & Bernander, R. Nucleoid Structure and Partition in Methanococcus jannaschii: An Archaeon With Multiple Copies of the Chromosome. *Genet.* **152 ,** 1315–1323 (1999).

40. Ma, Y., Galinski, E. a, Grant, W. D., Oren, A. & Ventosa, A. Halophiles 2010: life in saline environments. *Appl. Environ. Microbiol.* **76,** 6971–81 (2010).

41. Oren, a. Diversity of halophilic microorganisms: Environments, phylogeny, physiology, and applications. *J. Ind. Microbiol. Biotechnol.* **28,** 56–63 (2002).

42. Andrei, A.-Ş., Banciu, H. L. & Oren, A. Living with salt: metabolic and phylogenetic diversity of archaea inhabiting saline ecosystems. *FEMS Microbiol. Lett.* **330,** 1–9 (2012).

43. Oren, A., Ventosa, A. & Grant, W. D. Proposed Minimal Standards for Description of New Taxa in the Order Halobacteriales. *Int. J. Syst. Bacteriol.* **47,** 233–238 (1997).

44. Fendrihan, S. *et al.* Europe PMC Funders Group Extremely halophilic archaea and the issue of long-term microbial survival. **5,** 203–218 (2011).

45. Oren, A. Bioenergetic Aspects of Halophilism. **63,** (1999).

46. Vossenberg, J. L. C. M. Van De, Driessen, A. J. M., Grant, W. D. & Konings, W. N. Lipid membranes from halophilic and alkali-halophilic Archaea have a low H^+ and Na^+ permeability at high salt concentration. *Extremophiles* 253–257 (1999).

47. Tenchov, B., Vescio, E. M., Sprott, G. D., Zeidel, M. L. & Mathai, J. C. Salt tolerance of archaeal extremely halophilic lipid membranes. *J. Biol. Chem.* **281,** 10016–23 (2006).

48. Tindall, B. J., Ross, H. N. M. & Grant, W. D. Natronobacterium gen. nov. and Natronococcus gen. nov., Two New Genera of Haloalkaliphilic Archaebacteria. *Syst. Appl. Microbiol.* **5,** 41–57 (1984).

49. Madern, D., Ebel, C. & Zaccai, G. Halophilic adaptation of enzymes. *Extremophiles* **4,** 91–8 (2000).

50. Lanyi, J. K. Salt-dependent properties of proteins from extremely halophilic bacteria. *Bacteriol. Rev.* **38,** 272–90 (1974).

51. Kamekura, M., Dyall-smith, M. L., Upasani, V., Ventosa, A. & Kates, M. Diversity of Alkaliphilic Halobacteria : Proposals for Transfer of Natronobacterium vacuolatum , Natronobacterium magadii , and Natronobacterium pharaonis to Halorubrum , Natrialba , and Natronomonas gen . nov ., Respectively, as Halorubrum. *Int. J. Syst. Bacteriol.* 853–857 (1997).

52. Horikoshi, K. Alkaliphiles : Some Applications of Their Products for Biotechnology. *Microbiol. Mol. Biol. Rev.* **63,** (1999).

53. Horikoshi, K. *Extremophiles Handbook*. (Springer, 2011).

54. De Castro, R. E., Maupin-Furlow, J. a, Giménez, M. I., Herrera Seitz, M. K. & Sánchez, J. J. Haloarchaeal proteases and proteolytic systems. *FEMS Microbiol. Rev.* **30,** 17–35 (2006).

55. D'Alessandro, C. P., De Castro, R. E., Giménez, M. I. & Paggi, R. a. Effect of nutritional conditions on extracellular protease production by the haloalkaliphilic archaeon Natrialba magadii. *Lett. Appl. Microbiol.* **44,** 637–42 (2007).

56. Jones, B. E., Grant, W. D., Duckworth, a W. & Owenson, G. G. Microbial diversity of soda lakes. *Extremophiles* **2,** 191–200 (1998).

57. Witte, A. *et al.* Characterization of Natronobacterium magadii phage phi Ch1, a unique archaeal phage containing DNA and RNA. *Mol. Microbiol.* **23,** 603–16 (1997).

58. Cline, S. W. & Doolittle, W. F. Efficient transfection of the archaebacterium Halobacterium halobium. *J. Bacteriol.* **169,** 1341–4 (1987).

59. Dyall-Smith, M. The halohandbook. (2009). at <www.haloarchaea.com>

60. Mayrhofer-Iro, M. *et al.* Utilization of virus ϕCh1 elements to establish a shuttle vector system for Halo(alkali)philic Archaea via transformation of Natrialba magadii. *Appl. Environ. Microbiol.* **79,** 2741–8 (2013).

61. Ng, W. L. & DasSarma, S. Minimal replication origin of the 200-kilobase Halobacterium plasmid pNRC100. *J. Bacteriol.* **175 ,** 4584–4596 (1993).

62. Zhou, M., Xiang, H., Sun, C. & Tan, H. Construction of a novel shuttle vector based on an RCR-plasmid from a haloalkaliphilic archaeon and transformation into other haloarchaea. *Biotechnol. Lett.* **26,** 1107–13 (2004).

63. Lam, W. L. & Doolittle, W. F. Mevinolin-resistant mutations identify a promoter and the gene for a eukaryote-like 3-hydroxy-3-methylglutaryl-coenzyme A reductase in the archaebacterium Haloferax volcanii. *J. Biol. Chem.* **267 ,** 5829–5834 (1992).

64. Holmes, M. L., Nuttall, S. D. & Dyall-Smith, M. L. Construction and use of halobacterial shuttle vectors and further studies on Haloferax DNA gyrase. *J. Bacteriol.* **173 ,** 3807–3813 (1991).

65. Kixmüller, D. & Greie, J.-C. Construction and characterization of a gradually inducible expression vector for Halobacterium salinarum, based on the kdp promoter. *Appl. Environ. Microbiol.* **78,** 2100–5 (2012).

66. Svoboda, T. Characterization of putative repressors of the temperate phage ϕCh1 and analysis of the flagellum operon as a putative receptor of ϕCh1. *Diploma thesis* (2011).

67. Large, A. *et al.* Characterization of a tightly controlled promoter of the halophilic archaeon Haloferax volcanii and its use in the analysis of the essential cct1 gene. *Mol. Microbiol.* **66,** 1092–106 (2007).

68. Kixmüller, D., Strahl, H., Wende, A. & Greie, J.-C. Archaeal transcriptional regulation of the prokaryotic KdpFABC complex mediating K(+) uptake in H. salinarum. *Extremophiles* **15,** 643–52 (2011).

69. Alte, B. Konstruktion einer Flagellum-Deletionsmutante in Natrialba magadii und Charakterisierung bestehender Natrialba magadii Mutanten. *Diploma thesis* (2011).

70. D'Herelle, F. An invisible microbe that is antagonistic to the dysentery bacillus. *Comptes rendus Acad. Sci. Paris* (1917).

71. D'Herelle, F. *The bacteriophage; It's role in immunity.* (Baltimore: Williams and Wilkins, 1922).

72. Prangishvili, D. Viruses of the Archaea : a View on the Viral World from the Perspective of Hyperthermophilic Viruses. (2011).

73. Stanley, W. M. Isolation of a Crystalline Protein Possessing the Properties of Tobacco-Mosaic Virus. *Science* **81,** 644–5 (1935).

74. Skern, T. *Coffee House Notes on Virology*. 190 (Facultas Verlags- und Buchhandels AG, Facultas Universitätsverlag, 2009).

75. Madigan, M., Martinko, J., Stahl, D. & Clark, D. *Brock Biology of Microorganisms.* (Benjamin-Cummings Publishing Company, San Francisco, 2012).

76. Torsvik, T. & Dundas, I. Bacteriophage of Halobacterium salinarium. *Nature* **248,** 2 (1974).

77. Prangishvili, D., Forterre, P. & Garrett, R. a. Viruses of the Archaea: a unifying view. *Nat. Rev. Microbiol.* **4,** 837–48 (2006).

78. Prangishvili, D., Garrett, R. a & Koonin, E. V. Evolutionary genomics of archaeal viruses: unique viral genomes in the third domain of life. *Virus Res.* **117,** 52–67 (2006).

79. Pietilä, M. K., Roine, E., Paulin, L., Kalkkinen, N. & Bamford, D. H. An ssDNA virus infecting Archaea: a new lineage of viruses with a membrane envelope. *Mol. Microbiol.* **72,** 307–319 (2009).

80. Pina, M., Bize, A., Forterre, P. & Prangishvili, D. The archeoviruses. *FEMS Microbiol. Rev.* **35,** 1035–54 (2011).

81. Häring, M., Vestergaard, G. & Rachel, R. Virology: independent virus development outside a host. *Nature* **426,** 1101–1102 (2005).

82. Brumfield, S. K. *et al.* Particle assembly and ultrastructural features associated with replication of the lytic archaeal virus sulfolobus turreted icosahedral virus. *J. Virol.* **83,** 5964–70 (2009).

83. Snyder, J. C., Brumfield, S. K., Peng, N., She, Q. & Young, M. J. Sulfolobus turreted icosahedral virus c92 protein responsible for the formation of pyramid-like cellular lysis structures. *J. Virol.* **85,** 6287–92 (2011).

84. Bize, A. *et al.* A unique virus release mechanism in the Archaea. *Proc. Natl. Acad. Sci. U. S. A.* **106,** 11306–11 (2009).

85. Atanasova, N. S., Roine, E., Oren, A., Bamford, D. H. & Oksanen, H. M. Global network of specific virus-host interactions in hypersaline environments. *Environ. Microbiol.* **14,** 426–40 (2012).

86. Dyall-Smith, M., Tang, S.-L. & Bath, C. Haloarchaeal viruses: how diverse are they? *Res. Microbiol.* **154,** 309–13 (2003).

87. Oren, a, Bratbak, G. & Heldal, M. Occurrence of virus-like particles in the Dead Sea. *Extremophiles* **1,** 143–9 (1997).

88. Sime-Ngando, T. *et al.* Diversity of virus-host systems in hypersaline Lake Retba, Senegal. *Environ. Microbiol.* **13,** 1956–72 (2011).

89. Schnabel, H. *et al.* Halobacterium halobium phage ϕH. *EMBO J.* **1,** 87–92 (1982).

90. Schnabel, H. An immune strain of Halobacterium halobium carries the invertible L segment of phage PhiH as a plasmid. *Proc. Natl. Acad. Sci. U. S. A.* **81,** 1017–20 (1984).

91. Guo, P., Bailey, S., Bodley, J. W. & Anderson, D. Charcterization of the small RNA of the bacteriophage phi 29 DNA packaging machine. *Nucleic acid research* **15,** 7081–7090 (1987).

92. Guo, P. X., Erickson, S. & Anderson, D. A small viral RNA is required for in vitro packaging of bacteriophage phi 29 DNA. *Science* **236,** 690–4 (1987).

93. Geier, G. & Modrich, P. Recognition sequence of the dam methylase of Escherichia coli K12 and mode of cleavage of Dpn I endonuclease. *J. Biol. Chem.* (1979).

94. Hattman, S., Brooks, J. E. & Masurekar, M. Sequence specificity of the {P1} modification methylase (M·Eco P1) and the {DNA} methylase (M·Eco dam) controlled by the Escherichia coli dam gene. *J. Mol. Biol.* **126,** 367–380 (1978).

95. Lodwick, D., Ross, H. N., Harris, J. E., Almond, J. W. & Grant, W. D. Dam Methylation in the Archaebacteria. *J. Gen. Microbiol.* **132,** 3055–9 (1986).

96. Baranyi, U., Klein, R., Lubitz, W., Krüger, D. H. & Witte, A. The archaeal halophilic virus-encoded Dam-like methyltransferase M. phiCh1-I methylates adenine residues and complements dam mutants in the low salt environment of Escherichia coli. *Mol. Microbiol.* **35,** 1168–79 (2000).

97. Klein, R., Greineder, B., Baranyi, U. & Witte, A. The structural protein E of the archaeal virus phiCh1: evidence for processing in Natrialba magadii during virus maturation. *Virology* **276,** 376–87 (2000).

98. Klein, R. *et al.* Natrialba magadii virus phiCh1: first complete nucleotide sequence and functional organization of a virus infecting a haloalkaliphilic archaeon. *Mol. Microbiol.* **45,** 851–63 (2002).

99. Gropp, F., Grampp, B., Stolt, P., Palm, P. & Zillig, W. The immunity-conferring plasmid pϕHL from the Halobacterium salinarium phage ϕH: Nucleotide sequence and transcription. *Virology* **190,** 45–54 (1992).

100. Rössler, N., Klein, R., Scholz, H. & Witte, A. Inversion within the haloalkaliphilic virus phi Ch1 DNA results in differential expression of structural proteins. *Mol. Microbiol.* **52,** 413–26 (2004).

101. Ptashne, M. *A Genetic Switch–Phage Lambda Revisited. 3rd*. (Cold Harbor Spring Laboratory Press, 2004).

102. Gottesman, M. E. & Weisberg, R. A. Little Lambda , Who Made Thee ?†. Microbiology and *Molecular Biology Reviews* **68,** 796–813 (2004).

103. Klaus, S., Krüger, D. & Meyer, J. *Bakterienviren.* (Gustav Fischer Verlag, Stuttgart, 1992).

104. Stolt, P. & Zillig, W. Transcription of the halophage phi H repressor gene is abolished by transcription from an inversely oriented lytic promoter. *FEBS Lett.* **344,** 125–8 (1994).

105. Anderson, W. F., Ohlendorf, D. H., Takeda, Y. & Matthews, B. W. Structure of the cro repressor from bacteriophage lambda and its interaction with DNA. *Nature* **290,** 754–758 (1981).

106. Iro, M. *et al.* The lysogenic region of virus phiCh1: identification of a repressor-operator system and determination of its activity in halophilic Archaea. *Extremophiles* **11,** 383–96 (2007).

107. Reiter, M. Gene regulation of ϕCh1: characterization of ORF49 and further characterization of the origin of replication of the halophage ϕCh1. *Diploma thesis* (2010).

108. Holmes, M. L. & Dyall-Smith, M. L. Sequence and expression of a halobacterial β-galactosidase gene. *Mol. Microbiol.* **36,** 114–122 (2000).

109. Derntl, C. Construction of the first deletion mutant of a haloalkaliphilic archaeon and analysis of gene expression of the methyltransferase M. NmaϕCh1I of the halophage ϕCh1. *Diploma thesis* (2009).

110. Selb, R. Construction of mutants of Nab. magadii and ϕCh1. *Diploma thesis* (2010).

111. Beraha, J. ORF79 - a putative regulator of gene expression in ϕCH1 and analysis of $gp34_{52}$ as a tail fibre protein of Nab. magadii“. *Diploma thesis* (2013).

5. List of Figures

Acknowledgement

First of all, I want to thank my supervisor Prof. Dr. Angela Witte. Working in her group was a valuable and great experience. Her support, help and patience in all stages during my thesis means a lot to me. Angela always had time for questions and discussions and I enjoyed working together with her and the whole team of our lab.

I also want to thank my dear colleagues and friends Katharina Dimmel, Judith Beraha, Hans Jörg Hellinger, Johannes Kassmannhuber and Stephan Rindler for their support for my work and for the fun and great time we had in our lab.

I want to thank my best friends Kloster Klaus, Bunny, Roland and Joanna for their mental support, which was very important to me. They encouraged me during the whole time of studying and during my master thesis.

Not at least, I want to express my gratitude to my parents who always supported me during the long time as a student. My very special thanks go to my father Karl Schöner who made it possible for me to study and finally graduate.

Abstract

Gene expression systems that allow controlled expression of proteins require strong, tightly controlled and inducible promoters, which are still nearly missing for halophilic *Archaea*. Recently, a tryptophan inducible promoter for *Nab. magadii* was established, called p*tna*N, but overexpression of proteins other than the reporter protein BgaH failed so far. A possible explanation could be that the inducer tryptophan is degraded. Upon induction, the promoter of the tryptophanase gene (*tna*A) located on the chromosome is induced too leading to expression of tryptophanase, an enzyme that is responsible for the degradation of tryptophan. In course of this study, the *tna*A gene was deleted by replacing it with the novobiocin resistant cassette via homologous recombination. The deletion mutant *Nab. magadii* L13Δ*tna*A was confirmed to be homozygous for the deleted gene by southern blot analysis, but the capability of *Nab. magadii* L13Δ*tna*A to enable controlled overexpression of proteins from ϕCh1 as well as from *Nab. magadii* still has to be verified.

The second part of this work focuses on the characterization of putative regulators of the virus ϕCh1. ORF79 encodes a putative regulatory protein, and investigation started with the creation of the deletion mutant *Nab. magadii* L11Δ79. Compared to the wild type strain *Nab. magadii* L11, an earlier onset of lysis could be observed which was the first indication for a repressor function of ORF79. Furthermore it was demonstrated that protein expression of certain ϕCh1 ORFs is altered in the mutant strain. Among these proteins is the putative tail fiber protein $gp34_{52}$. Expression of $gp34_{52}$ seemed to be completely de-regulated in the deletion mutant. In course of this study, the putative influence of ORF79 on the expression of $ORF34_{52}$ was further analyzed. ORF79 and $ORF34_{52}$ were co-expressed in *Nab. magadii* L13 and it could be demonstrated that induced expression of ORF79 leads to a decrease in the production of $gp34_{52}$. Furthermore, ORF79 was expressed in strain *Nab. magadii* L11 leading to reduced lysis and reduced expression of $gp34_{52}$ compared to the wild type strain.

Bioinformatic prediction suggests that ORF56 of ϕCh1 is a putative transcriptional regulator. For the first time, in course of this study a putative influence of ORF56 on ϕCh1 development was examined. ORF56 was expressed in the strain *Nab. magadii* L11 leading to an altered growth behavior. Compared to the wild type strain nearly no lysis could be observed and furthermore, expression of certain viral proteins is reduced. The obtained data provide first indications for a regulatory function of ORF56.

Zusammenfassung

Für die kontrollierte Expression von Proteinen bedarf es starker und regulierbarer Promotoren, jedoch sind solche für halophile *Archaeen* nahezu nicht beschrieben. Aus diesem Grund wurde unlängst ein mit Tryptophan induzierbarer Promoter für *Nab. magadii* etabliert, jedoch war die Expression von anderen als dem Reporter-Protein BgaH nicht erfolgreich. Ein Grund dafür könnte eine mögliche Degradierung des Inducers Tryptophan sein. Durch Induktion wird nicht nur der p*tna*N Promoter induziert, der auf dem Plasmid vorhanden is, sondern auch der Promoter des Tryptophanase Gens (*tna*A) das auf dem Chromosom lokalisiert ist. Daher wird das Enzym Tryptophanase, welches für den Abbau von Tryptophan verantwortlich ist, produziert. Im Rahmen dieser Arbeit wurde das *tna*A Gen deletiert. Mittels homologer Rekombination wurde das Gen durch eine Novobiocin Resistenzkassette ersetzt. Der daraus resultierende homozygote Deletionsstamm *Nab. magadii* L13Δ*tna*A konnte mit einem Southern blot bestätigt werden. Nachfolgende Experimente werden zeigen, ob eine Überexpression von ϕCh1 und *Nab. magadii* Proteinen in dem Deletionsstamm erzielt werden kann.

Der zweite Teil dieser Masterarbeit beschäftigt sich mit ORFs des Virus ϕCh1 die vermutlich eine regulatorische Funktion während der Virusentwicklung haben. Durch die Entwicklung der Deletionsmutante *Nab. magadii* L11Δ79 wurden die erste Anzeichen für eine regulatorische Funktion von ORF79 ersichtlich. Verglichen zum Wildtyp Stamm lysiert der Deletionsstamm deutlich früher und darüberhinaus ist die Expression von viralen Proteinen verändert. Die Expression des vermeintlichen tail fiber Proteins $gp34_{52}$ scheint vollständig dereguliert zu sein. Im Rahmen dieser Arbeit wurde der Einfluss von ORF79 auf die Expression von $ORF34_{52}$ genauer untersucht. Dafür wurden beide ORFs in dem Stamm *Nab. magadii* L13 co-expremiert. Es konnte gezeigt werden, dass durch die Induktion von ORF79 Expression die Produktion von $gp34_{52}$ sinkt. Des weiteren wurde ORF79 in dem Stamm *Nab. magadii* L11 exprimiert. Dieser Stamm zeigt im Vergleich zum Wildtyp Stamm eine reduzierte Form der Lyse sowie reduzierte Expression von $gp34_{52}$.
Bioinformatische Vorhersagen schlagen vor, dass der ϕCh1 ORF56 für einen transkriptionellen Regulator codiert. Im Rahmen dieser Arbeit wurde zum Ersten mal ein möglicher Einfluss von ORF56 auf die Virusentwicklung untersucht. Zunächst wurde der ORF56 in dem Stamm *Nab. magadii* L11 exprimiert, was zu einem veränderten Lyse Verhalten geführt hat. Nur eine sehr schwache Form der Lyse konnte für diesen Stamm festgestellt werden, und darüber hinaus ist die Expression von viralen Proteinen stark reduziert. Die gesammelten Daten lieferten erste Hinweise für eine regulatorische Funktion des ORF56.

Curriculum Vitae

Personal details:

Name:	Léa Schöner
Date and place of birth:	18. Juli 1981, Vienna
Nationality:	Austria

Education:

2012 - 2013	Master thesis: Laboratory of Prof. Dr. Angela Witte, Department of Microbiology, Immunbiology and Genetics; University of Vienna, Austria
2011 - 2013	Study "Molecular Microbiology and Immunbiology" (Master), University of Vienna, Austria
2008 - 2011	Study "Biology" (Bachelor), University of Vienna, Austria
2000 - 2008	Studies in "Genetics and Microbiology" (Diploma), University of Vienna, Austria
1995 - 2000	Höhere Bildungslehranstalt für wirtschaftliche Berufe, St. Pölten, Austria
1991 - 1995	Hauptschule Altlengbach Laabental, Austria
1987 - 1991	Volkschule Altlenbach, Austria

Working experience:

SS 2013	*University of Vienna, Austria:* Tutor of students for practical training in "Übungen in Molekularer Mikrobiologie"
WS 2012	*FH Campus Wien (University of Applied Sciences), Austria:* Tutor of students for practical training in course of the studies "Molekulare Biotechnologie"

SS 2012	*University of Vienna, Austria:* Tutor of students for practical training in "Übungen in Molekularer Mikrobiologie"
2002 - 2013	*BTG Spedition und Logistik GmbH* Assistent to the management - organization
2000 - 2002	*NÖ Pressehaus, Druck- und Verlagsgesellschaft m.b.H.*